ABSTRACT

McGuffey, Matthew Kenneth. Thermal Stability of α-Lactalbumin. (Under the Direction of E. Allen Foegeding.)

The first objective of this research was to quantitatively describe the denaturation and aggregation processes of α-lactalbumin at neutral pH in order to understand their interrelationship and effect on protein stability. Three different preparations of α-La (two pure and one commercial) had similar denaturation temperatures, enthalpies and % reversibility values as measured by differential scanning calorimetry. However, heated pure preparation reveled three non-native monomer bands that corresponded to three distinct dimer bands (as measured by Native PAGE). This suggested that specific intramolecular disulfide bond shuffling lead to formation of disulfide-specific dimers. The apo protein was the most thermostable to turbidity development and this was independent of preparation. The Cα-La was the most thermostable holo- preparation. Turbidity development at 95°C ($\tau_{95°C}$) suggested pure preparations intensely associate through hydrophobic interactions through bridging by divalent phosphate and this effect was mitigated by decreasing the ionic strength, decreasing the phosphate charge to –1 (at pH 6.6) or decreasing the temperature. The second objective was to investigate the aggregation behavior of a commercial α-La at neutral pH and 95°C in a nutritional beverage mineral salt environment. The variables explored were α-La lot variation, relative β-lactoglobulin concentration and excess calcium on the aggregate size development as measured by light scattering and turbidity development. The lot of holo-α-La possessing a higher intrinsic β-Lg concentration had higher solubility at pH ≤ 6.80, evolved more reactive thiol groups, had a 25% faster first order rate constant, dissociated only slightly with cooling and formed spherical aggregates with a much higher molecular weight. Aggregates intrinsic to the

protein powder may play a role in aggregate growth and shape. Adding increasing quantities of β-Lg generally decreased solubility. The highest β-Lg concentrations investigated demonstrated a net thiol oxidation and, subsequently, had a diminished ability to aggregate through hydrophobic interactions. Adding excess calcium caused a dramatic loss of solubility at pH 7.0 and required an increase in pH to 7.5 to regain solubility.

Thermal Stability of α-Lactalbumin

by

Matthew K. McGuffey

A dissertation submitted to the Graduate Faculty of
North Carolina State University
in partial fulfillment of the
requirements for the Degree of
Doctor of Philosophy

Food Science

Raleigh

2004

Approved by:

E. Allen Foegeding, Ph.D. Chair of Advisory Committee	**Brian Farkas, Ph.D.**
Tyre Lanier, Ph.D.	**John van Zanten, Ph.D.**

BIOGRAPHY

Matthew Kenneth McGuffey was born 5/24/1975 in East Lansing, MI to Rodney Kenneth and Patricia Harston McGuffey right about the time Ken was finishing his Ph.D. dissertation in Animal Science (Dairy Cattle Nutrition). After living in New Brunswick, NJ and Brookings SD, Matt's family settled down in New Palestine, IN from age five through high school graduation. Ken's love for agriculture and land grant Universities spurred Matt to attend Purdue University as a Food Science major. Matt graduated in four years with a B.S.-Honors degree under the tutelage of Suzanne Nielsen. Matt was active in his fraternity, Sigma Phi Epsilon, throughout college as well as other organizations. Matt married Jamie L. Miles from Fortville, IN and had a daughter, Madison, during the latter stages of his studies. After graduation, he went to work for Kellogg Co. for one year as an intern while Jamie finished her B.S. degree at Ball State University. After Jamie's graduation, the McGuffey family moved to Cary, NC where Matt began his graduate studies in Food Science at North Carolina State University in Raleigh, NC. He earned his M.S. degree on the Physical Properties of Whey Protein Isolate Gels in December, 2000 and successfully defended his Ph.D. dissertation on April 26th, 2004. Matt, Jamie and Madison currently reside in Minneapolis, MN where Matt is working as a Product Development Scientist for General Mills, Jamie works for Cargill and Madison attends Northrop Elementary school.

ACKNOWLEDGEMENTS

- Having aged in the corporate world for about a month prior to writing this, I have added perspective on the impact of my 5 ¾ years in the NCSU FS Dept. It is easily the most accepting, caring environment that I have ever worked in and it is easy to understand why people choose to make their entire careers there. I have met a large number of great people there that I anticipate keeping in touch with throughout my life and FS career.
- To my best friends throughout my tenure at NCSU: Jack Davis, Dany Doucet and Jeff Resch. I can't imagine three people that I have more in common with on every level than them.
- To Kris Freideck and Josh Payne who I only got to hang out with for a very short time before we moved on, but who added an extra dimension to my time there. I highly value the time I spent with them
- To all the people that I attended IFT with, partied with, had intellectual conversations with etc.; I'll try to name a few: Mary, Katie, Myke, Brad, Dorin, Christina, Jon, Kelly C., Katie S., Chris P, Chris W., Kelly S., Wendy, Lacey, Tracy,
- To my outstanding 'later years' labmates: Lisa, Mandy, Jessy, Amanda, Jennifers, Erin, Paul, Karin. What an eclectic, great group of people to balance work and fun with
- To the international labmates: Stan, Shinya, Ok Jin, Jeab, Jennifer, Don O., Guoyan. The experience would not have been the same without you
- To Paige Luck, the person I have the least in common with that I have the most in common with☺ Thanks for being my deskmate and offering me a different perspective and helping me through the peaks and valleys of graduate school

- To those people that I just couldn't get away from (i.e. Mills employees): Amy, Mike, Kara, Arnie, Rob, Michelle, Noel. I've had a great past and anticipate having a great feature with these folks.
- To the coaches I had early in life that molded me into someone that had the capacity to be successful: Marvin Shepler, Larry Sparks, Brian Kehrt, Bruce Haynes
- To the people and institutions who helped me immensely in my professional development: David Smith, George Bewley, Rich Wullschleger, Suzanne Nielsen, Purdue University and Sigma Phi Epsilon IA
- To the handful of teenage friends that I still keep in touch with: Harper, Jay, Corby, Mitchell, Holder, Q, Reid, Lee, Darren, Lake, Smucker
- To my mother and sister who always provided love, support and phone calls showing that they cared throughout the process
- An enormous thanks to Allen Foegeding for being a great academic mentor by giving me the independence and space to be a free-thinker at my own pace and never allowing me to oversimplify my system…and for being a great friend and someone that I always enjoyed spending time around…so much time that I can't think of any hours of the day that we haven't spent together.
- I couldn't choose an individual to dedicate my dissertation to, but there are two people that I have chosen to emphasize as the big reasons that I am where I am today. My father and my wife. My dad has always been there to offer attention and interaction on every level without imposing himself on me, which has allowed me to grow into an independent person. His empathy and support throughout graduate school has been very important in my success. To Jamie, for putting up with a low income earner who had a

completely different pace of life (i.e. non-professional) and providing me with all the love and support that I needed. We've grown up so much in the past 6 years that this Minnesota thing will be easy.

- Finally, to my wonderful daughter Madison. Pre-Madison, I always worked very hard and was very focused on work. Her presence has allowed me to balance home and work life without any guilt. She is my inspiration and I relish every moment I spend with her

TABLE OF CONTENTS

LIST OF TABLES

Review of Literature

Denaturation and Aggregation of Three α-Lactalbumin Preparations

Aggregation of α-Lactalbumin Isolate in a Neutral pH Nutritional Beverage Mineral Salt Environment

LIST OF FIGURES

Review of Literature

Denaturation and Aggregation of Three α-Lactalbumin Preparations

Aggregation of α-Lactalbumin Isolate in a Neutral pH Nutritional Beverage Mineral Salt Environment

REVIEW OF LITERATURE

During cheesemaking, a casein curd is formed and whey flows out of its pores. Whey contains lipids, lactose, salts and the small globular proteins present in milk. Ultrafiltration is used to purify whey proteins from the salts and lactose to produce whey protein concentrates (WPC; >50% protein) whey protein isolates (WPI; >90%) (Morr and Foegeding 1990). Recently, processors have further optimized their separation technologies so that α-lactalbumin and β-lactoglobulin can be offered as relatively pure protein ingredients (~ 90% of the total protein by weight). These ingredients can be tailored to specific functional applications like gelation, emulsification, foaming or solubility. α-Lactalbumin has the most potential for its solubility properties because of its relatively slow reaction rate; however there are few studies that have evaluated its solubility under different environmental conditions.

α-Lactalbumin (α-La) is secreted into the mammary gland and is the specifier protein in the lactose synthestase complex. Here, it binds with galactosyltransferase to modify its substrate specificity for converting glucose to lactose during lactation (Ivatt and Rosemeyer 1976).

Bovine α-La is a globular, calcium metalloprotein with a molecular weight (M_w) of 14,147 Da for variant A and 14,175 Da for B (Brew and Grobler 1992; Wong et al. 1996). Acharya et al. (1989) first elucidated the three dimensional structure of baboon α-La using x-ray crystallography (XRC); only recently has the very similar bovine structure been determined (Chrysina et al. 2000). It has an ellipsoid shape with two distinct lobes divided by a cleft (Figure 1). One lobe is comprised of four helices and the other loop is comprised of two β-strands with a loop-like chain. It has no free thiol groups and four disulfide bonds (Vanaman et al. 1970). The native calcium metalloprotein is referred to as holo-α-LA and when calcium is removed from the structure it is referred to as apo-α-LA. In this review, the abbreviation α-La implies holo-α-La.

Metal Ion Binding Properties of α-Lactalbumin

All α-lactalbumin species bind calcium at one strong affinity site, which dramatically affects its biophysical properties. Besides calcium, this primary site can also bind Na^{+}, Mn^{2+} and Mg^{2+} with a much lower affinity. Kronman et al. (1989) reviewed cation binding to various α-La species at various conditions and the reader is referred to this review for a more thorough treatise of the subject. This review will focus on how cation binding at the various sites affects the thermal behavior of bovine α-La species with an emphasis on cations commonly found at millimolar levels in food.

Since it was first revealed that α-La was a calcium metalloprotein (Hiraoka *et al.* 1980), multiple studies have disagreed on the calcium binding strength with values ranging from 10^6 to 10^9 M^{-1}. These values include: 2.5 X 10^6 M^{-1} (Hummel-Dryer procedure) (Bratcher and Kronman 1984a), 1.35 X 10^{10} M^{-1} (a calcium sensitive electrode) (Hamano *et al.* 1986), 2.9 X 10^8 M^{-1} (Vanderheeren *et al.* 1996), 5 X 10^7 M^{-1} (Griko and Remeta 1999) (isothermal titration calorimetry) and 2.9 X 10^8 M^{-1} (microsensitive differential scanning calorimetry) (Hendrix *et al.* 2000). Bratcher and Kronman (1984b) found the calcium binding affinity is relatively constant from pH 7.4 down to 5.7, but decreases dramatically below pH 5.

The calcium-binding elbow of α-La is a rigid structure that differs from the more flexible EF-handed calcium-binding loops in calmodulin and troponin. A total of 7 oxygen molecules coordinate calcium to α-La including 4 aspartic acid residues (Asp82, 84, 87 and 88), lysine-79 and 2 water ligands. This distorted pentagonol bipyramid arrangement provides a favorable geometry for coordinating Ca^{2+} (Acharya *et al.* 1989). Desmet and Van Cauwelaert (1988) discussed the longer-range structural implications of calcium binding. The Asp-87 and –88 residues are part of both the calcium-binding loop and the rigid α-helix that is directed towards

the C-terminal. Upon calcium binding, the rigid elbow at the top of the molecule and the Cys73-91 disulfide bridge toward the bottom act as a hinge swinging the helix away from the center of the molecule (Figure 1). When this occurs, hydrophobic surfaces exposed in the apo- conformer become buried (Desmet and Vancauwelaert 1988; Lindahl and Vogel 1984).

Bovine α-La also binds Ca^{2+} at a secondary site (Brew and Grobler 1992). The pH-dependence of this site ($pK_a' = 6.3$) implicates the involvement of His-68 (Aramini *et al.* 1992), the only solvent-exposed native His residue (Berliner and Kaptein 1981). Chandra et al. (1998) have characterized the crystal structure of human-α-La and found a secondary calcium site that is populated when an excess calcium concentration exists. The four oxygen atoms involved in coordinating calcium are from Thr-38, Glutamine-39 (Gln), Leu-81 and Asp-83. However, this structure may not be related to the bovine molecule as the 39 residue (Glu in bovine) is not conserved between species and the human variant has a much lower calcium affinity (Chandra *et al.* 1998).

In the absence of calcium, sodium can bind to the primary Ca^{2+}-binding site ($K_d = 10^2$-10^3 M^{-1}) and stabilize the molecule (Hiroka and Sugai 1984). Relkin et al. (1993) found an almost linear increase in heat capacity of apo-α-LA unfolding with Na^+ addition. They attributed this to an increase in the hydrophobic exposure (Relkin *et al.* 1993), indicating counterions reduce the intramolecular charge repulsion allowing hydrophobic regions to remain intact. This would presumably increase the rate of aggregation, but no studies have demonstrated this.

Zinc is only present in ~50 μM concentrations physiologically and would be found at similar to less concentrations in food. The α-La of bovine, human, guinea pig and rabbit possess a distinct Zn^{2+}-binding site and an excess molar ratio causes immediate aggregation (Kronman

1989). Therefore, understanding Zn^{2+}-binding may uncover structural domains that are critical to the solubility of α-La. Murakami and Berliner (1983) determined that Ca^{2+}- and Zn^{2+}-binding to the bovine variant is mutually exclusive (i.e. these ligands cannot bind simultaneously) and there is no difference in the rate of lactose biosynthesis between them. They calculated a Zn^{2+} binding strength of 1.8×10^5 M^{-1} (using electron spin resonance), which is consistent with the value found by Permyakov et al. (1991) of 5×10^5 M^{-1} (determined by tryptophan (Trp) fluorescence). Musci and Berliner (1986) calculated a distance of 1.15 nm between the Zn^{2+}-binding site (located on α-helix #3 (see Figure 1) near the Met-90 residue) and the primary Ca^{2+} site. In the latter study, Permyakov et al. (1991) concluded that α-La possesses several strong Zn^{2+}-binding sites that are filled sequentially and accompany protein aggregation. As the molar ratio of Zn^{2+} is increased from 1:1 to 16:1, the thermal denaturation temperature gradually shifts downwards and the trypsin and chymotrypsin susceptibility is increased. However, the Trp fluorescence is not altered and the affinity for the bis-ANS probe is dramatically decreased indicating hydrophobic regions are not responsible for the aggregation behavior (Permyakov *et al.* 1991). Finally, spherical "amorphous" aggregates were observed by TEM at pH 7.4 for α-La with 5 mM $ZnCl_2$, although no increase in fluorescence was observed (Goers *et al.* 2002). It appears that Zn^{2+} binding causes a long-range structural perturbation in the molecule that prevents Ca^{2+} binding and the destabilization is electrostatic in nature. The negative charges near Met-90 may aid molecular solvation and when Zn^{2+} binds, rapid aggregation results.

PROTEIN FOLDING AND UNFOLDING

One of the most intensively studied phenomena in biology today is protein folding. α-Lactalbumin happens to be a favorite protein to utilize in folding studies because it shares ~40% sequence homology with lysozyme (Brew *et al.* 1967; McKenzie and White 1991) and it forms a

stable folding intermediate under multiple denaturing conditions (a search of lactalbumin and protein folding on ISI Web of Science yielded 315 hits from 1985 to present). The now ubiquitous molten globule (MG) state of proteins was first applied to α-La (Dolgikh *et al.* 1981; Ohgushi and Wada 1983) as a general term used to describe a partially-unfolded, non-native protein conformation (Hirose 1993; Kuwajima 1989). The MG state of α-La can be formed at: (1) moderate, strong denaturant concentration (e.g. GdnHCl or urea), (2) acid denaturation, or (3) removal of calcium at low salt concentration and neutral pH (Kuwajima 1989; Kuwajima 1996). The global properties of α-La at these conditions include native-like secondary structure (Hiroka and Sugai 1984), a slightly expanded structure (10-20% larger radius) (Dolgikh *et al.* 1985; Kataoka *et al.* 1997; Pfeil 1987), and an absence of tertiary structure packing (Kuwajima *et al.* 1976). In contrast to the MG state, the fully unfolded state (in 6M GuHCl) has a much faster Trp rotational relaxation rate, an increase in intrinsic viscosity (6.1 vs. 3.1 cm^3/g), and very little remaining secondary structure (Dolgikh *et al.* 1985; Dolgikh *et al.* 1981).

It would be an intensive undertaking to review all of the molten globule studies and several excellent reviews already exist (Kronman 1989; Kuwajima 1989; Kuwajima 1996; Permyakov and Berliner 2000). In this section, some general α-lactalbumin unfolding phenomena will be discussed with an emphasis on manipulating its thermal unfolding.

Unfolding/Denaturation of apo- and holo-α-Lactalbumin

Holo-α-LA demonstrates first order, denaturation reaction kinetics with an Arrhenius temperature dependence from 70°-150°C as studied by isoelectric focusing (Dannenberg and Kessler 1988), PAGE (Anema 2001; Anema and McKenna 1996; Hillier and Lyster 1979), and immunodiffusion (Lyster 1970). There is a break in the temperature dependence of the rate constant at 80°C (Anema and McKenna 1996; Dannenberg and Kessler 1988).

According to DSC studies, α-La has the lowest denaturation (T_d) of the whey proteins (~61°C), but it is considered the most thermostable because it fully renatures upon cooling (>90% thermoreversible) (de Wit and Klarenbeek 1984; Ruegg *et al.* 1977). Bernal and Jelen (1984) found a 20°C decrease in T_d when calcium was chelated with 0.1M EDTA (in skim milk ultrafiltrate). Until the early 1990's, the standard model for α-La thermal denaturation assumed two-states, the calcium-bound, native protein and the apo-unfolded conformer (Hiroka and Sugai 1984; McKenzie and White 1991). However, a Ca^{2+}-bound, thermally-unfolded intermediate has been detected by both ellipticity change at 270 nm ($\Delta\varepsilon_{270\ nm}$) and DSC at temperatures up to 80°C (Vanderheeren and Hanssens 1994; Vanderheeren *et al.* 1996). At 215 μM α-La, increasing the Ca^{2+} from 260 to 1400 μM increases the population of this intermediate from 40 to 80% (calculated by $\Delta\varepsilon_{270\ nm}$) or from <20% to 50% (calculated from DSC) relative to the apo-form at 80°C (Vanderheeren *et al.* 1996). This Ca^{2+}-bound intermediate maintains an intact hydrophobic core, as detected by fluorescence measurements (Vanderheeren and Hanssens 1994). It was stressed that this does not refute previous results indicating calcium is released upon denaturation because those studies utilized stoichiometric quantities of Ca^{2+} to α-La and not an excess (Vanderheeren and Hanssens 1994). This has important implications for its solubility properties. It indicates that as calcium molar ratio is increased, a higher proportion of α-La molecules will maintain intact hydrophobic surfaces at temperatures relevant to food processing. Future research will demonstrate if this has an effect on the aggregation of α-La.

The T_d for α-La is only slightly pH-dependent ranging from 59°C at pH 3.5 (Bernal and Jelen 1985) to 65°C at pH 8 (Bernal and Jelen 1985; de Wit and Klarenbeek 1984). Below pH 3.5, no thermal transition can be detected because of a conformational transition (Kronman *et al.*

1965) caused by ionization of carboxyl and tyrosyl residues resulting in the total loss of calcium binding ability (Kuwajima *et al.* 1981).

PROTEIN AGGREGATION

In vivo, protein aggregation is associated with diseases like Down's syndrome, Alzheimer's disease and cataracts. In protein manufacture using recombinant technology, protein can precipitate into inclusion bodies in the host cell and recovering them is an expensive operation that reduces efficiency. *In vitro*, protein aggregation occurs in agricultural and biomedical products and can reduce their shelf life and efficacy. It is of great benefit to control this phenomenon, but science is just now beginning to understand its causes. Like many other molecules, proteins can crystallize, which is of great interest to crystallographers; however this review will focus on general physical considerations for amorphous aggregate formation. This will include colloidal physics, aggregation kinetics and some basic thermodynamic considerations.

A protein molecule is a charged colloidal particle and physical models have been utilized to describe the intermolecular interactions and association properties. At most pH values, a protein is a polyelectrolyte possessing both positive and negative charges that reside near the protein surface. However, initially, we will consider a much simpler case. The Guoy-Chapman theory begins with an infinite plane of homogenous surface charge with a given concentration of both positive and negative point charges existing in space at a distance x (Dickinson 1992). The change in electrical potential ψ as a function of distance from the surface can be calculated from Poisson's equation:

$$\frac{d^2\psi}{dx^2} = -\frac{\rho}{\varepsilon_r \varepsilon_o} \qquad (1)$$

where ρ is the charge density, ε_r is the relative dielectric constant ε_o is the permittivity of free space (Chapman 1913; Gouy 1910). The Debye length (κ^{-1}) represents the thickness of the electric "double-layer" in solution (i.e. region of local, elevated counterion concentration):

$$\kappa^2 = \frac{2z^2e^2n_o}{\varepsilon_r\varepsilon_o kT} \qquad (2)$$

where z represents the charge valence (e.g. +1 for Na^+ and +2 for Ca^{2+}) and n_o the concentration of ions in the bulk solution. This represents the distance, κ^{-1}, where ψ decays to $1/e$ of its surface value. Therefore, the counterion concentration has a strong influence on the Debye length. For example, increasing the ionic strength from 0.01 to 0.1 M NaCl decreases κ^{-1} from 3 nm to 1 nm (Dickinson 1992).

Verwey and Overbeek (1948) extended this treatment to two approaching particles, either large spheres with thin double-layers or small spheres with thick double layers. When two similarly-charged particles approach one another, their double layers begin to overlap, which creates a region of higher concentration of counterions and subsequently osmotic pressure. Because this situation is energetically unfavorable, the bulk solvent "rushes in" to reduce this region of higher concentration, which stabilizes the particles to association.

The combination of repulsive electrostatic stabilization term with an attractive van der Waals (vdW) term leads to the well-known DLVO theory (named for the two sets of scientists, Deryagin-Landau from Russia and Verwey-Overbeek from the Netherlands) that contributed to it (Derjaguin and Landau 1941; Verwey and Overbeek 1948). Figure 2 demonstrates the net attraction (negative values) or repulsion of two approaching spherical particles. There is a primary minimum (i.e. attraction) at short distances (≤ 1 nm) and a secondary minimum at large distances (~ 15 nm) due to van der Waals forces. However, at intermediate distances (~3 nm; the

distance corresponding to the electric double-layer) there is a primary maximum, which is sufficient to maintain particle stability.

In order to apply DLVO theory to food biopolymer systems, counterion concentration must be considered. At low counterion concentration, there is a high electrostatic repulsion between the molecules and their approach is energetically unfavorable. This large kinetic barrier to particle association (>10-20 kT) stabilizes the macromolecules to association (De Young *et al.* 1993). At intermediate counterion concentration, some of the surface charges will be shielded and a combination of the repulsive (electrostatic) and attractive vdW terms must be considered to determine the net interactions. Consequently, monomer-monomer contacts will have a much smaller barrier height and they may aggregate over time (De Young *et al.* 1993). At high counterion concentration, the surface charges are completely shielded and the attractive vdW term dominate causing rapid, irreversible aggregation with a deep free energy well (>5-10 kT) (De Young *et al.* 1993). Of course, attempting to model protein aggregation with this theory alone has its shortcomings, but understanding the physics is a useful starting point to understanding polyelectrolyte aggregation phenomena.

Aggregation Kinetics

Aggregate structure is related to the kinetics of monomer attachment to the growing cluster. Smoluchowski (1917) first provided a kinetic model for colloidal aggregation in dilute systems that will be reviewed here. For concentrated systems, the equilibrium theories of Flory-Stockmayer (Flory 1953) and de Gennes (1979) can be applied (Nicolai *et al.* 1996).

The features of any kinetic aggregation model include the monomer and aggregate concentration at time *t*, the aggregation rate constant, and the solvent viscosity. Complexity is added to these models when monomers must collide in a specific orientation to cause

aggregation. Smoluchowski (1917) developed a kinetic model for diffusion-limited cluster aggregation (DLCA) where the number of aggregates $N_m(t)$ at time, t, containing m-monomers is:

$$N_m(t) = N_o \frac{\tau^{m-1}}{(1+\tau)^{m+1}} \qquad (3)$$

where N_o is the number of monomers and the dimensionless aggregation time $\tau = kN_o t$, where k is the second-order aggregation rate constant (Wang *et al.* 2002). When aggregation is only limited by diffusion of the monomers into the aggregates then $k_R = 4k_BT/3\eta$ where k_B is the Boltzmann constant and η is the solvent viscosity. When the number of binding sites is limited or repulsive forces exist, k_R will deviate from this idealized case and a collision frequency must be introduced so that $k = \alpha k_R$ (Wang *et al.* 2002).

The kinetics of aggregate formation can be deduced by their structure as determined by scattering methods or microscopy. The limiting cases of aggregate formation are DLCA and reaction-limited cluster aggregation (RLCA). These cases can be differentiated by the fractal dimension (d_f) their structure. This is a non-integer value from 1 to 3 that is a measure of the structural self-similarity from the macro- to microscopic length-scales. For three dimensions, a structure that is space-filling with a scale-invariant structure would have a $d_f = 3$ (Dickinson 1992). As d_f decreases, the structure becomes more string-like as it approaches the Euclidian limit of 1 (not self-similar). This can be envisioned as the microscopic appearance of cork. In macromolecular aggregation, d_f describes the scaling of aggregate mass (M) with its size (R_g) (Mandelbrot 1982) as:

$$M = \left(\frac{R_g}{a}\right)^{d_f} \qquad (4)$$

where *a* is the monomer radius (Lin *et al.* 1990). In DLCA, the sticking probability of the particles tends to unity due to the lack of monomer-monomer repulsion and the aggregation rate is regulated by the diffusion coefficient ($\sim k_B T / \eta$) (Kolb *et al.* 1983). This phenomenon results in smaller sized aggregates with a narrow polydispersity and a $d_f \sim 1.80$ (Nicolai *et al.* 1996), because the monomer concentration is rapidly depleted. In RLCA, the energy barrier to aggregation is increased (i.e. intermolecular repulsion) and the sticking probability approaches zero (Lin *et al.* 1990). These aggregates are much larger with a wider polydispersity and $d_f \sim 2.1$ (Nicolai *et al.* 1996). This occurs because the growing aggregates have a much larger surface area and, therefore, probability of reacting with monomers or other aggregates. Interestingly, this limiting case has been found for a diverse range of substances such as gold, silica and polystyrene (Lin *et al.* 1990).

Once the kinetics of the monomer to aggregate reaction have been established, the next consideration is the change in system thermodynamics with each additional monomer attachment (De Young *et al.* 1993). Specifically, the free energy of monomer addition is a measure of the energy barrier of the process. The three idealized cases of this phenomenon are *simple*, *nucleation-controlled* and *exponential* aggregate growth. For the case of simple growth, the addition of each monomer is equivalently favorable and the free energy linearly decreases with aggregate size (De Young *et al.* 1993). The nucleation-controlled condition disfavors monomer incorporation into small aggregates (positive free energy), but after a nucleus of some critical dimension is formed, the free energy of monomer addition is negative. Exponential aggregation exhibits positive cooperativity where the addition of each additional monomer is more favorable than the last. Thus, larger aggregates are stickier than smaller ones (De Young *et al.* 1993).

Large supremolecular protein aggregates may sediment and this phenomenon leads to instability of protein-containing beverages. According to Russell *et al.* (1999), the two major considerations for understanding macromolecular sedimentation are: 1) the variation of settling velocity with volume fraction and interparticle potential; and 2) the net effect of this potential on the stabilizing forces. The obvious starting point is the Stokes equation, which states that a dilute sphere possessing a different density, ρ, than the solvent moves at a Stokes velocity U_o so that:

$$U_o = \frac{2r^2 \cdot \Delta\rho \cdot g}{9\mu} \qquad (5)$$

where r is the particle radius, g is the acceleration due to gravity and μ is the solvent viscosity (Russell *et al.* 1999). Essentially, this equation represents a balance between the gravitational (numerator) and viscous drag forces (denominator) (Russell *et al.* 1999). When intermolecular forces are repulsive the biopolymer radius will remain constant and the sedimentation rate will remain slow. Attractive forces cause biopolymer aggregation or flocculation, which increases their effective radius and increases settling velocity.

Aggregation of α-Lactalbumin at Physiological Temperatures

In a recent review, de la Fuente *et al.* (2002) stated that, "it is generally accepted that α-lactalbumin does not polymerize by itself when heated above 70°C." However, recent studies in both the food science (Bertrand-Harb *et al.* 2002; Hong and Creamer 2002) and biochemical literature (Goers *et al.* 2002; Li *et al.* 2001; Lindner *et al.* 2001) have described conditions where α-La and its derivatives aggregate at temperatures ranging from 20-95°C. First, these biochemistry papers will be described so that the conformational prerequisites for α-La aggregation are understood, then the food science papers will be reviewed so that conditions where aggregation does or does not occur can be reconciled.

As previously described, the MG-state of α-La can be induced by removal of calcium at neutral pH or simply by lowering the pH (< 3.5). These conditions have been further studied to determine if they lead to aggregation (Goers *et al.* 2002). They studied α-La "fibrillation" of the acid and apo- (neutral pH) MG-conformers of both the intact and disulfide-reduced protein (1SS-α-La; where 3 of the 4 disulfides are reduced with DTT and subsequently carboxymethylated to inhibit further reaction). They analyzed α-La solutions using Fourier transform infrared spectroscopy (FTIR), transmission electron microscopy (TEM) and intrinsic fluorescence. At all pH values, the highly flexible 1SS-α-La conformation formed fibrils rich in β-sheet structure. However, the intact protein only fibrillates at pH 2. The evidence for fibril formation is a sigmoidal increase in fluorescence, linear entangled aggregates and a turbid, slightly viscous dispersion. This process had a normal concentration dependence, was highly sensitive to ionic strength (the lag time decreases 200-fold by increasing NaCl from 25 to 150 mM NaCl) and increasing the temperature to 55°C has no effect (Goers *et al.* 2002).

With the 6-120 disulfide bond reduced, 3SS-α-La retains its native secondary and tertiary structure (Kuwajima *et al.* 1990) and it does not aggregate unless the basic peptide lactoferricin is present (Takase *et al.* 2002). They concluded that the free –SH groups from 3SS-α-La and lactoferricin probably do not participate in disulfide bond formation and that "subtle structural changes" are involved in its aggregation (Takase *et al.* 2002).

Li *et al.* (1999) more critically evaluated the role of hydrophobic surfaces and solvent environment in inducing multiple α-La conformers to aggregate. In this study, they incubated holo-, apo- and reduced-α-La (r-La) with preformed aggregates of other proteins (e.g. BSA, lysozyme, GADPH) that possessed significant quantities of hydrophobic surfaces. Only r-La associates with the preformed aggregates as measured by turbidity and fluorescence. If glycerol,

ethyleneglycol or polyethylene glycol (PEG) are present, the aggregation rate is dramatically reduced (Li *et al.* 1999). These solvents compete for intra- and inter-molecular hydrophobic interactions and reduce the dielectric constant of the solvent (i.e. its polarity) (Schein 1990). Likewise, increasing concentration of potassium phosphate buffer from 0.1 to 0.5M increases the aggregation rate (Li *et al.* 1999). This is consistent with the Hofmeister series of stabilizing salts $SO_4^{2-} = HPO_4^{2-} > F^- > Cl^- > Br^- > I^- = ClO^{4-} > SCN^-$. Anions at the beginning of the series increase the surface tension (σ_T) of water, Cl^- is neutral and the anions after it decrease the σ_T of water (Collins and Washabaugh 1985). Increasing σ_T enhances the hydrophobic effect as the water surrounding the hydrophobic clusters is more polar and less favorable to non-polar structures.

Lindner *et al.* (2001) extended the analysis of Hofmeister series effects to the aggregation and precipitation of r-La with no salt, 0.1M NaCl or 0.1M Na_2SO_4 by monitoring the $OD_{360\ nm}$. Without the addition of salt, aggregation proceeds very slowly due to intermolecular electrostatic repulsion. With NaCl, the lag time for aggregation and precipitation is ~35 min., but reduces to ~18 minutes with Na_2SO_4. This result is consistent with fluorescence emission (using ANS) indicating hydrophobic surface exposure increases as: Na_2SO_4 > NaCl > no salt (Lindner *et al.* 2001).

Taking all of this into account, it is obvious that the state of the disulfide bonds, hydrophobic environment and electrostatic interactions all play some role in the self-association of α-La under physiological conditions, but in what order? This will be put into perspective at the end of the next section.

Heat-Induced Aggregation of α-Lactalbumin

α-Lactalbumin aggregates at ambient temperatures when the conditions are highly reducing, hydrophobically favorable, or if Zn^{2+} is available. This provides an understanding of the protein conformations and pathways that lead to rapid aggregation. At temperatures relevant to food processing (>70°C), the solvent conditions should not direct α-La aggregation down these pathways.

Table 1 provides an overview of studies where the aggregation properties of pure α-lactalbumin were studied. The specific findings of these papers and the progression of thought up to the present day will be discussed throughout this section. The next section describes the aggregation properties of mixtures of α-La and sulfhydryl-containing proteins (e.g. β-Lg and BSA). The pertinent data to glean from Table 1 concerning the four studies that found no aggregation includes: (1) three out of the four studies used the less-sensitive size exclusion chromatography (SEC) for analysis; (2) three out of the four studies used Sigma α-La; (3) three out of four studied utilized ≤ 80°C; (4) the only study utilizing severe temperatures (Calvo *et al.* 1993), used the lowest concentration (0.15%) and analyzed by SEC.

Chaplin and Lyster (1986) heated α-La at 95°C for 14 minutes (in 0.1M phosphate buffer at pH 7) where it was 60% irreversibly denatured into disulfide-bonded aggregates and 40% renatured to the native state as determined by DSC. When heated at 100°C for 10 min., native PAGE shows small oligomers (dimers, trimers, etc.), native α-LA and faster bands that occur due to hydrolysis of glutamine and asparagine residues (Chaplin and Lyster 1986). More recently, Bertrand-Harb *et al.* (2002) and Hong and Creamer (2002) published similar studies where low concentrations (≤1%) of α-La were heated from 65°C to 95°C at pH ~ 7.5. At 85°C, PAGE reveals small amounts of aggregated material appear in the gels and at 95°C both gels

have a significant amount of large aggregates at the top of the stacking gel and at the stacking gel / resolving gel interface. Both authors concluded that β-ME fully reduced the aggregates back to monomer so disulfide bond formation predominates at neutral pH. Circular dichroic spectra for both far- (Bertrand-Harb *et al.* 2002) and near- (Hong and Creamer 2002) UV indicate that heating α-La diminishes native secondary structure (predominately α-helix) and tertiary contacts, respectively. Bertrand-Harb *et al.* (2002) determined that heating α-La (≥ 85°C) exposes buried tryptic cleavage sites (Lys-X and Arg-X bonds). However, they found no change in protein solubility (~85% soluble) when increasing the heating temperature from 25-95°C. Most likely, this temperature independence occurred because they used a good solvent that stabilized the protein (1:1 Calcium and 200 mM phosphate), the pH was too high, the concentration too low (10 mg/mL) and the centrifugal force too low (10,000 *x g*) to spin aggregated proteins out of solution.

Rheological testing has revealed elasticity development that occured after extensive aggregation. Hines and Foegeding (1993) found that 7% α-La (calcium depleted from Sigma) in 50 mM TES and 0.1M NaCl formed a weak network (400 Pa) after heating at 90°C for 3 hr and cooling to room temperature. Ikeda and Nishinari (2001) formed a weak network (100 Pa) after heating calcium saturated α-La in 0.1M NaCl at 70°C for 2.5 hr (gelpoint occurred at 118 min).

α-Lactalbumin Aggregation in the Presence of Sulfhydryl-Containing Proteins

The enhancement of protein aggregation from the disulfide bonds of α-La by sulfhydryl-containing proteins has been thoroughly studied. The aggregation properties of α-La mixed with β-Lg (Bertrand-Harb *et al.* 2002; Calvo *et al.* 1993; Dalgleish *et al.* 1997; Gault and Fauquant 1992; Gezimati *et al.* 1997; Havea *et al.* 2001; Hong and Creamer 2002; Matsudomi *et al.* 1992; Schokker *et al.* 2000), BSA (Havea *et al.* 2000; Havea *et al.* 2001), ovalbumin (Sun and

Hayakawa 2001) and κ-casein (Doi *et al.* 1983) have been studied. In all cases, α-La monomer reacted rapidly with these proteins.

To obtain a broad, mechanistic review of the aggregation of pure whey proteins and their mixtures, the reader is referred to a recent review (de la Fuente *et al.* 2002). This review will focus on results obtained for mixtures containing significant proportions (≥50% mass weight) of α-lactalbumin with a focus on its coaggregation with β-Lg.

Elfagm and Wheelock (1978) were the first to describe the synergistic interaction between β-Lg and α-La. They studied the loss of β-Lg and α-La by SEC and discovered a dramatic loss of α-La when heated in the presence of β-Lg, but almost no aggregation when heated alone. This effect could not be seen until a temperature of 77°C was reached (the approximate T_d of β-Lg). Also, the aggregation rate increased as pH was increased from 6.4 to 7.2 due to the increasing pKa of the thiol groups. They also concluded that thiol-disulfide interchange reactions initiated primary aggregation, but was not involved in secondary aggregation (Elfagm and Wheelock 1978). Calvo *et al.* (1993) was the first to correlate the disappearance of α-La monomer with the concentrations of free sulfhydryls (from BSA and β-Lg).

Hines and Foegeding (1993) found that the aggregation rate of α-La increased 13-14-fold at 80°C when heated in the presence of β-Lg (1:1 ratio of β-Lg:α-La) and that mixed gels (5:1) had a similar ultimate G' to β-Lg alone. Matsudomi *et al.* (1992) found that adding α-La to β-Lg gels enhanced the gel hardness where a 6% α-La/ 2% β-Lg formed a strong gel; however, the individual proteins did not form a gel at these concentrations.

Gezimati *et al.* (1997) studied the aggregation and gelation of β-Lg and α-La (10% w/v) heated alone and in specific ratios. Suprisingly, they found no G' development when 8% α-La

was heated with 2% β-Lg to 90°C at a rate of 1°C/min.; however, the temperature was not held at 90°C and the G' was not measured upon cooling. The strongest gels were formed by a 1:1 ratio. The aggregation rate was much faster for both proteins when heated together and dispersing these solutions in SDS caused significant dissociation; this indicates hydrophobic interactions were important. From this work, they were the first group to propose that β-Lg and α-La initially associate through hydrophobic interactions and this contact facilitates sulfhydryl-disulfide interchange reactions (Gezimati *et al.* 1997).

Dagleigh *et al.* (1997) provided the first study that determined the approximate M_w values for coaggregated solutions of different ratios of α-La and β-Lg. They heated (75°C for ≤ 10 min) the proteins individually and with α-La weight fractions of 0.3, 0.49, 0.68 and 0.95 (10% total protein). The samples were fractionated by a SEC column and analyzed by SDS-PAGE (reducing and nonreducing conditions). As the α-La weight fraction was increased from 0.3 to 0.95, the aggregate M_w progressively decreased from ≥ 300 kDa (all material eluting at the void volume) to ~ 100 kDa (all material eluting at intermediate M_w), respectively. The intermediate weight fractions contained a mixture of large and intermediate M_w. Also, it was demonstrated that during the early stages of heating, the β-Lg/α-La ratio of the aggregates was much higher than was in the original composition; subsequently, α-La reacted more rapidly over time. In other words, β-Lg initially reacts much faster than α-La. They also found that both hydrophobic association and sulfhydryl-disulfide interchange play an important role in aggregation in this system. Finally, it was concluded that β-Lg does not act as a catalyst when coaggregated with α-La because the chain termination steps are more efficient than the propagation steps; thus, small quantities of β-Lg heated with α-La should not start a sulfhydryl-disulfide chain reaction polymerization (Dalgleish *et al.* 1997).

Schokker et al. (2000) compared the aggregation of 1:1 mixtures of α-La with either β-Lg A or β-Lg B at 75°C and analyzed results by SEC-MALLS and PAGE. At the longer times used in this study (≥ 15 minutes), α-La disappeared at a faster rate than either variant of β-Lg, and the aggregation rate was slightly faster with β-Lg B than β-La A. Hydrophobic incorporation into aggregates played a larger role for β-Lg A than β-Lg B, which was incorporated primarily through disulfide bond formation. Also, hydrophobic interactions were more important at early stages in the aggregation process and were more important for α-La than β-Lg. Apparently, consistent with the results of Dagleish et al. (1997), β-Lg initially reacts faster than α-La, but after a lag phase where α-La becomes activated, it reacts more quickly than β-Lg. Their possible explanations for this include the higher number and/or reactivity of the disulfide bonds or its lower transition temperature (Schokker *et al.* 2000). The aforementioned study by Hong and Creamer (2002) did not focus on the coaggregation of β-Lg and α-La, but did find the α-La reacts more slowly when β-Lg is preheated at 80°C for 30 seconds.

In order to determine the degree of participation of specific thiol and disulfide bonds in β-Lg and α-La, Livney *et al.* (2003) heated them (10 mg/mL total protein; 1:1 molar ratio) at 85°C for 10 minutes at pH 5.9 at low (no added NaCl) and high (0.1 M NaCl) ionic strength. They analyzed the whole tryptic digests (uncentrifuged and unfiltered) by MALDI-TOF-MS and the soluble products (i.e. centrifuged and filtered) by reverse phase high performance liquid chromatography (HPLC) with MS analysis to determine the degree of thiol participation in intermolecular aggregate formation. The high ionic strength treatment formed a gel and had many more identifiable mass peaks indicating reduced electrostatic repulsion promotes thiol-disulfide interchange reactions (Livney *et al.* 2003). They reiterated previous assertions (Gezimati *et al.* 1997; Katsumata *et al.* 1996; McGuffey *et al.* 2004) that hydrophobic

interactions probably facilitate more extensive disulfide bond formation and that electrostatic repulsion plays a role in protein solubility (Livney *et al.* 2003; McGuffey *et al.* 2004). In their low ionic strength treatment, there were many more soluble disulfide-linked peptides produced (Livney *et al.* 2003). Increasing electrostatic repulsion by decreasing ionic strength or increasing pH promotes more energetically favorable disulfide bond orientations and/or simply mitigates the hydrophobic attractions.

Now, we will describe the aggregation of α-La with other sulfhydryl-containing proteins. Doi et al. (1983) studied the aggregation of α-La and κ-casein alone and in a 1:1 mixture at 90°C by SEC, PAGE and intrinsic fluorescence. α-La and κ-casein rapidly aggregates through sulfhydryl-disulfide interchange when heated in 0.035 M potassium phosphate, 0.4 M NaCl, pH 7.6, but not when heated in 0.01 M imadizole, 0.07-0.5 M KCl at pH 7.6. When heated alone, the α-La sulfhydryl concentration (measured as $Abs_{412\ nm}$ for DTNB) evolved linearly from A≈0 at t = 0 to A ≈ 0.175 at 60 minutes where it leveled off through 150 min. Apparently, a free sulfhydryl is not required to break indigenous disulfide bonds in order to evolve free sulfhydryl groups. Fluorescence spectra indicate the release of aromatic (Tyr) residues upon heating; if these residues are acetylated, κ-casein did not complex with α-La and very little sulfhydryl development (A<0.01) could be detected. Apparently, tyrosine residues are critical in facilitating sulfhydryl-disulfide interchange in α-La (Doi *et al.* 1983).

The studies with BSA (Havea *et al.* 2000) and ovalbumin (Sun and Hayakawa 2001) essentially implicated the same phenomenon observed in β-Lg coaggregation with α-La. The sulfhydryl-containing protein initiates sulfhydryl-disulfide interchange with α-La, forming copolymers of the two proteins as observed in SEC and PAGE.

At this point, the multitude of results regarding the role of disulfide bond formation in the aggregation of α-La alone, and with sulfhydryl-containing proteins will be summarized. With a severe enough heat treatment (≥85°C), α-La is able to evolve free sulfhydryl groups to initiate sulfhydryl-disulfide interchange (Doi *et al.* 1983) and form intermediate sized, disulfide-bonded aggregates (Bertrand-Harb *et al.* 2002; Hong and Creamer 2002). This is not surprising considering the 6-120 disulfide bond is 140 times more reactive to DTT than the other 3 disulfide bonds in native conditions (Kuwajima *et al.* 1990) due to the geometric strain in the native fold (Gohda *et al.* 1995; Kuwajima *et al.* 1990). When a sulfhydryl-containing protein is present, the –SH group rapidly reacts with one of the disulfides of α-La and causes rapid aggregation of both species.

Hydrophobic interactions play an important role in the coaggregation of β-Lg and α-La (Schokker *et al.* 2000), but their role in α-La aggregation is still not well understood. Eynard *et al.* (1992) demonstrated a dramatic increase in fluorescence when heating α-La from 60-70°C, but a dramatic decrease from 70-80°C (pH 6.8). This indicates that aromatic clusters remain intact up to 70°C, but become disorganized above this temperature in dilute solution (Eynard *et al.* 1992) with low levels of calcium (Vanderheeren and Hanssens 1994). Also, modification of tyrosine groups inhibits sulfhydryl development of α-La (Doi *et al.* 1983). This indicates hydrophobic associations may help facilitate monomer-monomer contact so that sulfhydryl-disulfide exchange can take place, but, clearly, more research is needed in this area.

There are no studies in the food science literature that evaluates the effect of solvent environment (aside from extremes in pH) on α-La aggregation. However, a few observations can be made by the results attained with the solvent choices made in the different studies. Most all of the studies had high concentrations (>0.02 M) of phosphate (Table 1). High concentrations

of phosphate can complex calcium in either an insoluble precipitate (K_{sp} = 2.1 x 10^{-33}) (Lide 1994) or a soluble complex like $CaHPO_4$ (K_{sp} = 2.7 x 10^{-7}) or $Ca(H_2PO_4)_2$ (K_{sp} = 1.0 x 10^{-3}) (Kotz and Purcell 1991). Also, there is a positive electrostatic surface potential in the vicinity of the 6-120-disulfide bond (Chandra *et al.* 1998) and PO_4^{3-} may stabilize this region to aggregation. These factors may increase protein solubility and minimize turbidity development and would be interesting for further study. Hong and Creamer (2002) provide the only study that compares the thermal stability of the holo- and apo- forms of α-La; they indicate the apo- form is more reactive in forming non-native monomers, although their evidence (PAGE) is not convincing that this reactivity forms larger aggregates. The only studied where it was surprising to see no α-La aggregation was that of Schokker *et al.* (2000). One possible explanation might be their choice of imidazole as their reaction buffer. It is an aromatic group similar to tyrosine that might be a good solvent for hydrophobic groups (i.e. tyrosine); as described earlier, Doi *et al.* (1983) found α-La to be particularly heat stable in imadizole when heated at 90°C.

STATIC LIGHT SCATTERING

In static light scattering (SLS), the time-integrated intensity of scattered light from a polymer solution is measured to obtain size or specific structural information. The former focuses on the determination of parameters like the radius of gyration (R_g) and weight-averaged molar mass (M_w). It is based on the theory attributed to Rayleigh-Gans-Debye (RGD); essentially, the intensity of light scattered from a homogenous, isotropic, monodisperse system of polymers with $R_g < \lambda/20$ is related to the concentration fluctuations (Cancellieri et al. 1974). Besides size information, SLS can be used to characterize the polymer structure, shape or fractal dimension. This review will attempt to cover SLS theory and pertinent applications for the utilization of 0° angle measurements (i.e. turbidimetry) and multiangle laser light scattering (MALLS).

Turbidity Measurements

In a spectrophotometer, optical density measurements (OD = log I_o/I) are made in non-absorbing regions at a 0° detector angle with respect to the light source. Turbidity is related to the OD and the path length, l by:

$$\tau = \left(\frac{2.303 \cdot OD}{l} \right) \qquad (6)$$

Utilizing the Rayleigh-Gans approximation, the turbidity can be related to the M_w (in g mol^{-1}) as:

$$\tau = H \cdot Q \cdot M \cdot c \qquad (7)$$

where H *is a constant that describes the optical contrast of the experimental setup:*

$$H = \frac{32\pi^3 \cdot n_s^{\,2} \cdot \left(\frac{dn}{dc} \right)^2}{3N_A \cdot \lambda^4} \qquad (8)$$

where n_s is the solvent refractive index, *dn/dc* the refractive increment of the particle in mL g^{-1}, N_A is Avogadro's number and λ is the wavelength of light *in vacuo* (Cancellieri *et al.* 1974; Doty and Steiner 1950).

Rearranging a virial expansion of equation 7 yields an equation for a straight line:

$$H \cdot Q \cdot c/\tau = \left(1/M_w\right) + 2A_2 \cdot Q \cdot c \quad \lambda >> R_g \qquad (9)$$

where A_2 is the second virial coefficient. From a plot of $H \cdot Q \cdot c/\tau$ vs. *c*, M_w and the A_2 can be determined for a monodisperse suspension. The second virial coefficient describes the mutual interaction between pairs of particles, therefore, equation 9 ignores 3-body and higher interactions. It is a qualitative measure of the solvent power (Burchard 1994) from thermodynamically good ($A_2 > 0$), through ideal ($A_2 = 0$; a theta solvent), to thermodynamically

bad ($A_2 < 0$) (Schorsch *et al.* 1999). Thus, in a good solvent, the polymer swells to interact with the solvent and these interactions are preferred over interpolymer contacts.

The Q factor is a shape-dependent, dimensionless number between 0 and +1 that accounts for intraparticle destructive interference. For a sphere, this is represented by:

$$Q = \frac{3}{8}\int_0^{\pi} P(\varphi)\cdot(1+\cos^2\varphi)\cdot\sin\varphi\, d\varphi \qquad (10)$$

where $P(\varphi)$ is the particle scattering factor that accounts for destructive interference by scattering from different parts of the same particle (Cancellieri *et al.* 1974). For particles having a much smaller diameter than the λ, $Q = 1$.

For small particles ($D << \lambda$), Rayleigh theory predicts the scaling of turbidity with wavelength is equal to –4 according to:

$$\frac{d\log\tau}{d\log\lambda} = -4 + \alpha + \alpha' + \beta \qquad (11)$$

where α and α' are the wavelength dependence of n_o and *dn/dc*, respectively (Cancellieri *et al.* 1974). These are small negative corrections that can typically be neglected. β is the wavelength dependence of Q and corrects for the particle size. Equation 11 can be used to directly calculate β and a plot of β vs. D/λ' (where D = the particle diameter) can give size information.

For a polydisperse system, there are no real physical advantages to turbidimetry over MALLS in the determination of size characteristics of biopolymers. However, turbidimetry is a convenient method utilizing the ubiquitous spectrophotometer; it can determine qualitative changes in solvent quality, an average M_w for a monodisperse system and a size value if the approximate particle shape is known.

Multiangle Laser Light Scattering

In a solution containing small particles ($R_g < \lambda/20$), the intensity of light scattered arises from density and concentration fluctuations (Debye 1944). Density fluctuations are typically negligible and can be approximated by the solvent density fluctuations (Burchard 1994). Concentration fluctuations are directly related to the Rayleigh ratio (R_θ; the normalized scattering intensity) through standard thermodynamics (Burchard 1994):

$$R_\theta = K\, c\, RT \frac{dc}{d\pi} \qquad (12)$$

where RT dc/dπ is the osmotic compressibility and K is an optical constant:

$$K = \frac{4\pi^2 n_o^2}{N_A \lambda_o^4}\left(\frac{dn}{dc}\right)^2 \qquad (13)$$

having a similar form to equation 8. The osmotic compressibility is proportional to the M_w and at finite concentration equation 12 can be rewritten as:

$$R_\theta = KcM_w P(q) \cdot S(q) \qquad (14)$$

where P(q) and S(q) are the intraparticle and interparticle interference factors, respectively. These account for the phase difference of light scattered from different elements of the same particle P(q) or different particles S(q). The wave vector, q, is a function of scattering angle, θ:

$$q = \frac{4\pi n_s}{\lambda_o}\sin\left(\frac{\theta}{2}\right) \qquad (15)$$

In dilute solutions, $S(q)_{c\to 0} = 1$ and P(q) can be expanded to yield the Zimm approximation:

$$\frac{Kc}{R_\theta} \approx \frac{1}{M_w}\left(1 + \frac{\left(qR_{gz}\right)^2}{3}\right)(1 + 2M_w A_2 c) \qquad (16)$$

where R_{gz} denotes the z-averaged R_g and A_2 represents the second virial coefficient (as described in the previous section). When scattering data is collected at multiple angles for multiple

concentrations, a Zimm plot can be constructed to determine M_w and R_{gz}. A plot of q^2 vs. Kc/R_θ extrapolated to zero angle and zero concentration yields the M_w and R_{gz} (the initial slope for the c = 0 curve) (Burchard 1994). For small particles ($R_g < \lambda/20$), the $\sin(\theta/2)$ term approaches zero and only one angle is required to calculate M_w (typically the 90° angle is used because it has the highest signal to noise ratio) (Harding 1997). When very dilute solutions are used (≤ 0.5 g/L), as in SEC-MALLS, the A_2c term approaches zero and a Zimm plot requires only an angular extrapolation (Harding 1997).

In MALLS detection, the sample features and the information desired dictate what variations in instrument setup and sample preparation are chosen. The two primary instrument setup modes are: 1) batch mode where a scintillation vial is centered within the detectors and the incident laser; and 2) a flow cell with exquisitely engineered optics that is typically used in tandem with SEC. Batch mode should be utilized when: 1) running time course experiments using elevated temperatures, 2) if samples are relatively monodisperse or only the M_w is desired, and 3) if the sample will be progressively diluted to determine structural parameters like fractal dimension. The disadvantage to batch mode is the more intensive data treatment required to characterize the size polydispersity in polymer mixtures. The major advantage to flow cell mode is in fractionating polymer mixtures by SEC then analyzing the monodisperse slices that elute from the column by MALLS. Most manufactures offer 4-5 columns designed to separate globular proteins that have resolving power gradations from 1,000 through 5,000,000 Da. To attain optimal resolution for mixtures of both native (≈ 10^4 Da) and aggregated globular proteins (≈ 10^5 to 10^6 Da), two columns with disparate resolution profiles often are utilized in series. The major disadvantage is the inability to make in situ measurements with SEC because of the ambient temperature requirement. Therefore a heat-quench experiment must be utilized to

measure time-course data. In this type of experiment, the sample is given the desired heat treatment then quickly cooled (typically in an ice bath) to ambient temperatures before analysis.

Table 1. Summary of treatment conditions found in α-lactalbumin aggregation studies

Study	Heat Treatment	Conc. (g/L)	$[Ca^{2+}]$[a] Form	Solvent	Protein Source	Aggregation Observed	Method Used
Chaplin & Lyster, 1986	100ºC for 10 min.	14	NS	0.061 M Na_2HPO_4, 0.03 M NaH_2PO_4, (pH 7) & 0.02% NaN_3	Separated from Skim Milk and purified by affinity chromatography (DEAE Affi-Gel Blue column)	Yes	PAGE
Calvo et al., 1993	90°C for 24 min.	1.5	NS	"Milk Ultrafiltrate" Composition not given	Sigma	No	SEC
Dagleigh et al., 1997	75°C for 10 min.	100	NS[b]	0.02 M Phosphate Buffer, pH 7	Purified from a commercial source by Q-Sepharose column	No	SEC
Gezimati et al., 1997	80°C for 15 min.	80	NS	"WPC-like"	Sigma	No	PAGE
Schokker et al., 2000	80°C for "prolonged heating"	10	Holo-	0.02 M imidazole, 0.05 M NaCl, 0.003 M NaN_3, pH 7	Sigma (calcium saturated)	No	SEC
Havea et al., 2000	75°C for 6 min.	50	Holo-	0.4 M total of K^+ & Na^+ w/ 0.035 M Ca^{2+}, pH 6.8	Sigma (calcium saturated)	Yes	PAGE
Bertrand-Harb et al., 2002	65°C, 85°C & 95°C for 30 min.	10	NS[c]	0.2 M sodium phosphate buffer, pH 7.5	Separated from skim milk[d] and purified by DEAE-sepharose anion exchange chromatography	Yes (≥ 85°C)	PAGE
Hong & Creamer, 2002	70-95°C (every 5°C) for 10 min.	2.4	Apo- & Holo-	0.015 M phosphate buffer, pH 6.7 or 7.4	Separated from skim milk[d] and purified using Superdex 75 prep. column	Yes (≥80°C)	PAGE

a) not specified (NS)
b) the protein was "dialyzed exhaustively" against deionized H_2O indicating very little calcium would be present
c) during purification, 10 mM $CaCl_2$ was present in the elution buffer and dialysis was not mentioned, so Ca^{2+} it may be present
d) utilized method of Maillart and Ribideau-Dumas (1988)

List of Figures

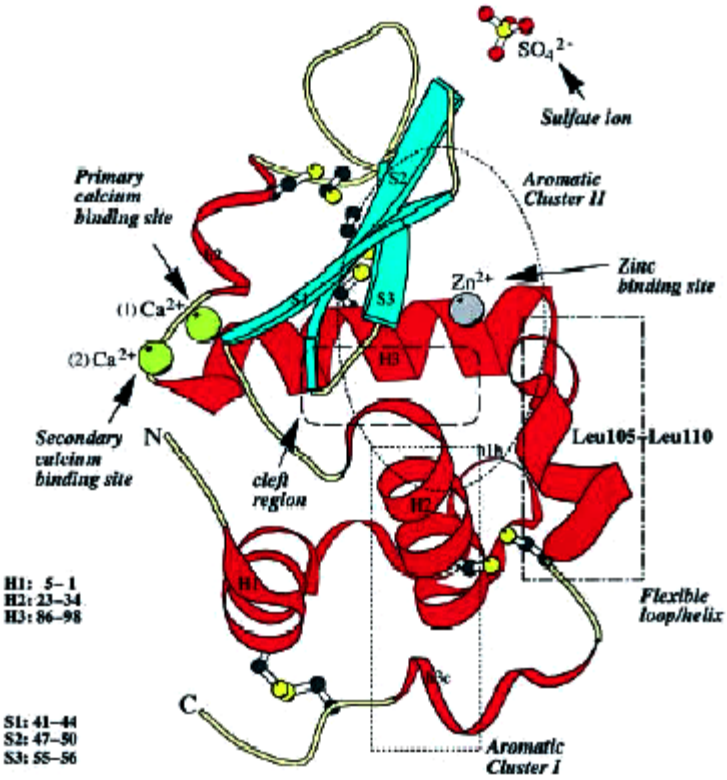
SO_4^{2-}
Sulfate ion
Primary calcium binding site
Aromatic Cluster II
Zinc binding site
Zn^{2+}
(1) Ca^{2+}
(2) Ca^{2+}
S2
S3
H3
Secondary calcium binding site
N
cleft region
Leu105–Leu110
H2
H1
Flexible loop/helix
H1: 5–1
H2: 23–34
H3: 86–98
S1: 41–44
S2: 47–50
S3: 55–56
C
Aromatic Cluster I

FIGURE 1

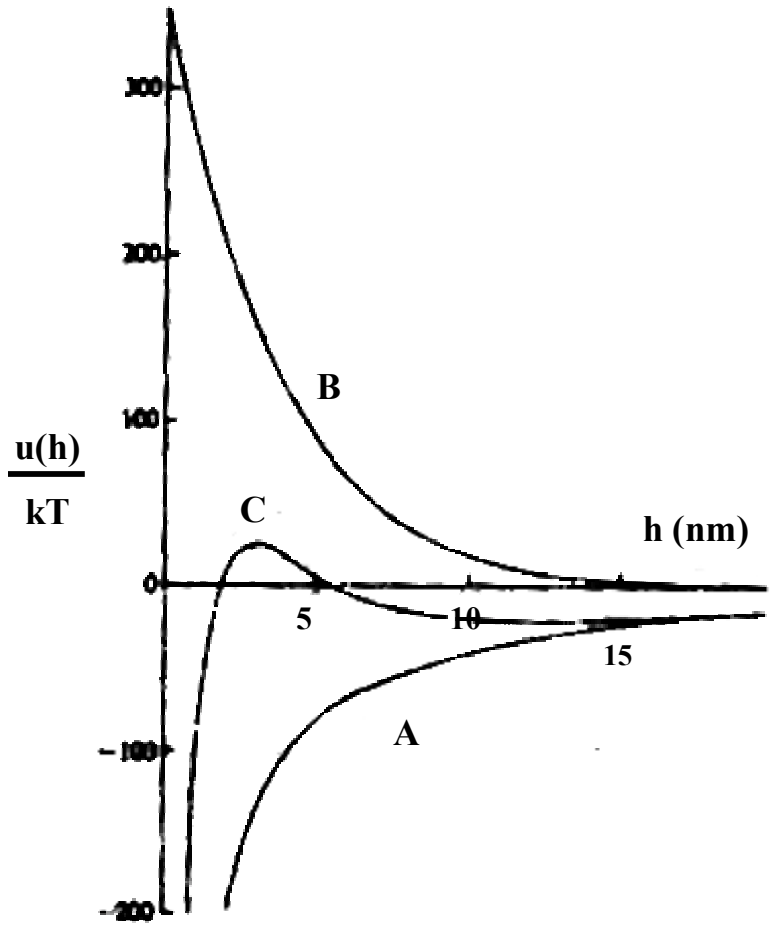

FIGURE 2

REFERENCES

ACHARYA, K.R.,STUART, D.I.,WALKER, N.P.,LEWIS, M. and PHILLIPS, D.C. 1989. Refined structure of babbon alpha-lactalbumin at 1.7A resolution. Comparison with c-type lysozyme. J. Mol. Bio. 208, 99-127.

ANEMA, S.G. 2001. Kinetics of the irreversible thermal denaturation and disulfide aggregation of α-lactalbumin in milk samples of various concentrations. Journal of Food Science 66, 2-9.

ANEMA, S.G. and MCKENNA, A.B. 1996. Reaction kinetics of thermal denaturation of whey proteins in heated reconstituted whole milk. Journal of Agricultural and Food Chemistry 44, 422-428.

ARAMINI, J.M.,DRAKENBERG, T.,HIRAOKI, T.,KE, Y.,NITTA, K. and VOGEL, H.J. 1992. Ca-43 Nmr-Studies of Calcium-Binding Lysozymes and Alpha- Lactalbumins. Biochemistry 31, 6761-6768.

BELL, K. and MCKENZIE, H.A. 1967. Isolation and properties of bovine β-lactoglobulin C. Biochimica Et Biophysica Acta 147, 109-&.

BERLINER, L.J. and KAPTEIN, R. 1981. Nuclear magnetic-resonance characterization of aromatic residues of α-lactalbumins - laser photo chemically-induced dynamic nuclear-polarization nuclear magnetic-resonance studies of surface exposure. Biochemistry 20, 799-807.

BERNAL, V. and JELEN, P. 1984. Effect of calcium binding on themral denaturation of bovine α-lactalbumin. J. Dairy Sci. 67, 2452-2454.

BERNAL, V. and JELEN, P. 1985. Thermal Stability of Whey Proteins - A Calorimetric Study. J. Dairy Sci. 68, 2847-2852.

BERTRAND-HARB, C.,BADAY, A.,DALGALARRONDO, M.,CHOBERT, J.M. and HAERTLE, T. 2002. Thermal modifications of structure and co-denaturation of α-lactalbumin and β-lactoglobulin induce changes of solubility and susceptibility to proteases. Nahrung-Food 46, 283-289.

BRATCHER, S.C. and KRONMAN, M.J. 1984a. Intermolecular and Intramolecular Interactions of Alpha- Lactalbumin .14. Metal-Ion Binding to the N and a Conformers of Bovine Alpha-Lactalbumin. Journal of Biological Chemistry 259, 875-886.

BRATCHER, S.C. and KRONMAN, M.J. 1984b. Metal ion binding to the N and A conformers of bovine α-lactalbumin. J. Biol. Chem. 259, 10875-10886.

BREW, K. and GROBLER, J.A. 1992. α-Lactalbumin. In *Advanced dairy chemistry: proteins*. (P.F. Fox eds.), 1: pp. 191-229. New York: Elsevier Applied Science.

BREW, K.,VANAMAN, T.C. and HILL, R.L. 1967. Comparison of Amino Acid Sequence of Bovine Alpha-Lactalbumin and Hens Egg White Lysozyme. Journal of Biological Chemistry 242, 3747-&.

BURCHARD, W. 1994. Light Scattering Techniques. In *Physical Techniques for the Study of Food Biopolymers*. (S. B. Ross-Murphy eds.): pp. New York: Blackie.

CALVO, S.,LEAVER, J. and BANKS, J.M. 1993. Influence of other whey proteins on the heat-induced aggregation of α-lactalbumin. International Dairy Journal 3, 719-727.

CANCELLIERI, A.,FRONTALI, C. and GRATTON, E. 1974. Dispersion Effect on Turbidimetric Size Measurement. Biopolymers 13, 735-743.

CHANDRA, N.,BREW, K. and ACHARYA, K.R. 1998. Structural evidence for the presence of a secondary calcium binding site in human α-lactalbumin. Biochemistry 37, 4767-4772.

CHAPLIN, L.C. and LYSTER, R.L.J. 1986. Irreversible heat denaturation of bovine α-lactalbumin. Journal of Dairy Research 53, 249-258.
CHAPMAN, D.L. 1913. A contribution to the theory of electroencapillarity. Phil. Mag. 25, 475-481.
CHRYSINA, E.D.,BREW, K. and ACHARYA, K.R. 2000. Crystal structure of apo- and holo-bovine α-lactalbumin at 2.2-A resolution reveal an effect of calcium on inter-lobe interactions. The Journal of Biological Chemistry 275, 37021-37029.
COLLINS, K.D. and WASHABAUGH, M.W. 1985. The Hofmeister effect and the behaviour of water at interfaces. Quaterly Reviews of Biophysics 18, 323-422.
DALGLEISH, D.G.,SENARATNE, V. and FRANCOIS, S. 1997. Interactions between α-lactalbumin and β-lactoglobulin in the early stages of heat denaturation. Journal of Agricultural and Food Chemistry 45, 3459-3464.
DANNENBERG, F. and KESSLER, H.-G. 1988. Reaction kinetics of the denaturation of whey proteins in milk. Journal of Food Science 53, 258-263.
DE GENNES, P.G. 1979. *Scaling Concepts in Polymer Physics*, Cornell University Press, London.
DE LA FUENTE, M.A.,SINGH, H. and HEMAR, Y. 2002. Recent advances in the characterisation of heat-induced aggregates and intermediates of whey proteins. Trends in Food Science & Technology 13, 262-274.
DE WIT, J.N. and KLARENBEEK, G. 1984. Effects of various heat treatments on structure and solubility of whey proteins. Journal of Dairy Science 67, 2701-2710.
DE YOUNG, L.R.,FINK, A.L. and DILL, K.A. 1993. Aggregation of globular proteins. Acc. Chem. Res. 26, 614-620.
DEBYE, P.J.W. 1944. Light scattering in solution. J. Appl. Phys. 15, 338-342.
DERJAGUIN, B.V. and LANDAU, L.D. 1941. Theory of the stability of strongly charged lyophobic sols and the adhesionof strongly charged particles in solutions of electrolytes. Acta Physicochim. URSS 14, 633-662.
DESMET, J. and VANCAUWELAERT, F. 1988. Calorimetric Experiments of Mn^{2+}-Binding to α-Lactalbumin. Biochimica Et Biophysica Acta 957, 411-419.
DICKINSON, E. 1992. *An Introduction to Food Colloids*, Oxford University Press, New York.
DOI, H.,TOKUYAMA, T.,KUO, F.-H.,IBUKI, F. and KANAMORI, M. 1983. Heat-induced complex formation between κ-casein and α-lactalbumin. Agricultural and Biological Chemistry 47, 2817-2824.
DOLGIKH, D.A.,ABATUROV, L.V.,BOLOTINA, I.A.,BRAZHNIKOV, E.V.,BYCHKOVA, V.E.,GILMANSHIN, R.I.,LEBEDEV, Y.O.,SEMISOTNOV, G.V.,TIKTOPULO, E.I. and PTITSYN, O.B. 1985. Compact state of a protein molecule with pronounced small-scale mobility - bovine α-lactalbumin. European Biophysics Journal 13, 109-121.
DOLGIKH, D.A.,GILMANSHIN, R.I.,BRAZHNIKOV, E.V.,BYCHKOVA, V.E.,SEMISOTNOV, G.V.,VENYAMINOV, S.Y. and PTITSYN, O.B. 1981. α-Lactalbumin: compact state with fluctuating tertiary structure? FEBS Letters 136, 311-315.
DOTY, P. and STEINER, R.F. 1950. Light scattering and spectrophotometry of colloidal solutions. J. Chem. Phys. 18, 1211-1220.
ELFAGM, A.A. and WHEELOCK, J.V. 1978. Interaction of bovine α-lactalbumin and β-lactoglobulin during heating. J. Dairy Sci. 61, 28-32.

EYNARD, L.,IAMETTI, S.,RELKIN, P. and BONOMI, F. 1992. Surface hydrophobicity changes and heat-induced modifications of α-lactalbumin. Journal of Agricultural and Food Chemistry 40, 1731-1736.

FLORY, P.J. 1953. *Principles of Polymer Chemsitry*, Cornell University Press, New York.

GAULT, P. and FAUQUANT, J. 1992. Heat-Induced Gelation of beta-Lactoglobulin - Influence of pH, Ionic Strength and Presence of Other Whey Proteins. Lait 72, 491-510.

GEZIMATI, J.,CREAMER, L.K. and SINGH, H. 1997. Heat-induced interactions and gelation of mixtures of β-lactoglobulin and α-lactalbumin. Journal of Agricultural and Food Chemistry 45, 1130-1136.

GOERS, J.,PERMYAKOV, S.E.,PERMYAKOV, E.A.,UVERSKY, V.N. and FINK, A.L. 2002. Conformational prerequisites for α-lactalbumin fibrillation. Biochemistry 41, 12546-12551.

GOHDA, S.,SHIMIZU, A.,IKEGUCHI, M. and SUGAI, S. 1995. The superreactive disulifide bonds in α-lactalbumin and lysozyme. J. Protein Chem. 14, 731-737.

GOUY, G. 1910. Sur la constitution de la electrique a la surface d'un electrolyte. J. Phys. Radium 9, 457-468.

GRIKO, Y.V. and REMETA, D.P. 1999. Energetics of solvent and ligand-induced conformational changes in α-lactalbumin. Protein Science 8, 554-561.

HAMANO, M.,NITTA, K.,KUWAJIMA, K. and SUGAI, S. 1986. Binding strength of calcium ion to bovine α-lactalbumin. J. Biochem. 100, 1617-1622.

HARDING, S.E. 1997. Hydrodynamic Properties of Proteins. In *Protein Structure A Practical Approach*. (T.E. Creighton eds.): pp. New York: Oxford University Press.

HAVEA, P.,SINGH, H. and CREAMER, L.K. 2000. Formation of new protein structures in heated mixtures of BSA and α-lactalbumin. Journal of Agricultural and Food Chemistry 48, 1548-1556.

HAVEA, P.,SINGH, H. and CREAMER, L.K. 2001. Characterization of heat-induced aggregates of beta- lactoglobulin, alpha-lactalbumin and bovine serum albumin in a whey protein concentrate environment. Journal of Dairy Research 68, 483-497.

HENDRIX, T.,GRIKO, Y.V. and PRIVALOV, P.L. 2000. A calorimetric study of the influence of calcium on the stability of bovine α-lactalbumin. Biophysical Chemistry 84, 27-34.

HILLIER, R.M. and LYSTER, R.L.J. 1979. Whey protein denaturation in heated milk and cheese whey. Journal of Dairy Research 46, 95-102.

HINES, M.E. and FOEGEDING, E.A. 1993. Interactions of α-lactalbumin and bovine serum albumin with β-lactoglobulin in heat-induced protein gelation. J. Agric. Food Chem. 41, 341-346.

HIRAOKA, Y.,SEGAWA, T.,KUWAJIMA, K.,SUGAI, S. and MURAI, N. 1980. α-Lactalbumin: A calcium metalloprotein. Biochem. Biophys. Res. Commun. 95, 1098-1104.

HIROKA, Y. and SUGAI, S. 1984. Thermodynamics of thermal unfolding of bovine apo-α-lactalbumin. Int. J. Peptide Protein Res. 23, 535-542.

HIROSE, M. 1993. Molten globule of food proteins. Trends Food Sci. Tech. 4, 48-52.

HONG, Y.H. and CREAMER, L.K. 2002. Changed protein structures of bovine β-lactoglobulin B and α-lactalbumin as a consequence of heat treatment. International Dairy Journal 12, 345-359.

IKEDA, S. and NISHINARI, K. 2001. Structural changes during heat-induced gelation of globular protein dispersions. Biopolymers 59, 87-102.

IVATT, R.J. and ROSEMEYER, M.A. 1976. Lactose Synthetase - Isolation and Characterization of Protein- Protein Complex. European Journal of Biochemistry 64, 233-242.
KATAOKA, M.,KUWAJIMA, K.,TOKUNAGA, F. and GOTO, Y. 1997. Structural characterization of the molten globule of a-lactalbumin by solution X-ray scattering. Protein Science 6, 422-430.
KATSUMATA, K.,OKAZAKI, A.,TSURUPA, G.P. and KUWAJIMA, K. 1996. Dominant forces in the recognition of a transient folding intermediate of alpha-lactalbumin by GroEL. Journal of Molecular Biology 264, 643-649.
KOLB, M.,BOTET, R. and JULLIEN, R. 1983. Scaling of kinetically growing clusters. Physical Review Letters 51, 1123-1126.
KOTZ, J.C. and PURCELL, K.F. 1991. *Chemistry and Chemical Reactivity*, Saunders College Publishing, Philadelphia.
KRONMAN, M.J. 1989. Metal-ion binding and the molecular conformational properties of α-lactalbumin. Critical Reviews in Biochemistry and Molecular Biology 24, 565-667.
KRONMAN, M.J.,CERANKOW.L and HOLMES, L.G. 1965. Inter- and Intramolecular Interactions of Alpha-Lactalbumin .3. Spectral Changes at Acid pH. Biochemistry 4, 518-&.
KUWAJIMA, K. 1989. The Molten Globule State as a Clue for Understanding the Folding and Cooperativity of Globular-Protein Structure. Proteins 6, 87-103.
KUWAJIMA, K. 1996. The molten globule state of α-lactalbumin. FASEB J. 10, 102-109.
KUWAJIMA, K.,IKEGUCHI, M.,SUGAWARA, T.,HIROKA, Y. and SUGAI, S. 1990. Kinetics of disulfide bond reduction in α-lactalbumin by dithiothreitol and molecular basis of superreactivity of the Cys6-Cys120 disulfide bond. Biochemistry 29, 8240-8249.
KUWAJIMA, K.,NITTA, K.,YONEYAMA, M. and SUGAI, S. 1976. Three state denaturation of a-lactalbumin by guanidine hydrochloride. J. Mol. Bio. 106, 359-373.
KUWAJIMA, K.,OGAWA, Y. and SUGAI, S. 1981. Role of the Interaction between Ionizable Groups in the Folding of Bovine Alpha-Lactalbumin. Journal of Biochemistry 89, 759-770.
LI, H.,ERRINGTON, A.D. and FOEGEDING, E.A. 1999. Isostrength comparison of large-strain (fracture) rheological properties of egg white and whey protein gels. J. Food Sci. 64, 893-898.
LI, J.,ZHANG, S. and WANG, C.C. 2001. Only the reduced conformer of α-lactalbumin is inducible to aggregation by protein aggregates. Journal of Biochemistry 129, 821-826.
LIDE, D.R., ed. 1994. *CRC Handbook of Chemistry and Physics*. Ann Arbor: CRC Press.
LIN, M.Y.,LINDSAY, H.M.,WEITZ, D.A.,BALL, R.C.,KLEIN, R. and MEAKIN, P. 1990. Universal reaction-limited colloid aggregation. Physical Review A 41, 2005-2020.
LINDAHL, L. and VOGEL, H.J. 1984. Metal-ion dependent hydrophobic interaction chromatography of α-lactalbumins. Analytical Biochemistry 140, 394-402.
LINDNER, R.A.,TREWEEK, T.M. and CARVER, J.A. 2001. The molecular chaperone α-crystallin is in kinetic competition with aggregation to stabilize a monomeric molten-globule form of α-lactalbumin. Biochemical Journal 354, 79-87.
LIVNEY, Y.D.,VERESPEJ, E. and DALGLEISH, D.G. 2003. Steric effects governing disulfide bond interchange during thermal aggregation in solutions of beta-lactoglobulin B and alpha-lactalbumin. Journal of Agricultural and Food Chemistry 51, 8098-8106.
LYSTER, R.L. 1970. The denaturation of α-lactalbumin and β-lactoglobulin in heated milk. Journal of Dairy Research 37, 233-243.

MAILLART, P. and RIBADEAU-DUMAS, B. 1988. Preparation of β-lactoglobulin and β-lactoglobulin-free proteins from whey retentate by NaCl salting out at low pH. J. Food Sci. 53, 743-745, 752.

MANDELBROT, B.B. 1982. *The Fractal Geometry of Nature*, Freeman, San Francisco.

MATSUDOMI, N.,OSHITA, T.,SASAKI, E. and KOBAYASHI, K. 1992. Enhanced heat-induced gelation of b-lactoglobulin by a-lactalbumin. Biosci. Biotech. Biochem. 56, 1697-1700.

MCGUFFEY, M.K.,OTTER, D.E.,VAN ZANTEN, J.H. and FOEGEDING, E.A. 2004. Aggregation of a-Lactalbumin Isolate in a Neutral pH Nutritional Beverage Mineral Salt Environment. International Dairy Journal Submitted.

MCKENZIE, H.A. and WHITE, F.H., JR. 1991. Lysozyme and α-lactalbumin: Structure, function, and interrelationships. Adv. Protein Chem. 41, 173-315.

MORR, C.V. and FOEGEDING, E.A. 1990. Composition and functionality of commercial whey and milk protein concentrates and isolates: A status report. Food Technology 44, 100, 102-104, 106, 108, 110 & 112.

MURAKAMI, K. and BERLINER, L.J. 1983. A Distinct Zinc-Binding Site in the Alpha-Lactalbumins Regulates Calcium-Binding - Is There a Physiological-Role for This Control. Biochemistry 22, 3370-3374.

MUSCI, G. and BERLINER, L.J. 1986. Intramolecular Distance Measurements in Alpha-Lactalbumin. Biochemistry 25, 4887-4891.

NICOLAI, T.,DURAND, D. and GIMEL, J.C. 1996. Scattering properties and modelling of aggregating and gelling systems. In *Light Scattering. Principles and Developments*. (W. Brown eds.): pp. Oxford: Clarendon Press.

OHGUSHI, M. and WADA, A. 1983. 'Molten-globule state': a compact form of globular proteins with mobile side-chains. FEBS Letters 164, 21-24.

OKAZAKI, A.,IKURA, T.,NIKAIDO, D. and KUWAJIMA, K. 1994. The chaperonin GroEL does not recognize apo-α-lactalbumin in the molten globule state. Nature Structural Biology 1, 439-446.

PERMYAKOV, E.A. and BERLINER, L.J. 2000. α-lactalbumin: structure and function. FEBS Letters 473, 269-274.

PERMYAKOV, E.A.,SHNYROV, V.L.,KALINICHENKO, L.P.,KUCHAR, A.,REYZER, I.L. and BERLINER, L.J. 1991. Binding of Zn(Ii) Ions to Alpha-Lactalbumin. Journal of Protein Chemistry 10, 577-584.

PETERS, T. 1985. Serum-Albumin. Advances in Protein Chemistry 37, 161-245.

PFEIL, W. 1987. Is thermally denatured unfolded? The example of α-lactalbumin. Biochimica et Biophysica Acta 911, 114-116.

RELKIN, P.,LAUNAY, B. and EYNARD, L. 1993. Effect of sodium and calcium addition on thermal denaturation of apo-α-lactalbumin: a differential scanning calorimetric study. J. Dairy Sci. 76, 36-47.

RENKEMA, J.M.S.,GRUPPEN, H. and VAN VLIET, T. 2002. Influence of pH and ionic strength on heat-induced formation and rheological properties of soy protein gels in relation to denaturation and their protein compositions. J. Agric. Food Chem 50, 6064-6071.

RUEGG, M.,MOOR, U. and BLANC, B. 1977. A calorimetric study of the thermal denaturation of whey proteins in simulated milk ultrafiltrate. J. Dairy Res. 44, 509-520.

RUSSELL, W.B.,SAVILLE, D.A. and SCHOWALTER, W.R. 1999. *Colloidal Dispersions*. Edited by G.K. Batchelor. Cambridge Monographs on Mechanics and Applied Mathematics, Cambridge University Press, New York.

SCHEIN, C.H. 1990. Solubility as a function of protein structure and solvent components. Biotechnology 8, 308-317.

SCHOKKER, E.P.,SINGH, H. and CREAMER, L.K. 2000. Heat-induced aggregation of β-lactoglobulin A and B with α-lactalbumin. International Dairy Journal 10, 843-853.

SCHORSCH, C.,JONES, M.G. and NORTON, I.T. 1999. Thermodynamic incompatibility and microstructure of milk protein/locust bean gum/sucrose systems. Food Hydrocoll. 13, 89-99.

SMOLUCHOWSKI, M.V. 1917. Versuch einer mathematischen theorie der koagulationkinetik kollider losungen. Z. Phys. Chem. 92, 129-168.

SUN, Y.X. and HAYAKAWA, S. 2001. Thermally induced aggregates in mixtures of alpha-lactalbumin with ovalbumins from different avian species. Journal of Agricultural and Food Chemistry 49, 2511-2517.

TAKASE, K.,HIGASHI, T. and OMURA, T. 2002. Aggregate formation and the structure of the aggregates of disulfide-reduced proteins. Journal of Protein Chemistry 21, 427-433.

VANAMAN, T.C.,BREW, K. and HILL, R.L. 1970. Disulfide Bonds of Bovine Alpha-Lactalbumin. Journal of Biological Chemistry 245, 4583-&.

VANDERHEEREN, G. and HANSSENS, I. 1994. Thermal unfolding of bovine α-lactalbumin. Journal of Biological Chemistry 269, 7090-7094.

VANDERHEEREN, G.,HANSSENS, I.,MEIJBERG, W. and VANAERSCHOT, A. 1996. Thermodynamic characterization of the partially unfolded state of Ca^{2+}-loaded bovine alpha-lactalbumin: Evidence that partial unfolding can precede Ca2+ release. Biochemistry 35, 16753-16759.

VERWEY, E.J.W. and OVERBEEK, J.T.G. 1948. *Theory of the Stability of Lyophobic Colloids*, Elsevier

WANG, K.,SINGH, A.K. and VAN ZANTEN, J.H. 2002. Aggregation rate measurements by zero-angle time-resolved multiangle laser light scattering. Langmuir 18, 2421-2425.

WETLAUFER, D.B. 1961. Osmometry and general characterization of a-lactalbumin. Comp. Ren. Trav. Lab. Carlsberg 31, 125-138.

WONG, D.W.S.,CAMIRAND, W.M. and PAVLATH, A.E. 1996. Structures and Functionalities of Milk Proteins. Crit. Rev. Food Sci. Nutr. 36, 807-841.

Denaturation and Aggregation of 3 α-Lactalbumin Preparations at Neutral pH

Matthew K. McGuffey[a], Kevin L. Epting[b], Robert M. Kelly[b] and E. Allen Foegeding[a,*]

To Be Submitted to Journal of Agricultural and Food Chemistry

*Corresponding Author

[a]Department of Food Science
Southeast Dairy Foods Research Center
North Carolina State University
236 Schaub Hall
Raleigh, NC 27695-7624

[b]Chemical Engineering Department

North Carolina State University

Raleigh, NC 27606-7270

ABSTRACT

The denaturation and aggregation of Sigma (Σα-La), ion-exchange chromatography purified (IEXα-La) and a commercial α-lactalbumin (Cα-La) was studied with microsensitive differential scanning calorimetry, polyacrylamide gel electrophoresis and turbidity measurement. All three preparations had denaturation temperatures near 64°C and the denaturation enthalpy (ΔH) was Cα-La > Σα-La > IEXα-La. The reversibility of the ΔH transition was ~35% for Cα-La and Σα-La and 24% for IEXα-La. Heating pure preparations produced three non-native monomer bands that corresponded to three distinct dimer bands indicating specific intramolecular disulfide bond shuffling leads to formation of disulfide-specific dimers. The apo protein was the most thermostable to turbidity development and the Cα-La was the most thermostable holo-preparation. Turbidity development at 95°C ($\tau_{95°C}$) indicated pure preparations intensely associate through hydrophobic interactions through bridging by divalent phosphate. This effect was mitigated by decreasing the phosphate charge to –1 (at pH 6.6). The Cα-La required 4 times the phosphate or excess Ca^{2+} to develop a similar $\tau_{95°C}$ to the pure preparations and displayed a complex pH-dependent $\tau_{95°C}$ behavior. The $\tau_{95°C}$ dramatically decreased at 85°C and was negligible at 75°C, indicating pronounced temperature dependence. A mechanism is provided and the interrelationship between specific electrostatic interactions and hydrophobic attraction in relation to the formation of disulfide-bonded products is discussed.

INTRODUCTION

The ability of whey protein manufacturers to isolate α-lactalbumin (α-La) and β-lactoglobulin (β-Lg) to a high degree of purity represents a tremendous opportunity to broaden their food applications (*1*). Human milk contains ~30% α-La (as a % of total protein) and the human and bovine variants have similar nutritional qualities including equally high tryptophan and cysteine contents (*2*). Since α-La is considered a heat stable protein (*3*), it is an excellent candidate for utilization in nutritional beverages like infant formulas and nutritional supplements.

α-La is a globular, calcium metalloprotein with a molecular weight (M_w) of 14.2 kDa, 4 disulfide bonds and no free thiol groups (*4*). The two lobes of the three dimensional structure (*5;6*) can be partitioned electrostatically (*7*): 1) an acidic lobe rich in β-sheet structure that contains the Ca^{2+} binding loop (residues 35-88) (*5;6*) with a calculated pI of 3.7 (including 10 Asp); and 2) a basic lobe rich in α-helical structure (residues 1-34 and 89-123) (*5;6*) with a calculated pI of 9.6 (including 9 Lys).

The competition between electrostatic stabilization and intermolecular hydrophobic aggregation in denatured forms of α-La has been studied by evaluation in different solvent environments (*8-10*). With no additional salt, aggregation proceeds very slowly, but it is dramatically enhanced with the addition of Na_2SO_4 (*9*), potassium phosphate (*11*) and NaCl (*9;10*). The aggregation rate follows normal Hofmeister series effects where salts that increase the surface tension of water increase the hydrophobic aggregation rate (*9*). This attraction can be significantly mitigated with the addition glycerol, ethyleneglycol or polyethylene glycol (i.e. solvents that interact with hydrophobic clusters) (*8*).

α-La denatures at relatively low temperatures (~64°C), but does not rapidly aggregate due to its lack of free thiol groups (*12*). However, when held at temperatures ≥ 85°C, α-La evolves free thiol groups (*13;14*) that form intermolecular disulfide-bonded aggregates (*15-17*). Of the disulfide bonds of α-La (C6-C120, C28-C111, C61-C77, and C73-C91) (*18*), the C6-C120 disulfide bond is considered "superreactive" (to DTT at 25°C) due to the geometric strain imposed by the native fold, the positive charge distribution in this region and its surface exposure (*19;20*). At 85°C, it drives initiation of thiol/disulfide interchange, and, subsequently, a neighboring thiol (C111) is the most reactive in forming intermolecular disulfide bonds (*21*). The high reactivity on the C-terminus chain may be a result of its known flexibility (*21;22*) and the enhanced reactivity of Cys thiols in the proximity of positive charge density (*23*). Also, it has been suggested that hydrophobic interactions facilitate intermolecular disulfide bond formation in the coaggregation of α-La and β-Lg (*17;24*).

Most studies have evaluated the coaggregation of α-La with β-Lg rather than α-La alone. The consensus is that mixtures of α-La and β-Lg have enhanced aggregation properties than either protein heated alone (*25*). Even minor "contamination" of α-La preparations by β-Lg considerably enhances thermal aggregation (*12;15;26*). Essentially, aggregate size increases as the β-Lg content is increased in α-La preparations (*12*). Chaplin and Lyster (*16*) provided the only study that focused solely on the heat-induced aggregation of α-La and their proposed mechanism has not been significantly altered by subsequent studies. When α-La is heated to 77°C (the temperature causing a complete unfolding transition as analyzed by DSC) and then cooled, it is >90% reversible. However, when α-La is held at 95°C for 14 min, only 40% renatures to the native state. Native polyacrylamide gel electrophoresis (PAGE) shows the

aggregates as small oligomers (dimers, trimers, etc.). Chaplin and Lyster (16) propose that irreversibility was due to a fraction of disulfide bonds are broken during heating of α-La at high temperatures, producing free thiol groups that can catalyze intermolecular thiol/disulfide interchange reactions resulting in the formation of soluble oligomers (*16*).

There is considerable variation exists among the studies investigating the heat stability of α-La. **Table 1** lists eight studies that have evaluated its ability to aggregate and their respective conditions. The pertinent data to glean from the four studies that found *no* aggregation (*12;24;27;28*) includes: (1) three out of the four studies used Sigma α-La; (2) three out of the four studies utilized ≤ 80°C; and (3) three out of the four studies used size exclusion chromatography (SEC) for analysis. The only study utilizing "severe" temperatures (90°C) (*27*), used the lowest concentration (1.5 $g \cdot L^{-1}$) and analyzed by SEC. The only study that detected aggregates at temperatures < 80°C (*29*) heated at the lowest pH with a high ionic strength. This indicates that multiple factors including α-La source, purity, temperature, concentration and solvent may influence its ability and the degree to which it aggregates.

The objective of this study was to evaluate the denaturation and aggregation of three α-La preparations predominantly used in **Table 1**: 1) ion-exchange chromatography purified (IEXα-La); 2) Sigma (Σα-La); and 3) a commercial preparation (Cα-La). This study evaluates the denaturation profile of these preparations in order to determine its relationship, if any, with aggregation. In order to provide some contrast to the existing literature methods, *in situ* turbidity measurements were used to characterize the solvent and temperature dependence of α-La aggregation.

MATERIALS AND METHODS

Materials. The commercial α-La was a gift from Davisco Foods International (Le Seur, MN) and contained 91.7% protein on a wet basis (N × 6.14) (30) based on micro-Kheldahl nitrogen analysis. As a % weight of total protein, this preparation contained 92.5, 2.8, 0.8, 1.1, 0.6 and 2.2% α-La, β-Lg, BSA, immunoglobulin, glycomacropeptide and proteose peptone, respectively, as determined by reverse phase high performance liquid chromatography. Approximately 7% of the α-La was glycosylated as determined by deglycosylation with PNGase and quantitation with laser densitometry. The Ca^{2+} concentration represented only ~20% saturation of the α-La. Two different lots of highly purified α-La (Product # L-5385) were obtained from Sigma Chemical Company (St. Louis, MO). A Q-Separose Fast Flow ion exchange resin was used to purify the aforementioned commercial α-La according to (21). All salts and chemicals used were USP or electrophoresis grade.

Methods. *Protein solution preparation*. Protein powder was hydrated with ~90% of the total deionized H_2O (>17 MΩ) required and stirred for 2 h at room temperature. The order of salt solution addition was: 0.2 M $CaCl_2$, 0.2 M sodium phosphate buffer (a blend of monobasic and dibasic solutions to yield the reaction pH) and 1M NaCl. The pH of this solution was then adjusted using 0.10 N HCl, then the balance of water was added. The intrinsic Ca^{2+} and Na^{+} composition of the commercial preparation was compensated for in the total added.

The protein concentrations for purified holo- and apo-α-La preparations were calculated using extinction coefficients of 2.01 (*31*) and 1.95 $L \cdot g^{-1} \cdot cm^{-1}$ (*4*), respectively. For the commercial α-La, an effective extinction coefficient was calculated using the protein content of the powder and determined to be $\varepsilon_{280} = 1.92\ L \cdot g^{-1} \cdot cm^{-1}$.

Native and SDS PAGE. Native polyacrylamide gel electrophoresis (PAGE) was performed using precast, 4-20% gradient gels made with Tris-HCl buffer (Bio-Rad Labs, Hercules, CA).

Samples were diluted 1:2 with Bio-Rad "Native Sample Buffer". The reservoir buffer was 0.02 M Tris and 0.2 M glycine at pH 8.0. Sodium dodecyl sulfate-(SDS) PAGE was performed under similar conditions except the protein samples were mixed with 1% SDS prior to 1:1 dilution in the Native sample buffer and 0.1% SDS was added to the reservoir buffer. Protein staining was performed with a Coomassie Stain Solution (Bio-Rad Labs) for 1 h and destained with 10% glacial acetic acid, 10% isopropanol overnight. A M_w marker containing myosin (200 kDa), β-galactosidase (116 kDa), phosphyorylase b (97.4 kDa), bovine serum albumin (66.2 kDa) and ovalbumin (45 kDa) from Bio-Rad was used. The naming convention of Hong and Creamer (17) was used to describe the products of heating α-La including: native-like and non-native monomers and SDS-dimers.

Differential Scanning Calorimetry. The thermal denaturation of α-La was monitored using a Nano-Cal Model 5100 differential scanning calorimeter (Calorimetry Sciences Corp., Provo, UT). The instrument reference and sample cell volumes were each ~0.90 mL. A scan rate of 1°C/min and an excess pressure (~2 atm) was used for all experiments. A typical experiment consisted of a buffer/buffer scan set followed by a buffer/protein scan set (a set consists of 2 heating and cooling cycles from 25°C to 95°C). The buffer was 10 mM sodium phosphate (buffered at pH 7.0) and was used to dissolve the α-La to ~2.5 mg/mL. All solutions were thoroughly degassed prior to analysis.

The heat capacity data of the buffer and protein scans was analyzed using the CpCalc 2.0 software provided by the instrument manufacturer. The buffer scan (i.e. baseline) was subtracted from the protein scan and the molar heat capacity was calculated using a molecular weight of 14,200 Da and a partial specific volume of 0.709 (*32*). A polynomial equation was used to fit the pre-transition baseline to the post-transition baseline. The area under this curve was used to

calculate the calorimetric enthalpy (ΔH). The % reversibility was calculated as the ratio of ΔH from the second heating scan to the first ($\Delta H_2/\Delta H_1 \cdot 100$). This data represents the average of three replications.

In Situ Turbidity Experiments. The time-dependent optical density development was monitored at 400 nm in a Shimadzu 160U spectrophotometer equipped with a jacketed cuvette holder attached to a recirculating water bath (RWB). Initially, the circulating water temperature was set to 100°C to improve heat transfer and reduce the sample temperature lag. As the sample temperature approached 95°C (~5 min), the RWB temperature was reduced to maintain a 95°C sample temperature. The sample temperature was monitored with a thermocouple every 2-3 min during the early stages of heating and every 10 min after it stabilized. The temperature accuracy was typically ±0.5°C. At the end of the heating period, the protein solutions were rapidly cooled in water and the OD was remeasured to assess the reversibility of aggregate formation.

The optical density (OD) values from the spectrophotometer were converted to turbidity (τ) values by the relationship ($\tau = 2.303 \times OD/l$) where *l* is the path length (*33*). The reversibility was calculated as: $(\tau_{95°C} - \tau_{25°C})/\tau_{95°C} \cdot 100$. The data represents the average of three replications for IEXα-La and Cα-La and two replications for Σα-La.

RESULTS AND DISCUSSION

Purity of α-La Preparations. Figure 1A (lanes 2, 4 and 6) demonstrates the purity of the three preparations utilized in this study. The lanes were overloaded (40 μg total protein) to visualize minor impurities. In the Cα-La (lane 6), the two higher mobility bands were the two variants of β-Lg with β-Lg B being present at much higher concentrations. The two bands of lower mobility were glycosylated α-La and either a α-La dimer or α-La/β-Lg dimer. In the SDS-PAGE (Figure 1B), the glycosylated α-La and β-Lg have identical mobilities and cannot be

delineated (*34*). The presence of a dimer band in unheated Cα-La suggests that the rigors of the commercial process (pasteurization and spray drying) caused some aggregation. The Cα-La was used as the α-La source for IEX purification to provide a context in comparing results from the Σα-La and Cα-La preparations. Σα-La (Lane 2) and IEXα-La (Lane 4) demonstrated a similar high degree of purity with faint bands visible in the SDS-PAGE patterns corresponding to β-Lg and dimeric α-La.

Denaturation Profiles of α-La Preparations. Figure 2 shows the DSC denaturation profiles for Σα-La and IEXα-La. The dashed line represents the polynomial baseline fit with the area under the curve representing the calorimetric enthalpy (ΔH) and the peak of the curve representing the denaturation temperature (T_d). The only observation not consistent with previous work was a second peak observed in Σα-La with a T_d of ~85°C that was not present in the IEXα-La. This is not seen when α-La is heated in pH 8.0 Tris (*32*) and was not present on the second heating scan. Only the first peak was used to calculate the denaturation parameters described in Table 2. There was little difference in T_d between all three preparations (~63-64°C). These values are consistent with studies using "microsensitive" DSC that found T_d values of 64.1°C (*32*) and 64.2°C (*35*) using 1°C/min scan rates and similar concentrations. Previous investigations found a wider range of values including ~60°C (*36;37*), 65°C (*16;38*) and 70°C (*39*). This variation arises from the use of widely varying solvent conditions, but more importantly, they use exceedingly higher protein concentrations (up to 200 mg/mL) to compensate for lack of instrumental sensitivity. Also, much higher scan rates were used (2.5-20°C/min) and extrapolated down to 0°C/min.

Table 2 shows the ΔH values obtained for the three preparations. Of the pure preparations, Σα-La (286 kJ/mol) required ~25 kJ/mol more energy to denature than IEXα-La (261 kJ/mol). The Cα-La required the most energy to denature (309 kJ/mol). The differences in ΔH for the purified preparations may represent a difference in their preparation procedures. The Σα-La was freeze dried in the holo-form whereas IEXα-La was freeze dried in the apo-form and Ca^{2+} was added to the hydrated protein. The ΔH values for Σα-La and IEXα-La were consistent with previous determinations using microsensitive DSC: 264 kJ/mol (*32*) and 276 ± 9 kJ/mol (*40*).

The ability of α-La to undergo reversible denaturation transitions through multiple heat/cool cycles makes it unique among the whey proteins (*38;41*). Table 2 shows the similar % reversibility values for Σα-La and Cα-La (~35%) with the slightly lower value obtained for IEX α-La (24%). The DSC automatically held the sample at the programmed terminal temperature (i.e. 95°C) for 10 min before the cooling cycle to allow for system equilibration. These values are in reasonable agreement with the findings of Chaplin and Lyster (*16*) that found 40% reversibility when α-La is heated and held at 95°C for 15 min before rescanning (10°C/min; 1.6 mg/mL). When Σα-La was only heated to 90°C, it was 72% reversible (data not shown), indicating that irreversible denaturation occurs much more rapidly at >90°C. The apo- protein demonstrated an endothermic transition at 38°C with no endothermic transition on the second scan (data not shown).

There are several examples in the literature where α-La displays very high reversibility including 80-90% (62 mg/mL; T_{max} = 110°C at 10°C/min) (*38*), >90% (~90 mg/mL; T_{max} = 95°C at 21.4°C/min) (*41*) and 100% through 4 heating cycles (200 mg/mL; T_{max} = 100°C at 5°C/min) (*39*). It is interesting that increased % reversibility values correlate with higher protein

concentration. Eggers and Valentine (*42*) have demonstrated that the thermal stability of α-La is dramatically enhanced while it is entrapped in a silica matrix (as compared to dilute solution). They found that at 95°C, α-La had not approached complete unfolding and they estimated an increase in T_d of 25 to 32°C based on circular dichroism data (*42*). This type of phenomenon cannot be discounted in explaining the high degrees of renaturation in the very "crowded" systems sometimes utilized to obtain DSC data.

Analysis of Heated Preparations by PAGE. Figure 1A shows the loss of monomer and formation of non-native monomers of higher mobility when α-La preparations were heated and analyzed by Native PAGE. The Cα-La had a greater loss of native-like monomer and formed no non-native monomers (Lane 7), although it was heated for 60 min. The pure preparations (Lanes 3 and 5) formed three bands of higher mobility (two intense bands and one faint band) that corresponded to the non-native monomer bands described in previous studies (*16;17*). Differences in migration on Native PAGE are based on differences in both net charge and hydrodynamic size so, assuming these species did not become more compact, they must possess a higher net negative charge than the native-like monomer. The two studies that observed these species proposed different mechanisms for their formation. Chaplin and Lyster (*16*) proposed that higher mobility is caused by partial deamidation of glutamine and asparagines residues (thus, increasing net negative charge) due to their observation that heating α-La at 100°C evolves ammonia (*16*). Hong and Creamer (*17*) suggested that intramolecular disulfide bond shuffling increases negative charge exposure due to the loss of Ca^{2+} binding ability and that the differences in mobility among non-native species represents a difference in hydrodynamic size. However, they acknowledged the need for "further fruitful study…to resolve these issues" (*17*).

Both Native and SDS PAGE results resolved 5 distinguishable bands of lower mobility (Figure 1A and 1B, lanes 3, 5 and 7) that Chaplin and Lyster (*16*) identified as oligomers by Native PAGE. In SDS PAGE patterns, three of these bands had similar mobility corresponding to SDS-dimeric species (two intense bands and one faint band) as observed by Hong and Creamer (*17*). They implicated differences in disulfide bond specificity that resulted in differences in hydrodynamic size (*17*). In Cα-La (lane 7), the oligomer bands were much less intense and there was only one distinct dimer band.

The other studies did not demonstrate the aggregate smearing observed in these PAGE patterns, however, they used a stacking/resolving gel system that appeared to trap aggregates at its interface. The addition of SDS without any reducing agent did not appear to alter aggregate mobility indicating they were covalently bound as has been demonstrated (*15;16*). The Cα-La preparation had more of a smearing effect and formed aggregates that extended up to the 200 kDa. The purified preparations (heated for 30 min) formed aggregates that extended up near the 116 kDa marker.

Concentration Dependence of Turbidity Development. The data in Figure 3 shows the turbidity of the three α-La preparations (5 to 60 g/L) heated at 95°C for 30 min then cooled to 23 ± 2°C. All of the treatments had equal ionic strength (μ) where the absence of $CaCl_2$ in the apo-treatments was compensated for with NaCl. In the treatments containing no Ca^{2+} (the apo-conformer), there was very little turbidity development (i.e. formation of large aggregates) over the entire concentration range studied. This phenomenon was similar between preparations with turbidity only deviating at ≥ 50 g/L. Holo-α-La developed higher turbidity than apo-α-La at all protein concentrations (Figure 3). To illustrate, at 20 g/L, the Ca^{2+} concentration is only 1.4

mM, yet this causes a 28-fold larger turbidity value than the apo- treatment with the same ionic strength.

The apo-α-La conformer has a much lower transition temperature (T_d ~ 38°C) (*32;43*) and renaturation ability (*39*) than holo-α-La and has been referred to as more heat "labile" (*21*). It has also been found to be more "reactive" in the formation of non-native monomers and dimers (*17*). Also, the "slow reacting" disulfide bonds (C28-C111, C61-C77 and C73-C91) are reduced by DTT ~40X (at 25°C) faster in the apo- conformer than the holo- (*19*). It appears that these cases of reactivity/lability bear no relationship to its ability to form large aggregates (Figure 3), which is the most important consideration for beverage manufactures.

There is more than one explanation to the increased aggregation of holo-α-La relative to apo-α-La. The presence of Ca^{2+} stabilizes the adjacent C61-C77 and C73-C91 disulfide bonds to thermal denaturation (*44*) and only the C61 forms disulfide bonded aggregates when heated at 85°C (*21*). Since denaturation probably leads to Ca^{2+} release (*35*), the Ca^{2+} either interacts favorably with the negative charge density on this lobe or it can bridge negative charges intermolecularly and facilitate hydrophobic interactions. This has been described for whey protein aggregation (*45*).

The Σα-La and IEXα-La preparations produced a significantly higher turbidity than Cα-La at all concentrations except 10 g/L (Figure 3). At concentrations ≥ 20 g/L, Σα-La formed white precipitates that settled out of solution (these were resuspended prior to turbidity measurement). Only at 60 g/L did this occur for IEXα-La. The data for all holo-α-La preparations included one replication using extensively dialyzed preparations. This data was consistent with undialyzed preparations indicating a dialyzable component (like residual salts) was not responsible for the differences in behavior. Potential causes for these differences are discussed in the next section.

The remaining experiments were performed at 10 g/L to attempt to understand the phenomena that lead to aggregate stabilization or precipitation that occured at higher concentration.

Turbidity Evolution and Reversibility at 95°C. Of the studies listed in Table 1, there were no measurements actually made at the temperature to which the protein was heated. For α-La, monitoring the turbidity development at 95°C ($\tau_{95°C}$) proved to be valuable in understanding the pertinent interactions responsible for aggregate formation. Figure 4 shows the $\tau_{95°C}$ development for the three preparations in the same electrostatic conditions (10 mM sodium phosphate, pH 7.0) as the DSC experiments. The highly purified Σ and IEX preparations formed very large aggregates that caused intense scattering as soon as the temperature exceeded T_d (~3 min), and then plateaued throughout the remaining heating period. However, the $\tau_{95°C}$ of Cα-La did not begin its gradual increase until ~15 minutes and its plateau value was far lower than for purified α-La. Apparently, the minor protein constituents present in Cα-La or some other factor diminish rapid turbidity development. The presence of β-Lg in Cα-La would be the first logical explanation. However, when β-Lg was added to IEXα-La at levels mimicking the Cα-La, the $\tau_{95°C}$ trend was identical with a 28% decrease in its plateau turbidity value (Figure 4). There were two bands (not including the β-Lg variants) removed from Cα-La by the IEX chromatography purification process (Figure 1A) that caused it to behave similarly to Σα-La. They corresponded to glycosylated α-La and a dimer of α-La or α-La/β-Lg. Glycosylation increases the net negative charge through a post-translational modification that adds glucose to a solvent exposed loop N45 (*46*). A dimer would also represent a charge alteration due to the loss of Ca^{2+} binding ability (*17*). When these were removed, making the charge state distribution more homogenous, there was a general instability created that resulted in intense turbidity development (Figure 4) and the formation of three separate non-native monomer bands (Figure

1A). Secondary structure analysis on heated α-La reveals the formation of a new α-helix that may represent a charge alteration (*47*). This may occur during the ingredient manufacturing process and provide thermal stability to Cα-La. When the charge altered component was removed by IEX chromatography, rapid turbidity development occurred that lead to precipitation at higher concentrations.

The importance of net charge in the reaction medium can be illustrated by changing the pH. When the sodium phosphate buffer pH was lowered to pH 6.60, there was very little turbidity development (data not shown). This is opposite of what would be expected relative to the pKa of a-La; however, this may be related to the pKa_2 of NaH_2PO_4 (6.86). Thus, α-La aggregated more rapidly when phosphate had a –2 charge (at pH 7.0) than when the charge was –1 (at pH 6.6). This is the first reported evidence of the role divalent phosphate plays in α-La aggregation. Given the prevalence of phosphate buffer as the reaction medium of choice for many aggregation studies (Table 1), and its use in protein beverages, these observations are important considerations for the stabilization of α-La. The pH dependence of $\tau_{95°C}$ development is discussed further in the next section.

Figure 4 shows that the turbidity developed at 95°C in α-La preparations was partially reversible upon cooling. The purified preparations had 15-20% reversibility and the Cα-La was 35% reversible. Although the reversibility for Cα-La was large, it represented a slight decrease in a very low plateau turbidity value. The observed dissociation further implicates hydrophobic interactions, which are favored at high temperatures and disfavored near room temperature (*48*), as the logical explanation to the rapid turbidity development in denatured, purified α-La preparations. The interrelationship of hydrophobicity and electrostatic interactions is further explored in the General Discussion.

Turbidity is not just a measure of aggregate size (i.e. M_w), but shape, isotropy and refractive properties (*49*). Purified preparations heated for 30 min had a 4× higher $\tau_{25°C}$ than Cα-La heated for 1 hour, yet the aggregates of Cα-La had lower mobility when analyzed by PAGE. The turbidity profile of purified preparations indicated the intermolecular association was intense and immediate while that of Cα-La was more gradual. This indicates the aggregates may have had different shapes. Since Cα-La demonstrated the greatest thermal stability, it was used for the remaining aggregation experiments.

Effect of Solvent Environment on Turbidity Development in Cα-La. Figure 5a shows the increase in turbidity development with increasing Na^+ concentration (added as NaCl with constant phosphate concentration). Increasing the ionic strength (μ) from 0.025 (16 mM Na^+) to 0.04 (30 mM Na^+) resulted in a similar $\tau_{95°C}$ trend with a slightly higher value. Further increasing the μ to 0.07 (60 mM Na^+) resulted in a more abrupt $\tau_{95°C}$ increase. Interestingly, this treatment demonstrated a brief plateau in $\tau_{95°C}$ near 15 min before rapidly increasing suggesting its aggregation was controlled by an intermediate. Also, this treatment demonstrated much more variability than the other treatments. This indicates that the aggregate growth process was rather heterogeneous and highly sensitive to slight experimental deviations. Increasing the ionic strength from 0.04 to 0.07 decreased the reversibility from 31% to 16%.

Figure 5b shows the increase in $\tau_{95°C}$ when phosphate concentration was increased from 10 to 40 mM. Doubling the phosphate concentration to 20 mM (μ = 0.045) caused a rapid increase at ~8 min that reached its plateau at 20 min and had 2× the plateau $\tau_{95°C}$ value over 10 mM phosphate. A further increase to 40 mM phosphate (μ = 0.09) caused rapid $\tau_{95°C}$ development that was similar in magnitude to the pure preparations with only 10 mM phosphate. Increasing the ionic strength from 0.045 to 0.09 increased the reversibility from 16% to 34%.

Figure 6 shows the effects of decreasing the pH below 7.0 or adding excess Ca^{2+} (all treatments had equal ionic strength). Decreasing the pH to 6.8 increased the lag time, but caused $\tau_{95°C}$ to develop to a higher terminal value than pH 7.0 (Figure 6). However, when the pH was further lowered to 6.6, there was almost no $\tau_{95°C}$ development. Similar behavior was observed with a higher concentration of total Na^+ (data not shown). When the pH was lowered to pH 6.0, the $\tau_{95°C}$ development was immediate, but it quickly reached a plateau value that was similar to pH 7.0. Decreasing the pH to 6.8 slightly increased its reversibility (44%) whereas the pH 6.0 treatment was not reversible at all (–6%). The $\tau_{95°C}$ results indicate the involvement of two general phenomena that have opposite effects on aggregation of α-La in this pH range. Decreasing the charge on phosphate from –2 to –1 (pKa_2 = 6.86) diminished $\tau_{95°C}$ at pH 6.6 whereas decreasing the protein net charge enhanced it at pH 6.0. Altering the protein surface charge and the extent to which it is screened has two effects on its ability to aggregate: 1) decreased intramolecular unfolding, and 2) a decreased repulsive barrier to aggregation. The behavior at pH 6.0 suggests that low surface charge facilitates immediate aggregation. At pH 6.6, the increased negative surface charge may promote more complete unfolding and the enhanced electrostatic repulsion without the screening of divalent phosphate would prevent turbidity development. Further increasing the pH towards and above the pKa_2 of $H_2PO_4^-$ would cause unfolded α-La to be screened by divalent phosphate, thus, enhancing $\tau_{95°C}$. A more specific interaction between phosphate near a specific hydrophobic clusters is discussed in the General Discussion. The stability to aggregation at pH > 6.5 has been demonstrated in a commercial α-La fraction (1.7% protein w/w) that remained soluble heated at 120°C in skim milk permeate (*26*).

There was a pronounced increase in $\tau_{95°C}$ in the presence of a 2:1 molar ratio of Ca^{2+} to α-La (Figure 6). Although not quite as abrupt as the pure preparations (Figure 4), $\tau_{95°C}$ development was much more rapid than its 1:1 molar ratio counterpart and attained its plateau value around 25 min. The turbidity decreased slightly with cooling (17%). There are multiple roles that excess Ca^{2+} may be playing in this system to enhance interactions and aggregation. When α-La (~3 mg/mL) is heated to 80°C in the presence of excess Ca^{2+}, it retains some surface hydrophobicity that does not exist when heated with a 1:1 molar ratio (*50*). Mechanistically, the denaturation is converted from a simple two-step process ($N \rightarrow U + Ca^{2+}$) to a three-step process that possesses a Ca^{2+} bound intermediate ($N \rightarrow I \rightarrow U + Ca^{2+}$) (*35*). Explained thermodynamically, adding excess Ca^{2+} reduces the highly positive entropy of Ca^{2+} mixing into the bulk solution that exists when a 1:1 molar ratio of Ca^{2+} to α-La is heated and loses its bound Ca^{2+} (*32*). Bovine α-La has a second, weaker Ca^{2+} binding site involving H68 (*51*) that is adjacent to a hydrophobic cluster. A reduction in surface charge caused by this specific effect or a more general intermolecular ionic cross-linking might enhance rapid aggregation through hydrophobic interactions.

Temperature Dependence of Turbidity Development. There is a pronounced decrease in turbidity with decreasing temperature (Figure 7). At 85°C, there was a modest turbidity increase from 6-10 min with a plateau throughout the remaining heating time. At 75°C, there was almost no turbidity development. Galani and Apenten (*52*) evaluated the contribution of hydrophobic interactions relative to disulfide bond formation in the aggregation of β-Lg (in WPI at pH 6.8) from 80-120°C. The rate constant for hydrophobically-driven aggregation is much larger at 95°C than other temperatures (*52*). The irreversible denaturation (i.e. aggregation) of α-La heated in milk demonstrates an Arrhenius temperature dependence with a break at 80°C (*53;54*). These studies demonstrating enhanced aggregation at temperatures >80°C are consistent with the

data seen in Figure 7 and helps to explain the findings in Table 1, where most of the studies found no aggregation when heating at ≤ 80°C.

General Discussion. DSC has been used as a primary tool for measuring protein denaturation and, often, these results are extended to describe the "thermostability" of a protein. Ruegg et al. (*38*) stated that, "thermostability…should be interpreted in terms of renaturation and not of high temperatures of denaturation." This parameter is valid in describing one facet of protein thermostability, because, in order to renature, a protein must remain monomeric; however it does not evaluate the ability of the irreversibly denatured protein fraction to aggregate and insolubilize. In this study, Cα-La and Σα-La had similar abilities to renature, but pronounced differences in turbidity development that lead to protein precipitation of Σα-La at ≥ 20 g/L. Furthermore, the most stable protein to aggregation, apo-α-La, had the lowest T_d and did not renature at all when heated and cooled under identical conditions. Any definition of protein thermostability for application to protein beverages should encompass its ability to retain solubility when heated. There was one denaturation parameter that was consistent with turbidity data. The increasing ΔH values for the three preparations (Table 2) corresponded to a decreasing extent of aggregation (Figure 4) in the same solvent conditions. Since protein aggregation is exothermic (*55*) this indicated that intermolecular interactions may have still been present at 2.5 g/L.

Scheme 1 describes the mechanism for the heat-induced aggregation of α-La in 10 mM sodium phosphate (Figures 1 and 4). Steps 1 – 3 were proposed by Hong and Creamer (*17*) where steps 1 and 3 were based on the mechanism of Chaplin and Lyster (*16*). The mechanism was expanded with three additional steps I and 4 to represent the observations at 95°C (Figure 4) and step 5 to represent the aggregate dissociation with cooling. When α-La is heated above T_d, it

releases Ca^{2+} and forms the molten globule (MG) state that does not rapidly undergo irreversible denaturation reactions at < 85°C and renatures when cooled (step 1). When held at ≥ 85°C, pure α-La irreversibly denatures through intramolecular disulfide bond shuffling (Step 2) forming three dominant non-native monomer species (Figure 1A) (*17*). In step 3, these species would have a free thiol group available to catalyze thiol/disulfide interchange and form the three dominant SDS-dimeric bands (Figure 1B) and larger oligomers. In Cα-La, irreversible denaturation proceeds directly through intermolecular thiol/disulfide interchange (Step 3). Step 4 represents the formation of larger aggregate smears (Figure 1A and 1B) that partially dissociate with cooling (step 5; Figures 4-6).

α-Lactalbumin is the best characterized molten globule protein and an abundance of literature exists describing the forces responsible for its folding/unfolding in various conditions (for a review, see (*56;57*). The role divalent phosphate played at high temperature in facilitating hydrophobic interactions in MG-monomers (Figure 4) suggests the involvement of the basic lobe of the molecule. This lobe possesses the two most reactive thiol groups (C111 and C120) at 85°C (*21*) and a hydrophobic cluster that is exposed upon Ca^{2+} release (*58;59*). This cluster contains the I27, M30, F31 and H32 residues from α-helix 2 and Q117 and W118 residues on the C-terminus (*6*). Its folding/unfolding behavior is intricately involved with the C28-C111 disulfide bond (*60-62*) and it is much more stable to unfolding than the other hydrophobic cluster (*61*). Moreover, this cluster is shielded by a positive charge from L114 and probably one other residue (*63*). When L114 is replaced with an uncharged residue, the thermal stability to denaturation (i.e. T_d) increases by ~11°C (*22*) indicating positive charge density in this region destabilizes the cluster. The H32 residue may be the charge pair of the L114 as it has a pKa' of ~6.6 (*64*) and is adjacent to L114 in the native fold (*6*). This suggests that the ionization

behavior of a specific residue like H32 might also be involved in the pH dependent phenomena observed in this study. At pH 7.0, the –2 charged phosphate may stabilize this positively region and cause the exposed hydrophobic cluster to remain intact and facilitate rapid monomer association. This specific monomer-monomer contact may play a role in producing the specific intra- and intermolecular disulfide bonded patterns seen in Figure 1. When α-La is heated to high temperatures at pH 6.6 (where phosphate has a –1 charge and some of the H32 is positively charged), the two positive charges might enhance reactivity of the neighboring C28-C111 disulfide bond (*23*), which would partially disorganize the native hydrophobic cluster and inhibit $\tau_{95°C}$ development (Figure 6). This is consistent with observations that C28 is unreactive and possibly "retracted inward" when heated at 85°C (pH 6.0) despite extensive molecular unfolding and high reactivity from C111, its partner in the native molecule (*21*). This lack of C28 reactivity further indicates this hydrophobic cluster remains intact and provides some protection to this part of the molecule, but more research is needed to verify this.

Conclusion. The aggregation of α-La through hydrophobic interactions was enhanced by the presence of calcium, a high degree of purity, excess screening by phosphate (-2 charge) or calcium (+2 charge) and by heating at 95°C (relative to lower temperatures). The aggregates formed at 95°C partially dissociated with cooling. The formation of distinct disulfide-shuffled monomers and disulfide-bonded dimers may be related to specific hydrophobic interactions.

Table 1. Summary of treatment conditions where the ability of α-lactalbumin to aggregate at high temperature was evaluated (listed chronologically)

Study	Heat Treatment	Protein ($g \cdot L^{-1}$)	Solvent	α-La Source	β-Lg Present[a]	Aggregation Observed	Method Used
Chaplin & Lyster, 1986	100ºC for 10 min.	14	0.10 M sodium phosphate buffer, pH 7	Affinity chromatography purified	No	Yes	PAGE
Calvo et al., 1993	90°C for 24 min.	1.5	"Milk ultrafiltrate" composition not given	Sigma	NA[b]	No	SEC
Dagleigh et al., 1997	75°C for 10 min.	100	0.02 M phosphate buffer, pH 7	Ion exchange chromatography purified	No	No	SEC
Gezimati et al., 1997	80°C for 15 min.	80	"WPC-like" composition not given	Sigma	NA	No	PAGE
Schokker et al., 2000	80°C for "pro-longed heating"	10	0.02 M imidazole, 0.05 M NaCl, 0.003 M NaN_3, pH 7	Sigma (calcium saturated)	NA	No	SEC
Havea et al., 2000	75°C for 6 min.	50	WPC permeate (0.4 M K^+ & Na^+; 0.035 M Ca^{2+}, pH 6.8	Sigma (calcium saturated)	NA	Yes	PAGE
Bertrand-Harb et al., 2002	65°C, 85°C & 95°C for 30 min	10	0.2 M sodium phosphate buffer, pH 7.5	Ion exchange chromatography purified	Yes	Yes (≥ 85°C)	PAGE
Hong & Creamer, 2002	70-95°C (every 5°C) for 10 min	2.4	0.015 M phosphate buffer, pH 6.7 or 7.4	Size exclusion chromatography purified	No	Yes (≥80°C)	PAGE

a) Is β-Lg visually present in the electrophoretograms or chromatograms of the α-La preparations?
b) Not applicable (NA); Sigma α-La has no β-Lg contamination

Table 2.
Denaturation parameters of commercial, ion exchange chromatography purified and Sigma holo-α-lactalbumin preparations as measured by microsensitive differential scanning calorimetry

Preparation	T_d (°C)	ΔH ($kJ \cdot mol^{-1}$)	% Reversibility
Commercial	63.1 ± 0.5	309 ± 2.0	34 ± 3.6
IEX	64.0 ± 1.4	261 ± 1.2	24 ± 1.7
Sigma	63.9 ± 0.3	286 ± 5.3	37 ± 0.6

LIST OF FIGURES

Figure 1. Native PAGE (A) and SDS PAGE (B) of the three preparations of native (even numbered lanes) and heated (odd numbered) α-La (all containing 40 μg of total protein). Sigma and IEXα-La were heated for 30 min and Cα-La was heated for 1 hr at 95°C. Lane 1 is the M_w marker; Lanes 2 and 3 are Sigma α-La; Lanes 4 and 5 are α-La isolated by ion-exchange chromatography; Lanes 6 and 7 are commercial α-La; Lane 8 is the whey protein standard (30 μg total protein). The heated solutions were obtained at the end of the heating periods from Figure 4.

Figure 2. Two representative curves from the analysis of Sigma (top curve) and IEX (bottom curve) α-La by microsensitive differential scanning calorimetry. Solutions (~2.5 mg/mL) were heated at 1°C/min in a 10 mM sodium phosphate buffer (pH 7) and the baseline was fit with a polynomial equation.

Figure 3. Concentration dependence of turbidity development after heating at 95°C for 30 min for apo-α-lactalbumin (open symbols) and three holo-α-lactalbumin preparations (closed symbols): Sigma (●), IEX (▲,Δ) and commercial (■,□). Solutions contained 10 mM sodium phosphate buffered at pH 7 and 60 mM total Na (excess Na^+ was added as NaCl). Holo-α-La preparations contained a 1:1 molar ratio of Ca^{2+} to α-La. The 30 and 50 g/L treatments were not evaluated for Sigma α-La for cost considerations.

Figure 4. Turbidity development at 95°C (open symbols) and its reversibility when cooled (closed symbols) of commercial (○,●), Sigma (□, ■) and IEX (Δ,▲) holo-α-La and IEXα-La with 1 g/L β-Lg (♦). Solutions contained 10 g/L total protein and 10 mM sodium phosphate buffered at pH 7.

Figure 5. Effect of increasing monovalent (NaCl, A) and divalent (phosphate, B) salts on the turbidity development at 95°C (open symbols) and its reversibility when cooled (closed symbols) of commercial holo-α-lactalbumin (10 $g \cdot L^{-1}$ total protein) at pH 7.0. The commercial α-La curve from Figure 4 was represented in both panels (○) to provide a visual reference. In panel A, NaCl was added to obtain a total Na concentration of 30 (■,□) and 60 mM (▲,Δ). In panel B, sodium phosphate (buffered at pH 7.0) was added to obtain a 20 mM (■,□) and 40 mM (▲,Δ) phosphate concentration. The intrinsic Na concentration contributed from the phosphate was 32 (20 mM) and 64 mM (40 mM).

Figure 6. Effect of lowering the pH to 6.80 (♦,◊), 6.60 (+) and 6.00 (▲,Δ) and adding a 2:1 molar ratio of Ca^{2+} to α-La at pH 7.0 (■,□) on the turbidity development at 95°C (closed symbols) and its reversibility when cooled (open symbols) for commercial holo-α-lactalbumin (10 $g \cdot L^{-1}$ total protein). Solutions contained 10 mM sodium phosphate buffered at the given pH and ~30 mM total Na^{+}. NaCl was used to compensate for the ionic strength (0.04 M) changes that occur with lowering the pH (on phosphate) or adding excess $CaCl_2$. The 30 mM Na curve from Figure 5A was represented (○) to provide a visual reference.

Figure 7. Temperature dependence of turbidity development for commercial α-La heated at 75°C (▲) and 85°C (■). Solutions contained 10 $g \cdot L^{-1}$ total protein and 40 mM sodium phosphate buffered at pH 7 (contributing 64 mM total Na). The 40 mM sodium phosphate curve from Figure 5B was represented (○) to provide a visual reference.

Scheme I. Mechanism for the heat-induced aggregation for both a pure and commercial source of holo-α-lactalbumin.

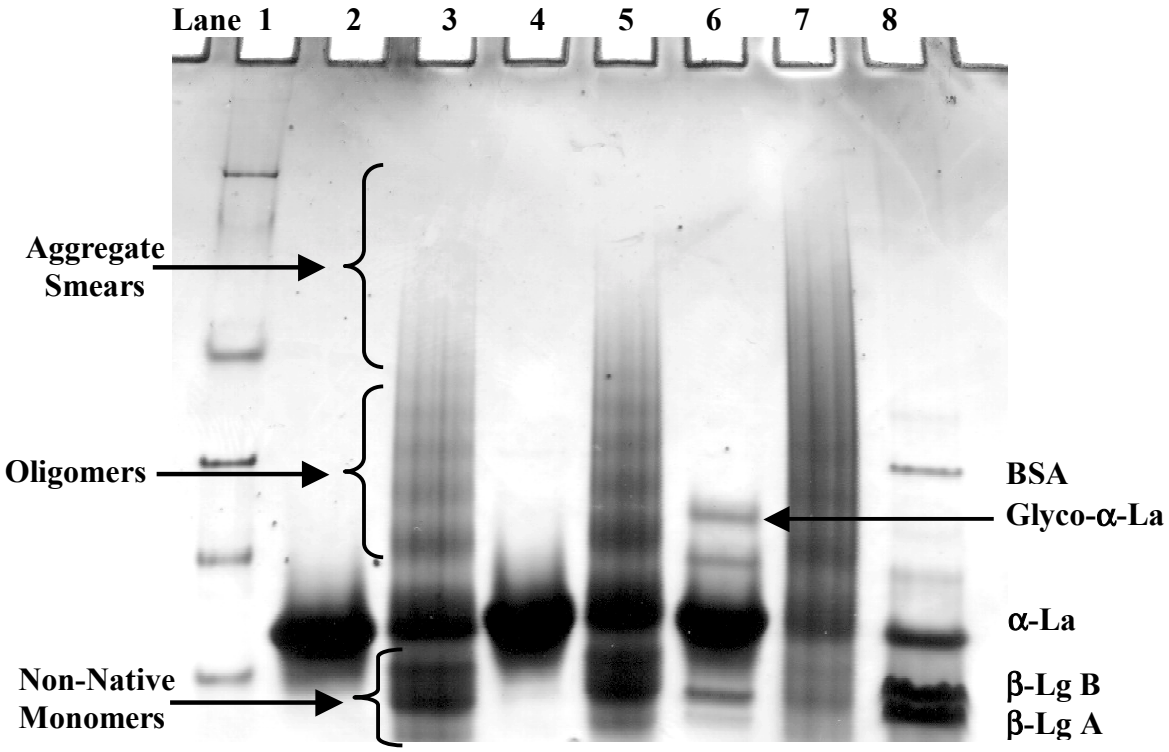
Lane 1
2
3
4
5
6
7
8
Aggregate Smears
Oligomers
Non-Native Monomers
BSA
Glyco-α-La
α-La
β-Lg B
β-Lg A

Figure 1A

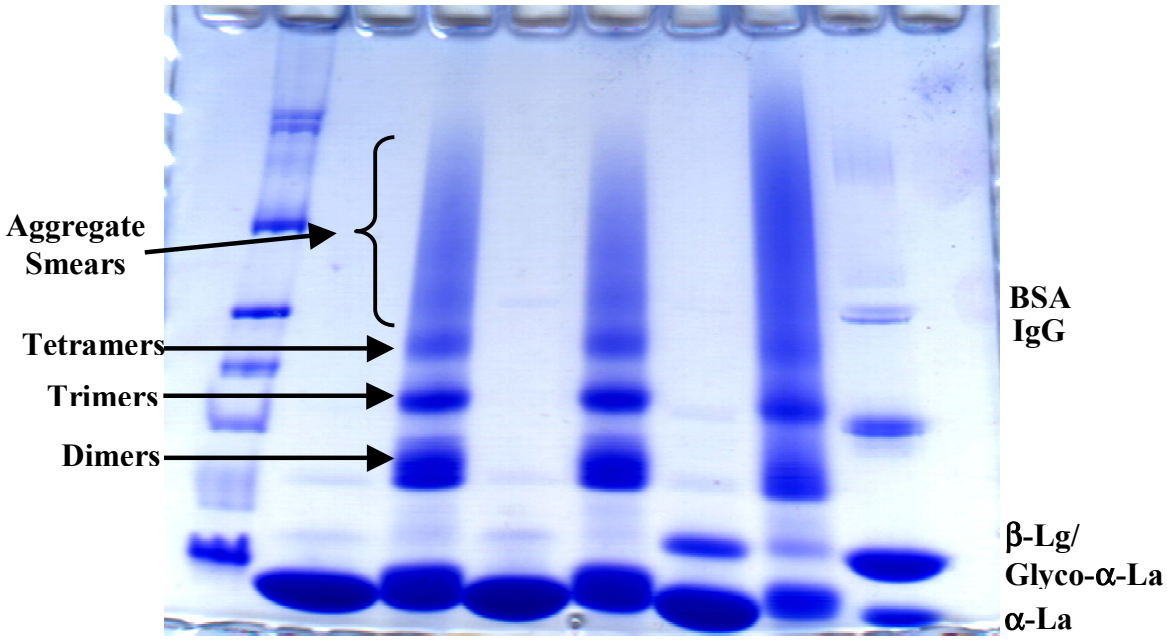
Aggregate
Smears
Tetramers
Trimers
Dimers
BSA
IgG
β-Lg/
Glyco-α-La
α-La

Figure 1B

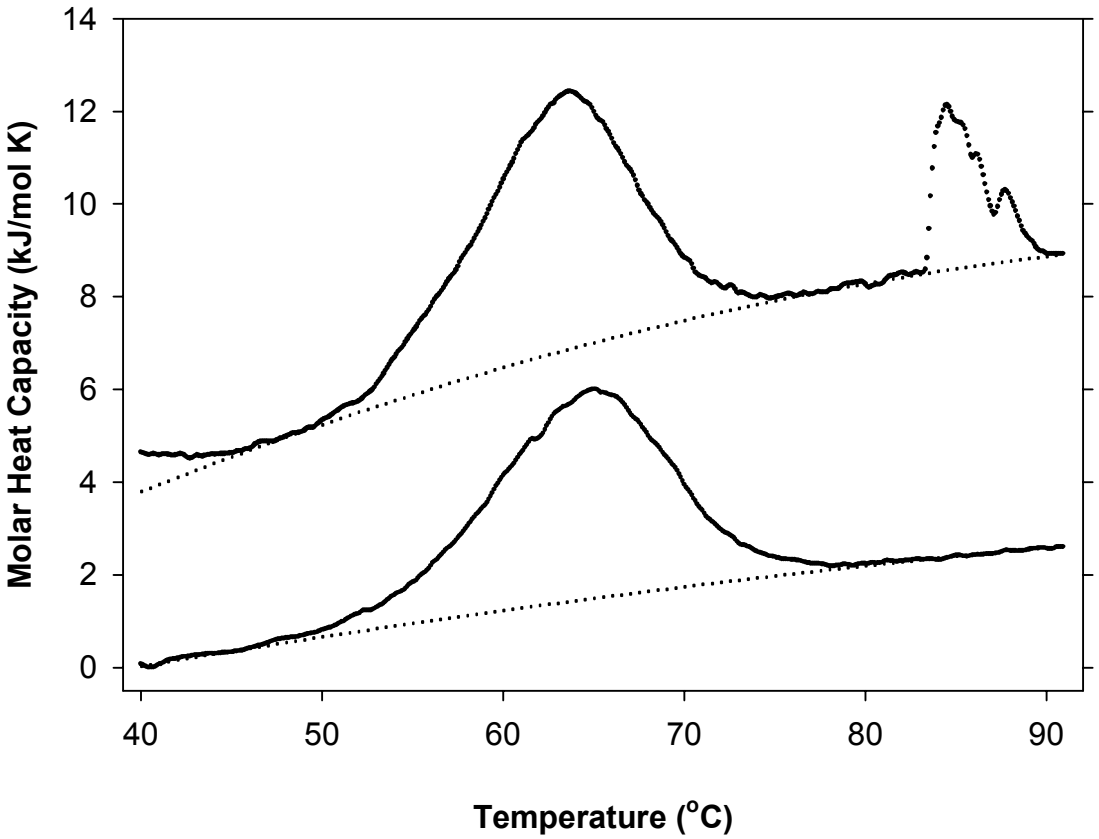
Molar Heat Capacity (kJ/mol K)
14
12
10
8
6
4
2
0
40
50
60
70
80
90
Temperature (°C)

Figure 2

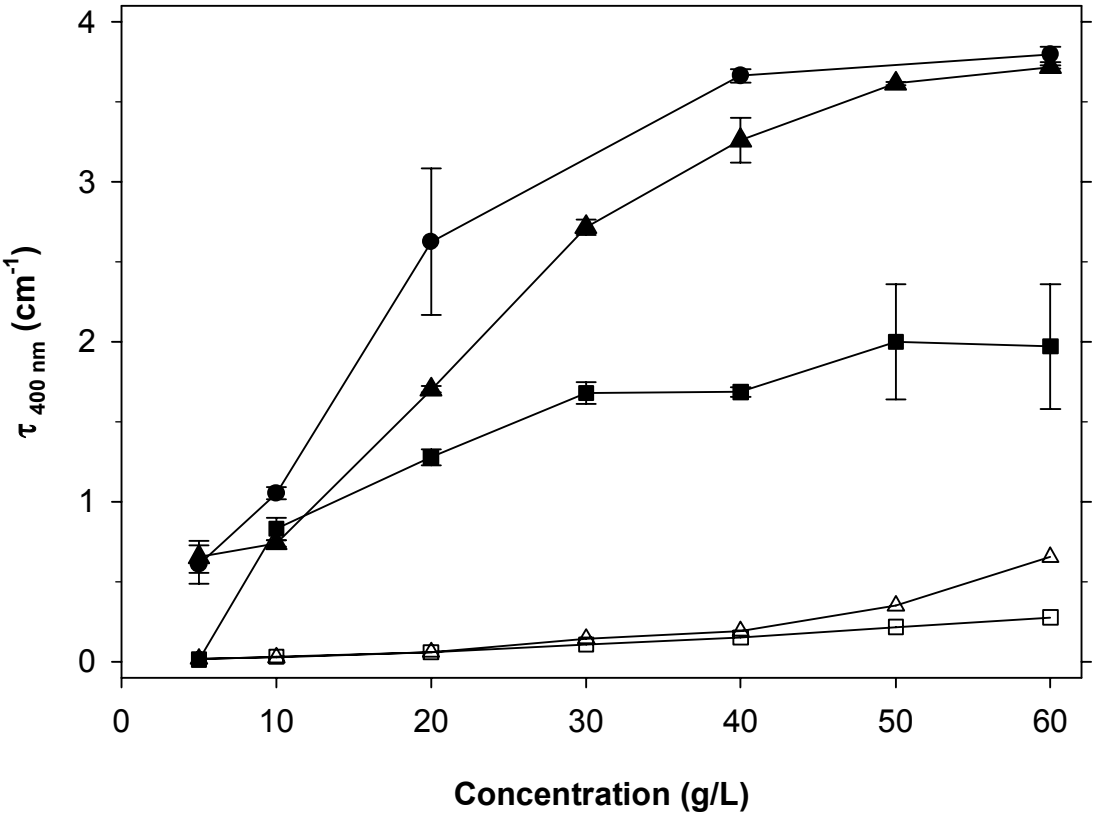

Figure 3

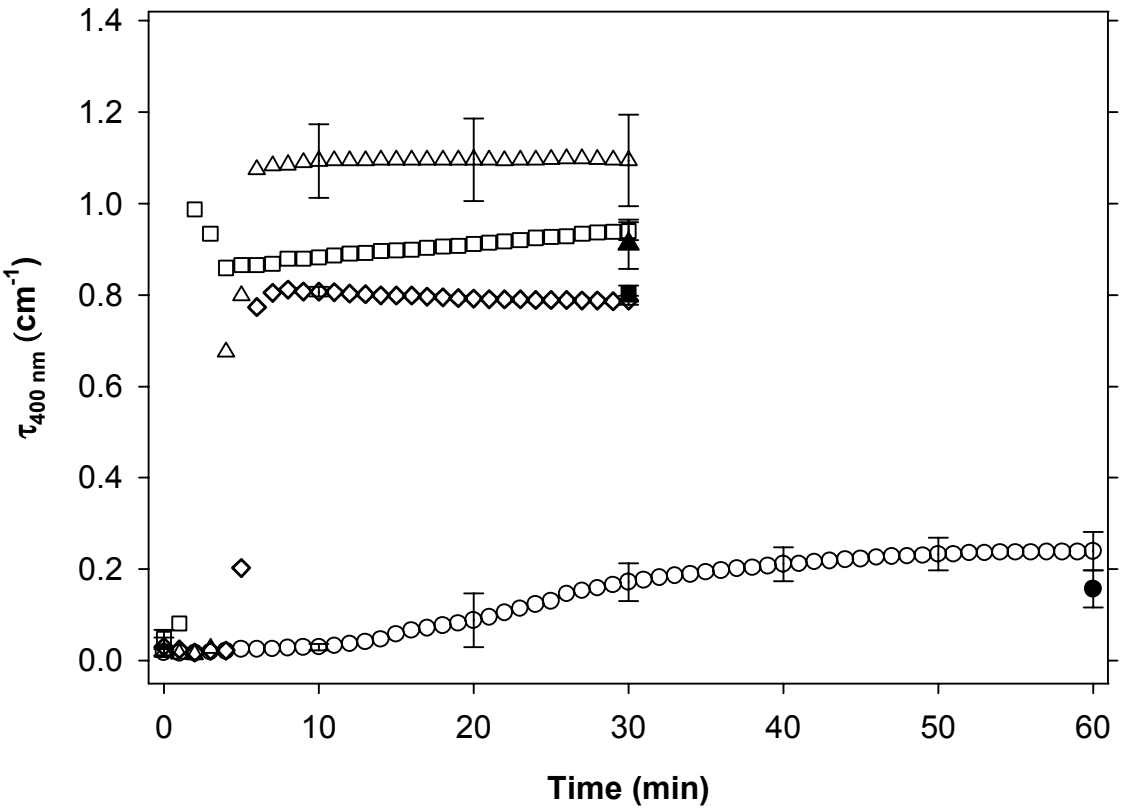

Figure 4

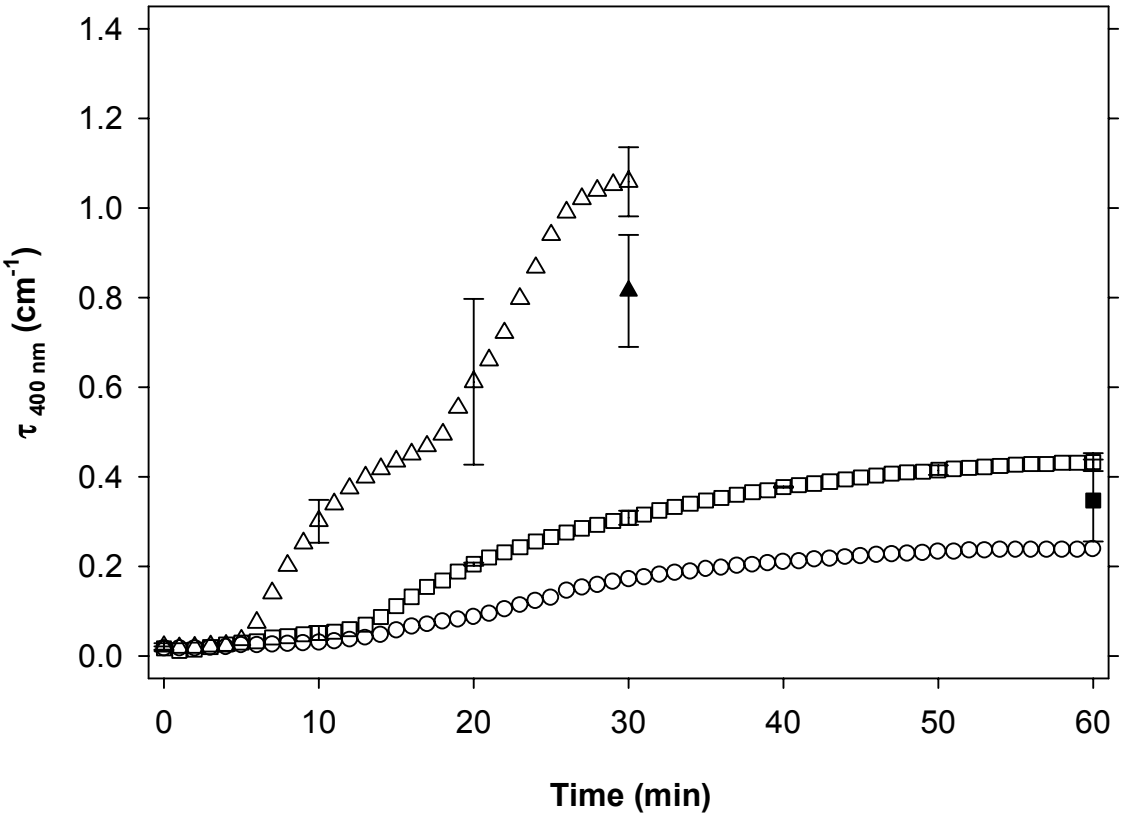

Figure 5A

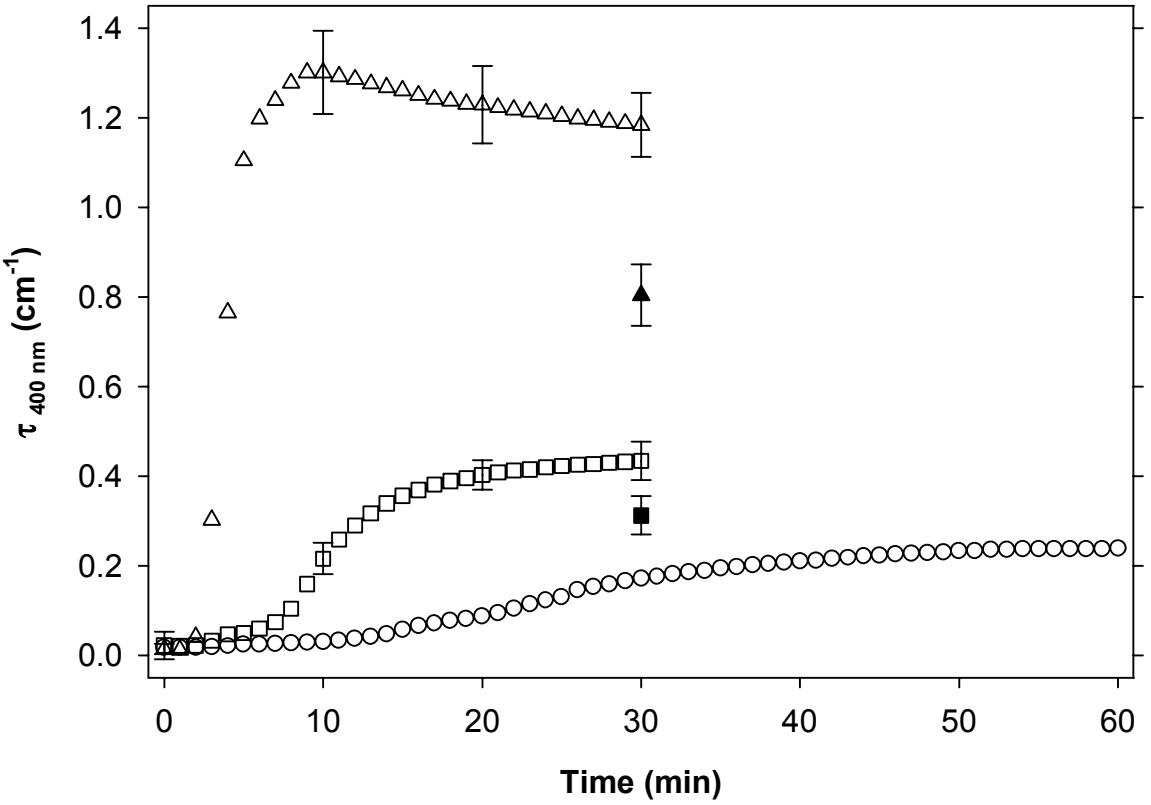

Figure 5B

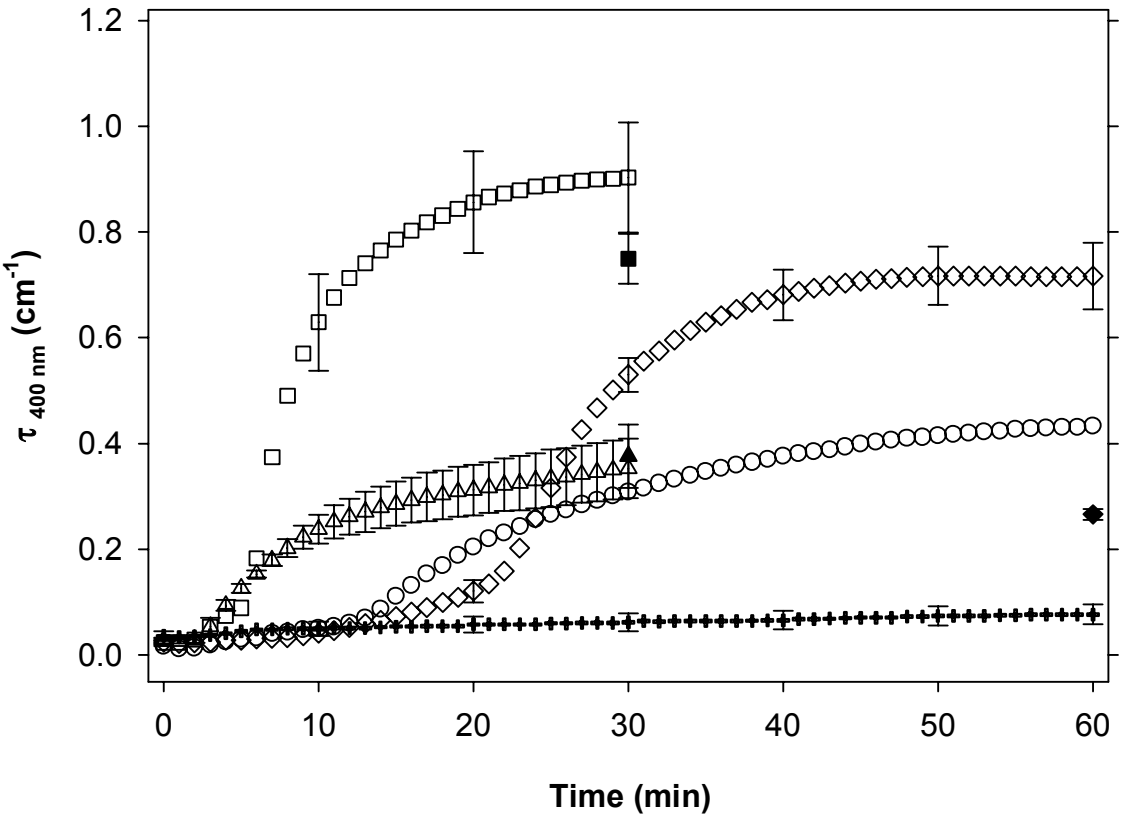

Figure 6

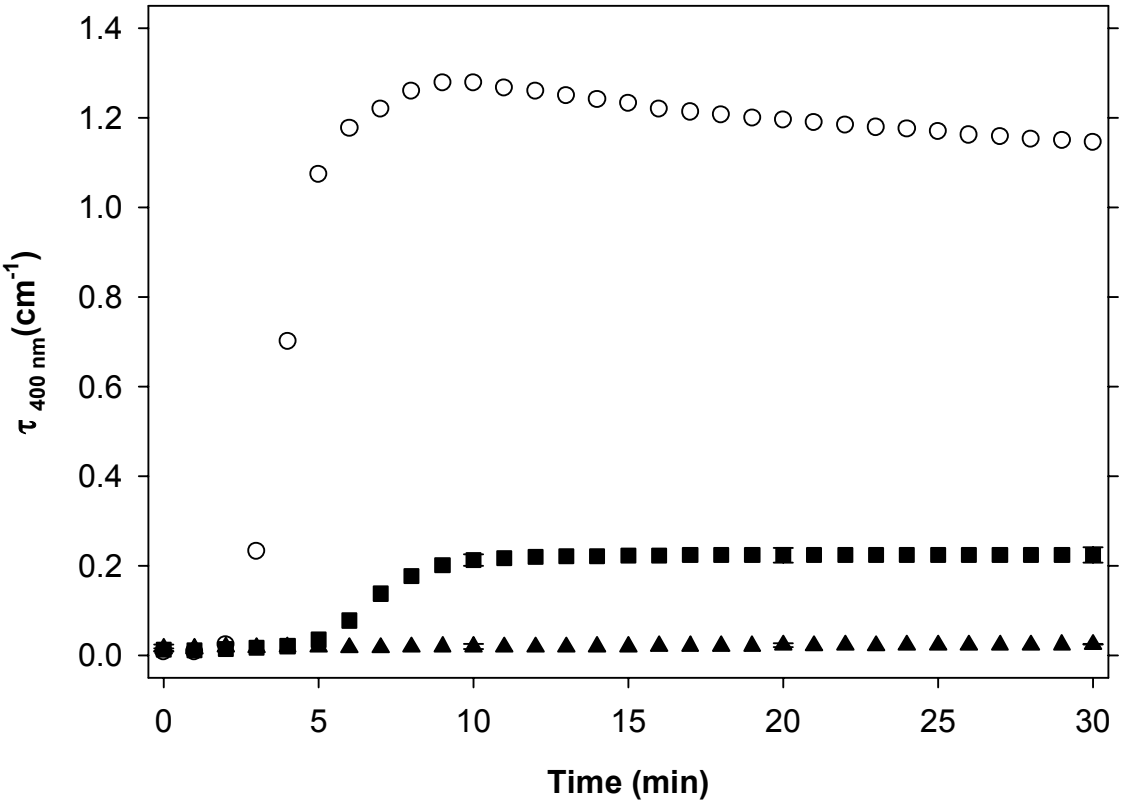

Figure 7

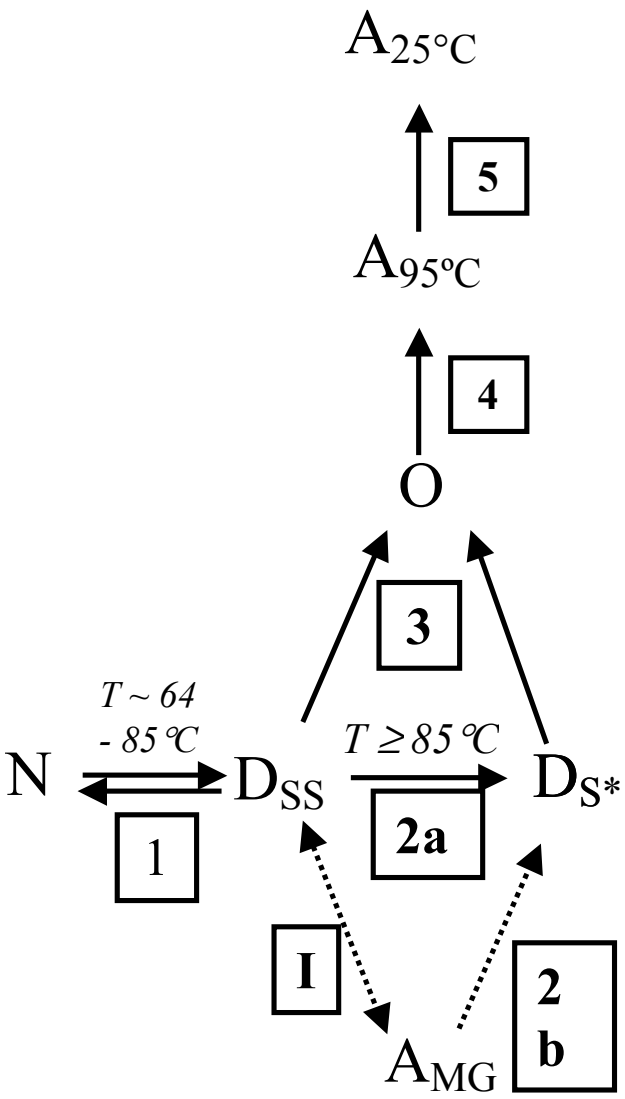

Scheme I

LITERATURE CITED

(1) Smithers, G. W.; Ballard, F. J.; Copeland, A. D.; De Silva, K. J.; Dionysius, D. A.; Francis, G. L.; Goddard, C.; Grieve, P. A.; McIntosh, G. H.; Mitchell, I. R.; Pearce, R. J.; Regester, G. O. New opportunities from the isolation and utilization of whey proteins. *J. Dairy Sci.* 1996, *79*, 1454-1459.

(2) Heine, W. E.; Klein, P. D.; Reeds, P. J. The importance of α-lactalbumin in infant nutrition. *J. Nutr.* 1991, *121*, 277-283.

(3) Foegeding, E. A.; Davis, J. P.; Doucet, D.; McGuffey, M. K. Advances in modifying and understanding whey protein functionality. *Trends Food Sci. Tech.* 2002, *13*, 151-159.

(4) Swaisgood, H. E. Developments in dairy chemistry. In *Developments in dairy chemistry*; P. F. Fox, Ed.; Elsevier Applied Science Publishers: London, 1982; pp 132-147.

(5) Acharya, K. R.; Stuart, D. I.; Walker, N. P.; Lewis, M.; Phillips, D. C. Refined structure of babbon alpha-lactalbumin at 1.7a resolution. Comparison with c-type lysozyme. *J. Mol. Bio.* 1989, *208*, 99-127.

(6) Chrysina, E. D.; Brew, K.; Acharya, K. R. Crystal structure of apo- and holo-bovine α-lactalbumin at 2.2-a resolution reveal an effect of calcium on inter-lobe interactions. *J. Biol. Chem.* 2000, *275*, 37021-37029.

(7) Vanhooren, A.; Vanhee, K.; Noyelle, K.; Majer, Z.; Joniau, M.; Hanssens, I. Structural basis for difference in heat capacity increments for ca^{2+} binding to two α-lactalbumins. *Biophys. J.* 2002, *82*, 407-417.

(8) Li, J.; Zhang, S.; Wang, C. C. Only the reduced conformer of α-lactalbumin is inducible to aggregation by protein aggregates. *J. Biochem. (Tokyo)* 2001, *129*, 821-826.

(9) Lindner, R. A.; Treweek, T. M.; Carver, J. A. The molecular chaperone α-crystallin is in kinetic competition with aggregation to stabilize a monomeric molten- globule form of α-lactalbumin. *Biochem. J.* 2001, *354*, 79-87.

(10) Goers, J.; Permyakov, S. E.; Permyakov, E. A.; Uversky, V. N.; Fink, A. L. Conformational prerequisites for α-lactalbumin fibrillation. *Biochemistry* 2002, *41*, 12546-12551.

(11) Li, H.; Errington, A. D.; Foegeding, E. A. Isostrength comparison of large-strain (fracture) rheological properties of egg white and whey protein gels. *J. Food Sci.* 1999, *64*, 893-898.

(12) Dalgleish, D. G.; Senaratne, V.; Francois, S. Interactions between α-lactalbumin and β-lactoglobulin in the early stages of heat denaturation. *J. Agr. Food Chem.* 1997, *45*, 3459-3464.

(13) Schnack, U.; Klostermeyer, H. Thermal decomposition of a-lactalbumin. 1. Destruction of cysteine residues. *Milchwissenschaft* 1980, *35*, 206-208.

(14) Doi, H.; Tokuyama, T.; Kuo, F.-H.; Ibuki, F.; Kanamori, M. Heat-induced complex formation between κ-casein and α-lactalbumin. *Agr. Biol. Chem. (Tokyo)* 1983, *47*, 2817-2824.

(15) Bertrand-Harb, C.; Baday, A.; Dalgalarrondo, M.; Chobert, J. M.; Haertle, T. Thermal modifications of structure and co-denaturation of α-lactalbumin and β-lactoglobulin induce changes of solubility and susceptibility to proteases. *Nahr.-Food* 2002, *46*, 283-289.

(16) Chaplin, L. C.; Lyster, R. L. J. Irreversible heat denaturation of bovine α-lactalbumin. *J. Dairy Sci.* 1986, *53*, 249-258.

(17) Hong, Y. H.; Creamer, L. K. Changed protein structures of bovine β-lactoglobulin b and α-lactalbumin as a consequence of heat treatment. *Int. Dairy J.* 2002, *12*, 345-359.

(18) Vanaman, T. C.; Brew, K.; Hill, R. L. Disulfide bonds of bovine alpha-lactalbumin. *J. Biol. Chem.* 1970, *245*, 4583-&.
(19) Kuwajima, K.; Ikeguchi, M.; Sugawara, T.; Hiroka, Y.; Sugai, S. Kinetics of disulfide bond reduction in α-lactalbumin by dithiothreitol and molecular basis of superreactivity of the cys6-cys120 disulfide bond. *Biochem.* 1990, *29*, 8240-8249.
(20) Gohda, S.; Shimizu, A.; Ikeguchi, M.; Sugai, S. The superreactive disulifide bonds in α-lactalbumin and lysozyme. *J. Protein Chem.* 1995, *14*, 731-737.
(21) Livney, Y. D.; Verespej, E.; Dalgleish, D. G. Steric effects governing disulfide bond interchange during thermal aggregation in solutions of beta-lactoglobulin b and alpha-lactalbumin. *J. Agr. Food Chem.* 2003, *51*, 8098-8106.
(22) Greene, L. H.; Grobler, J. A.; Malinovskii, V. A.; Tian, J.; Acharya, K. R.; Brew, K. Stability, activity and flexibility in alpha-lactalbumin. *Protein Eng.* 1999, *12*, 581-587.
(23) Bulaj, G.; Kortemme, T.; Goldenberg, D. P. Ionization-reactivity relationships for cysteine thiols in polypeptides. *Biochem.* 1998, *37*, 8965-8972.
(24) Gezimati, J.; Creamer, L. K.; Singh, H. Heat-induced interactions and gelation of mixtures of β-lactoglobulin and α-lactalbumin. *J. Agr. Food Chem.* 1997, *45*, 1130-1136.
(25) de la Fuente, M. A.; Singh, H.; Hemar, Y. Recent advances in the characterisation of heat-induced aggregates and intermediates of whey proteins. *Trends Food Sci. Tech.* 2002, *13*, 262-274.
(26) Rattray, W.; Jelen, P. Thermal stability of skim milk whey protein solution blends. *Food Res. Int.* 1997, *30*, 327-334.
(27) Calvo, S.; Leaver, J.; Banks, J. M. Influence of other whey proteins on the heat-induced aggregation of α-lactalbumin. *Int. Dairy J.* 1993, *3*, 719-727.
(28) Schokker, E. P.; Singh, H.; Creamer, L. K. Heat-induced aggregation of β-lactoglobulin a and b with α-lactalbumin. *Int. Dairy J.* 2000, *10*, 843-853.
(29) Havea, P.; Singh, H.; Creamer, L. K. Formation of new protein structures in heated mixtures of bsa and α-lactalbumin. *J. Agr. Food Chem.* 2000, *48*, 1548-1556.
(30) Karman, A. H.; van Boekel, M. A. J. S. Evaluation of the kjeldahl factor for conversion of the nitrogen content of milk and milk products to protein content. *Neth. Milk Dairy J.* 1986, *40*, 315-336.
(31) Okazaki, A.; Ikura, T.; Nikaido, D.; Kuwajima, K. The chaperonin groel does not recognize apo-α-lactalbumin in the molten globule state. *Nat. Struct. Biol.* 1994, *1*, 439-446.
(32) Hendrix, T.; Griko, Y. V.; Privalov, P. L. A calorimetric study of the influence of calcium on the stability of bovine α-lactalbumin. *Biophys. Chem.* 2000, *84*, 27-34.
(33) Schorsch, C.; Jones, M. G.; Norton, I. T. Thermodynamic incompatibility and microstructure of milk protein/locust bean gum/sucrose systems. *Food Hydrocolloid.* 1999, *13*, 89-99.
(34) Kinghorn, N. M.; Norris, C. S.; Paterson, G. R.; Otter, D. E. Comparison of capillary electrophoresis with traditional methods to analyse bovine whey proteins. *J. Chromatogr. A* 1995, *700*, 111-123.
(35) Vanderheeren, G.; Hanssens, I.; Meijberg, W.; VanAerschot, A. Thermodynamic characterization of the partially unfolded state of ca^{2+}-loaded bovine alpha-lactalbumin: Evidence that partial unfolding can precede ca2+ release. *Biochem.* 1996, *35*, 16753-16759.
(36) Bernal, V.; Jelen, P. Effect of calcium binding on themral denaturation of bovine α-lactalbumin. *J. Dairy Sci.* 1984, *67*, 2452-2454.

(37) Relkin, P.; Eynard, L.; Launay, B. Thermodynamic parameters of b-lactoglobulin and α-lactalbumin. A dsc study of denaturation by heating. *Thermochim. Acta* 1992, *204*, 111-121.
(38) Ruegg, M.; Moor, U.; Blanc, B. A calorimetric study of the thermal denaturation of whey proteins in simulated milk ultrafiltrate. *J. Dairy Res.* 1977, *44*, 509-520.
(39) Boye, J. I.; Alli, I.; Ismail, A. A. Use of differential scanning calorimetry and infrared spectroscopy in the study of thermal and structural stability of α-lactalbumin. *J. Agr. Food Chem.* 1997, *45*, 1116-1125.
(40) Pfeil, W. Thermodynamics of α-lactalbumin unfolding. *Biophys. Chem.* 1981, *13*, 181-186.
(41) de Wit, J. N.; Klarenbeek, G. Effects of various heat treatments on structure and solubility of whey proteins. *J. Dairy Sci.* 1984, *67*, 2701-2710.
(42) Eggers, D. K.; Valentine, J. S. Molecular confinement influences protein structure and enhances thermal protein stability. *Protein Sci.* 2001, *10*, 250-261.
(43) Relkin, P.; Launay, B.; Eynard, L. Effect of sodium and calcium addition on thermal denaturation of apo-α-lactalbumin: A differential scanning calorimetric study. *J. Dairy Sci.* 1993, *76*, 36-47.
(44) Chang, J.-Y.; Li, L. The structure of denatured a-lactalbumin elucidated by the technique of disulfide scrambling. *J. Biol. Chem.* 2001, *276*, 9705-9712.
(45) Xiong, Y. L. Influence of ph and ionic environment on thermal aggregation of whey proteins. *J. Agr. Food Chem.* 1992, *40*, 380-384.
(46) Slangen, C. J.; Visser, S. Use of mass spectrometry to rapidly characterize the heterogeneity of bovine alpha-lactalbumin. *J. Agr. Food Chem.* 1999, *47*, 4549-4556.
(47) Fang, Y.; Dalgleish, D. G. The conformation of α-lactalbumin as a function of ph, heat treatment and absorption at hydrophobic surfaces studied by ftir. *Food Hydrocolloid.* 1998, *12*, 121-126.
(48) Dill, K. A. Dominant forces in protein folding. 1990, *29*, 7133-7155.
(49) Cancellieri, A.; Frontali, C.; Gratton, E. Dispersion effect on turbidimetric size measurement. *Biopolymers* 1974, *13*, 735-743.
(50) Vanderheeren, G.; Hanssens, I. Thermal unfolding of bovine α-lactalbumin. *J. Biol. Chem.* 1994, *269*, 7090-7094.
(51) Aramini, J. M.; Drakenberg, T.; Hiraoki, T.; Ke, Y.; Nitta, K.; Vogel, H. J. Ca-43 nmr-studies of calcium-binding lysozymes and alpha- lactalbumins. *Biochem.* 1992, *31*, 6761-6768.
(52) Galani, D.; Apenten, R. K. O. Heat-induced denaturation and aggregation of β-lactoglobulin: Kinetics of formation of hydrophobic and disulphide-linked aggregates. *Int. J. Food Sci. Tech.* 1999, *34*, 467-476.
(53) Dannenberg, F.; Kessler, H.-G. Reaction kinetics of the denaturation of whey proteins in milk. *J. Food Sci.* 1988, *53*, 258-263.
(54) Anema, S. G.; McKenna, A. B. Reaction kinetics of thermal denaturation of whey proteins in heated reconstituted whole milk. *J. Agr. Food Chem.* 1996, *44*, 422-428.
(55) Marshall, W. E.; Zarins, Z. M. Exothermic transitions of glycinin determined by differential scanning calorimetry. *J. Agr. Food Chem.* 1989, *37*, 869-873.
(56) Kuwajima, K. The molten globule state of α-lactalbumin. *FASEB J.* 1996, *10*, 102-109.
(57) Permyakov, E. A.; Berliner, L. J. A-lactalbumin: Structure and function. *FEBS Lett.* 2000, *473*, 269-274.
(58) Lindahl, L.; Vogel, H. J. Metal-ion dependent hydrophobic interaction chromatography of α-lactalbumins. *Anal. Biochem.* 1984, *140*, 394-402.

(59) Desmet, J.; Vancauwelaert, F. Calorimetric experiments of mn-$^{2+}$-binding to α-lactalbumin. *Biochim. Biophys. Acta* 1988, *957*, 411-419.
(60) Peng, Z. Y.; Wu, L. C.; Kim, P. S. Local structural preferences in the alpha-lactalbumin molten globule. *Biochem.* 1995, *34*, 3248-3252.
(61) Wu, L. C.; Kim, P. S. A specific hydrophobic core in the α-lactalbumin molten globule. *J. Mol. Biol.* 1998, *280*, 175-182.
(62) Song, J. X.; Bai, P.; Luo, L.; Peng, Z. Y. Contribution of individual residues to formation of the native-like tertiary topology in the alpha-lactalbumin molten globule. *J. Mol. Biol.* 1998, *280*, 167-174.
(63) Richardson, R.; Brew, K. Lactose synthase. An investigation of the interaction site of alpha- lactalbumin for galactosyltransferase by differential kinetic labeling. *J. Biol. Chem.* 1980, *255*, 3377-3385.
(64) Bradbury, J. H.; Norton, R. S. Proton-magnetic-resonance spectroscopic study of histidine residues of bovine alpha-lactalbumin. *Eur. J. Biochem.* 1975, *53*, 387-396.

Aggregation of α-Lactalbumin Isolate in a Neutral pH Nutritional Beverage Mineral Salt Environment

Matthew K. McGuffey[a], Donald E. Otter[b], John H. van Zanten[c] and E. Allen Foegeding[a,*]

To Be Submitted to the International Dairy Journal

*Corresponding Author

[a]Department of Food Science
Southeast Dairy Foods Research Center
North Carolina State University
236 Schaub Hall
Raleigh, NC 27695-7624

[b]Fonterra Co-operative Group Limited
Private Bag 11 029, Dairy Farm Road
Palmerston North, New Zealand

[c]Chemical Engineering Department
North Carolina State University
Raleigh, NC 27695-7905

Keywords: β-lactoglobulin; thiol; disulfide; hydrophobic; solubility; light scattering; turbidity

Running Title: Aggregation of α-Lactalbumin

Abstract

The aggregation behavior of commercial α-La was investigated at neutral pH and 95°C in a complex mineral salt environment. The objective was to understand the effect of α-La lot variation, relative β-lactoglobulin concentration and excess calcium on the aggregate size development as measured by light scattering and turbidity development. The effect of protein net charge was evaluated with a solubility method and the role of thiol groups was evaluated by reaction with DTNB. The lot of holo-α-La possessing a higher intrinsic β-Lg concentration had higher solubility at pH ≤ 6.80, evolved more reactive thiol groups, had a 25% faster first order rate constant, dissociated only slightly with cooling and formed spherical aggregates with a much higher molecular weight. Aggregates intrinsic to the protein powder may play a role in aggregate growth and shape. Adding increasing quantities of β-Lg generally decreased solubility due to enhanced hydrophobic interactions. The highest β-Lg concentrations investigated demonstrated a net thiol oxidation and, subsequently, had a diminished ability to aggregate through hydrophobic interactions. Adding excess calcium caused a dramatic loss of solubility at pH 7.0 and required an increase in pH to 7.5 or increased phosphate concentration to regain solubility.

1. Introduction

The total category sales of nutritional beverages in 2002 was $2.3 billion and growing (Hollingsworth, 2003). These health-conscious markets are becoming increasingly aware of the role protein plays in nutrition and will desire higher quality protein sources as they become available. Whey protein isolates (WPI) possess a high nutritional quality, but when they are heat denatured, they rapidly aggregate and form precipitates or gels because of their high relative concentration of β-lactoglobulin (β-Lg) (Foegeding, Davis, Doucet & McGuffey, 2002). This property has limited their level of utilization in neutral pH nutritional beverages, however, ingredient suppliers now can produce high purity preparations (>90%) of the second most abundant whey protein, α-lactalbumin. α-Lactalbumin (α-La) is the most heat stable whey protein to aggregation (Dalgleish, Senaratne & Francois, 1997) and, therefore, has the most potential for utilization in a heat stable beverage.

α-La is a globular, calcium metalloprotein with a isoelectric point of 4.6, a molecular weight (M_w) of 14,200 Da, no free thiol groups and 4 disulfide bonds (Brew & Grobler, 1992; Swaisgood, 1982). It has the lowest denaturation temperature (~62°C) of the whey proteins, but this process is >90% reversible as measured by calorimetry (Chaplin & Lyster, 1986; de Wit & Klarenbeek, 1984). The reversibility is dramatically reduced when α-La is held at temperatures >90°C (Chaplin et al., 1986; McGuffey, Epting, Kelly & Foegeding, Submitted) or heated in the presence of thiol groups (Boye & Alli, 2000). However, Fang and Dalgleish (1998) found that some α-helical structure is irreversibly altered upon heating at neutral pH and that "restructuring" of secondary structure is distinct from disorganization of hydrophobic clusters (i.e. irreversible denaturation). McGuffey et al. (Submitted) found very little aggregation in

commercial α-La preparation, however, when a purified α-La fraction (by ion-exchange chromatography, there was intense aggregation that was similar to Sigma α-La.

When heated to high temperatures (≥ 90°C) at neutral pH (≥ 7.0), pure α-La forms aggregates linked by intermolecular disulfide bonds (Bertrand-Harb, Baday, Dalgalarrondo, Chobert & Haertle, 2002; Chaplin et al., 1986). Electrophoresis reveals multiple distinct monomer and dimer bands that are products of intramolecular disulfide bond shuffling that leads to the formation of specific dimer bands (Hong & Creamer, 2002; McGuffey et al., Submitted). These specific bands may be the result of hydrophobic interactions in the positively-charged, C-terminal region due to their enhancement by –2 charged phosphate (pH 7) (McGuffey et al., Submitted). Hydrophobic interactions can be diminished by removing calcium, lowering the pH to 6.6 (-1 charged phosphate) or reducing the temperature to ≤ 85°C (McGuffey et al., Submitted).

The disulfide bonds of α-La enhance the aggregation and gelation of both β-Lg (Schokker, Singh & Creamer, 2000) and BSA (Havea, Singh & Creamer, 2000) where the rate of α-La disappearance can be correlated to the quantity of free thiol groups (Calvo, Leaver & Banks, 1993) . Also, increasing the proportion of β-Lg in α-La preparations progressively increases the M_w of aggregates (Dalgleish et al., 1997). Essentially, β-Lg disappears more rapidly in the early stages of heating and α-La dominates the later stages (Dalgleish et al., 1997; Schokker et al., 2000). The free thiol of β-Lg (C121) probably initiates thiol-disulfide interchange with the C6-C120 disulfide bond of α-La, but subsequently, α-La is a good "chain carrier" for this reaction and extensively unfolds with significant participation by C111 and C61 thiols (Livney, Verespej & Dalgleish, 2003). Hydrophobic interactions seem to be especially important in the early stages of heating, are more significant for α-La than β-Lg (Schokker et al.,

2000) and have been suggested to facilitate thiol-disulfide interchange (Gezimati, Creamer & Singh, 1997; Hong et al., 2002).

There have been several studies that evaluated the effects of excess calcium and phosphate on whey protein solubility (de Rham & Chanton, 1984) and turbidity development (de Wit et al., 1984; Xiong, 1992). Essentially, increasing the Ca^{2+} concentration from ~2-4 mM (an excess molar ratio of Ca^{2+} to α-La) requires a corresponding increase in pH from ~6 to ~7 to retain protein solubility (de Rham et al., 1984; de Wit et al., 1984) or minimize turbidity (de Wit et al., 1984). However, citrate and phosphate form soluble complexes with Ca^{2+} in approximately 1:1 molar ratios, which enhances solubility (de Rham et al., 1984). The citrate complex is pH independent (pH 6 – 7) whereas phosphate is only effective at pH values above 6.8 (de Rham et al., 1984). This is likely due to the pKa_2 value (~ 6.86) of $H_2PO_4^-$.

The objective of this study was to quantitatively describe the aggregation of commercial α-La preparations at 95°C with a protein concentration (50 $g \cdot L^{-1}$) and electrostatic environment that simulates a nutritional beverage. This study was divided into three sections. First, the aggregation of α-La with a 1:1 molar ratio of Ca^{2+} to α-La was characterized with a focus on understanding differences between two lots of α-La and characterization of aggregate size and growth by size exclusion chromatography coupled to multiangle laser light scattering (SEC-MALLS). In the second section, the effect of increasing quantities of β-Lg on the aggregation of α-La was evaluated. In the final section, the solubility effect of increasing Ca^{2+} beyond excess molar ratios and its interaction with phosphate was investigated. The specific contributions of disulfide bond formation, net charge and hydrophobicity to the mechanisms of aggregation and insolubilization are described.

2. Materials and methods

2.1 Materials

Two lots of α-La were a gift from Davisco Foods International (Le Seur, MN) and contained 87.3% (lot A) and 91.7% (lot B) protein on a wet basis (N × 6.14; (Karman & van Boekel, 1986) based on micro-Kheldahl nitrogen analysis. All salts and chemicals used for preparing protein solutions were USP grade. HPLC grade chemicals were used for the chromatography eluent. Electrophoresis grade chemicals were utilized for the native PAGE experiments.

2.2 Protein powder characterization

The constituent protein content was determined by reverse phase HPLC according to the method of Elgar, Norris, Ayers, Pritchard, Otter & Palmano (2000). The α-La was approximately 7% glycosylated for both lots. The mineral composition was determined by inductively-coupled plasma, atomic emission spectroscopy. Certain cations that have a high affinity for α-La (i.e. Ca^{2+}, Mn^{2+}, Zn^{2+}, Na^{+}) (Kronman, 1989) and are present in high concentrations in WPI (i.e. Ca^{2+}, Na^{+} and K^{+}) (Morr & Foegeding, 1990) were quantified. Lot A and B had 430 and 505 ppm of Ca^{2+}, respectively, which represents ~20% saturation of the molecule. Lot A and B had 6500 and 4300 ppm of Na^{+}, respectively, which was the highest concentration of any ion. K^{+} and Mg^{2+} were were both present at <100 ppm and the concentrations of Zn^{2+} and Mn^{2+} were found to be <1 ppm.

2.3. Protein solution preparation

Protein powder was hydrated with deionized H_2O (>17 MΩ) to ~11% $w \cdot v^{-1}$ and allowed to stir for 2 h at room temperature before degassing for 30 min. All solutions were filtered through a 0.7 μm (prefilter)/0.20 μm PVDF syringe filter to remove dust and insoluble matter.

For all experiments, the following solution preparation protocol was followed: ~11% protein solutions were diluted with ca. 90% of the total water needed to make ~50 $g \cdot L^{-1}$ solutions (not including volume from salt solutions). The order of salt solution addition was: 0.2 M $CaCl_2$, 0.2 M sodium and potassium phosphate buffer (a blend of monobasic and dibasic solutions to yield pH 7.0) and monovalent salts (2M KCl and NaCl). The pH of this solution was then adjusted to 7.00 ± 0.02 using 0.25 or 0.5 N HCl, then the balance of water was added. This protocol was used to formulate a simulated, nutritional-beverage environment to contain 30 mM each of K^+ and Na^+, 10 mM phosphate and a 1:1 molar ratio of Ca^{2+}:α-La. This composition was utilized for all experiments. The intrinsic mineral composition of each lot was accounted for in all formulations.

An effective extinction coefficient was calculated using the protein content of the powder and determined to be ε_{280} = 1.90 and 1.92 $L \cdot g^{-1} \cdot cm^{-1}$ for lots A and B, respectively. This value was utilized to determine protein concentration for all solutions. It represents a weight-average of holo-α-La (ε_{280} = 2.01 $L \cdot g^{-1} \cdot cm^{-1}$) (Swaisgood, 1982), apo-α-La (ε_{280} = 1.95 $L \cdot g^{-1} \cdot cm^{-1}$) (Okazaki, Ikura, Nikaido & Kuwajima, 1994), β-Lg (ε_{280} = 0.966 $L \cdot g^{-1} \cdot cm^{-1}$) (Bell & McKenzie, 1967) and bovine serum albumin (BSA; ε_{280} = 0.667 $L \cdot g^{-1} \cdot cm^{-1}$) (Peters, 1985). All experiments were carried out using a protein concentration of 50 $g \cdot L^{-1}$, which constitutes a ~3.2 mM α-La concentration (M_w of 14,200 Da).

2.4. Protein solubility

The pH-dependence (6.0-7.5) of α-La solubility was evaluated using a modified method of Jegouic, Grinberg, Gingant and Haertle (1996). Protein solutions were formulated as above, heated at 95°C for 1 h in a water bath then immediately ice quenched to room temperature. The

heated solutions were spun at 30,000 *x g* for 30 min at 20°C using a Sorvall RC-5B centrifuge (DuPont Instruments, Wilmington, DE). The solubility was determined from a ratio of the absorbance of the supernatant relative to the unheated protein from 270-290 nm (at 2 nm intervals) to average out spectral shifts. The absorbance of the supernatant was corrected for the scattering caused from large aggregates by an extrapolation method from higher wavelengths described previously (Winder & Gent, 1971). The % solubility was calculated as:

$$\%\,Sol. = \frac{(Corrected\ Abs.Sntnt)_{\lambda}}{(Native\ Abs)_{\lambda}} \cdot 100 \qquad (1)$$

and is presented as the average value from the 10 wavelengths (λ). Each value represents the average of at least triplicate measurements.

2.5. Size exclusion chromatography with multiangle laser light scattering

Samples of α-La heated for early times (t = 1.9 – 15 min) were analyzed by SEC-MALLS in a high performance chromatography system. The samples were fractionated with two size exclusion columns connected in series (BioSep-S2000 and S4000; Phenomenex, Torrance, CA). The manufactures' exclusion range for these columns was 1-300 kDa and 15-2,000 kDa, respectively. The columns were eluted with 20 mM Tris-HCl, 0.1M NaCl, 0.02% NaN_3 pH 7.0 buffer (0.02 μm membrane filtered) that was continuously degassed and pumped at a flow rate of 0.9 mL/min with a Waters 2690 Separations Module (Waters Corporation, Franklin, MA). Heated samples were diluted to 2.5 $g \cdot L^{-1}$ with elution buffer and syringe filtered (0.2 μm PVDF) and 50 μL was injected onto the column.

The angular dependence of excess scattering was determined using a DAWN DSP (Wyatt Corporation, Santa Barbara, CA) equipped with a linearly polarized Ne-He laser (5 mW; λ_o = 632.8 nm) and a K5 flow cell with 15 available angles. Only 12 angles yielded an acceptable

signal to noise ratio making the range of scattering vectors $0.0097 < q < 0.0257$ nm^{-1}, where $q = (4\pi n_s/\lambda)\cdot\sin(\theta/2)$ and n_s is the solvent refractive index. The 90° detector was calibrated using filtered, HPLC grade toluene and the remaining detectors were normalized with BSA monomer (Sigma, St. Louis, MO). The concentration of each eluting slice was detected using a Waters 996 photodiode array detector set to 280 nm (Waters Corporation, Franklin, MA) and an Optilab DSP interferometric refractometer (Wyatt Corporation, Santa Barbara, CA). The data was collected and processed with the Astra for Windows, version 4.73.04.

The weight-averaged molar mass (M_w) and the z-averaged radius of gyration (R_g) were calculated for each eluting slice (set at 0.10 seconds) using a first order Zimm fit with the second virial coefficient set to zero and a specific refractive increment (dn/dc) for α-La of 0.188 mL·g^{-1}. The concentration of each eluting slice was calculated using the refractometer detector.

2.6. Turbidity development

The time-dependent optical density development was monitored at 400 nm in a Shimadzu 160U spectrophotometer equipped with a jacketed cuvette holder attached to a recirculating water bath (RWB). Initially, the circulating water temperature was set to 100°C to improve heat transfer and reduce the sample temperature lag. As the temperature approached 95°C (~5 min), the RWB temperature was reduced to maintain a 95°C sample temperature. The sample temperature was monitored with a thermocouple every 2-3 min during these early stages of heating and every 10 min after it stabilized. The temperature accuracy was ± 0.5°C. At the end of the heating period, the protein solutions were rapidly cooled in water and the OD was remeasured to assess the reversibility of aggregate formation. The optical density (OD) values from the spectrophotometer were converted to turbidity (τ) values by the relationship ($\tau = 2.303$

× OD/l) where *l* is the path length (Schorsch, Jones & Norton, 1999). The reversibility was calculated as: $(\tau_{95°C} - \tau_{25°C})/\tau_{95°C} \cdot 100$.

2.7. Reactive thiol quantitation

The concentration of reactive thiol groups was determined by reaction with DTNB (Ellman, 1959) based on the method of Pierce Biotechnology (Rockford, IL). All heated solutions were analyzed in a 0.1M sodium phosphate buffer (pH 8.0) containing 1 mM EDTA. This buffer was used to prepare the 8M urea solutions (for analysis of unheated solutions) and the DTNB (~4 $g \cdot L^{-1}$). For all experiments, heated samples were analyzed within 1 h of heating by appropriately diluting with buffer and DTNB solutions to obtain a ~2:1 DTNB to α-La molar ratio. The $Abs_{412\ nm}$ was measured for the samples ~30 min after DTNB addition and the reactive thiol concentration was calculated using an extinction coefficient of 14,150 $M^{-1} \cdot cm^{-1}$ for DTNB. The spectrophotometer was zeroed with an appropriately diluted DTNB solution (without protein) and blanked with heated protein solutions (without DTNB) to account for aggregate scattering effects. Values represent the average of triplicate measurements.

3. Results and Discussion

3.1. Simulating nutritional beverage conditions

In the first two sections of this study, experiments were carried out with 30 mM each of Na^+ and K^+, 10 mM phosphate, 50 $g \cdot L^{-1}$ α-La (3.2 mM) and a 1:1 molar ratio of Ca^{2+}:α-La. The relatively low concentrations of Ca^{2+} and phosphate were utilized to obtain a basic understanding of the aggregation process before exploring higher concentrations in the third section. Aside from the solubility experiments, the solution pH was adjusted to 7.00.

A temperature of 95°C was chosen to maximize the thermal exposure and approach industrial thermal processing conditions (i.e. 121.1°C for 3 min), while remaining practical from a laboratory perspective. This temperature has been utilized in several recent studies involving α-La aggregation (Bertrand-Harb et al., 2002; Hong et al., 2002).

3.2. Composition of commercial α-La

Table 1 summarizes the protein composition of the two α-La lots and the commercial β-Lg lot evaluated in this study. Figure 1 presents the native PAGE results for the two α-La lots to corroborate the HPLC protein quantitation. Increasing protein loads were utilized to demonstrate the presence of minor protein components and preformed aggregates. Both protein lots used in this study possess a relatively high purity of α-La. Lot A possesses ~75% more β-Lg and ~60% more BSA than Lot B, which suggests Lot A may demonstrate enhanced aggregation properties. The only discrepancy between the HPLC data and the Native PAGE was the BSA band. In lot A, it was very pronounced even with only a 20 μg load (Lane 2), but it was still only faintly present in Lot B when overloaded to 160 μg (Lane 9). This indicates the HPLC results may have overestimated BSA content. The β-Lg lot had no BSA contamination and minor contamination by α-La and IgG.

Besides quantitation of the native protein composition, it is also important to determine the degree of aggregation in the unheated sample. There were three observations that indicated lot A had a higher concentration of preformed aggregates than lot B. First, during 0.2 μm filtration of the 11% solutions, lot A demonstrated higher backpressure and would clog the filter after ~30 mL. Lot B had almost no backpressure and would not even clog when >100 mL was filtered. Second, when the native gel was overloaded (Figure 1, lanes 8 & 9) with 160 μg of

protein, there was a faint smearing of protein with very low mobility present in lot A that was not present in the lot B. Finally, during the turbidity development experiment the lot A turbidity values at t = 0 were double those of lot B.

3.3. Protein solubility

The pH dependence of α-La solubility was measured for both lots from pH 6.0-7.5 after heating samples for 1 h at 95°C (Figure 2). At pH ≤ 6.50, the solubility of both lots was less than 20% and both lots progressively increased with increasing pH to 6.80. Interestingly, lot A had higher solubility than Lot B from pH 6.50 to 6.80 where it reached ~98% before decreasing to ~69% at pH 6.85. This indicates multiple phenomena may be playing a role in the solubility of this lot. Lot B had a sharp jump in solubility from 31 to 84% when the pH was increased from 6.80 to 6.85 and it was higher than lot A at pH 6.85 and 6.90. At pH ≥ 7, the solubility was >93% and equal for both lots. For this reason, the remaining experiments were performed at pH 7 to exclude the effect of solubility on the interpretation of aggregation results.

The spectrophotometric method was highly reproducible for most of the treatments except pH 6.75 and 6.80 of Lot A. These samples were opaque and possessed large background scattering values indicating the presence of large, soluble aggregates. At pH 6.80, these aggregates were not sedimentable. A combustible total nitrogen method was used to verify this and these results were averaged into the reported values.

The temperature dependence of α-La solubility (10 $g \cdot L^{-1}$) has been measured (Bertrand-Harb et al., 2002) and found to be equally high when heating at 65, 85 and 95°C for 30 min due to their use of pH 7.5. de Rham and Chanton (1984) demonstrated a similar trend in pH dependence of whey protein solubility to Figure 2 where 100% solubility was reached around pH 7.1. Rattray and Jelen (1997) measured the heat coagulation time (HCT) of α-La (1.7% w/w

protein) at pH values from 6.7 down to 6.45, which represents the visual detection of large aggregate/floc formation. For solutions heated at 140°C, there is a sharp drop in the HCT from pH 6.7 (20 min) to 6.6 (~12 min) and at pH 6.5, it coagulates within 1 min. When the temperature is lowered to 120°C, pH 6.45 solutions are stable for ~23 min (Rattray et al., 1997).

Increasing the pH above the pI has multiple effects on protein structure that would explain the general trend of increasing solubility. First, the net negative protein surface charge increases slightly from –4 to –6 (approximately) when the pH is increased from pH 6 to 7 (Robbins, Andreott, Holmes & Kronman, 1967). This would result in increased intermolecular electrostatic repulsion that would prevent close approach required for hydrophobic interactions and thiol-disulfide interchange. The intramolecular repulsion would drive more complete unfolding with the major restriction being the 4 disulfide bonds that cause α-La to retain its compact structure even under denaturing conditions (Dolgikh et al., 1985). As the pH approaches the thiol pKa (~8.0-8.5 in proteins (Creighton, 1993), the thiol/disulfide reactions would increase in rate. Disulfide bond reduction is critical to molecular unfolding that would disrupt the native hydrophobic clusters and diminish their role in the development of large, insoluble protein aggregates.

The 45% increase in lot B solubility by increasing pH from 6.80 to 6.85 is difficult to explain using the gradual change in ionization behavior of the native molecule (as described above). A minor increase in pH in this range has been shown to dramatically increase the thermostability of whey proteins (McSweeney, Mulvihill & O'Callaghan, 2004) and commercial α-La (Rattray et al., 1997). This enhanced stability might represent increased chelation of calcium by phosphate at this pH (de Rham et al., 1984) or the ionization of a specific residue that is critical to maintaining protein solubility. Histidine is the only amino acid that typically has a

pKa in this range and a His residue has been implicated in the rapid aggregation of α-La at ambient temperatures when bound to metal ions (Permyakov, Morozova, Kalinichenko & Derezhkov, 1988; Veprintsev, Permyakov, Kalinichenko & Berliner, 1996).

The lower solubility of lot A (at pH 6.85 and 6.90) may be a result of its more extensive reactive thiol evolution (see next section), resulting in the formation of larger aggregates that become less soluble as the net charge is reduced. The enhanced solubility of lot A observed at pH 6.75 and 6.80 appears counterintuitive. However, McGuffey et al. (Submitted) found dramatic turbidity development of commercial α-La at pH 7.0 diminished at pH 6.6. They implicated –2 charged phosphate (pKa_2 ~ 6.86) may screen the positive charge density on the C-terminus at pH 7.0 and enhances hydrophobic interactions and that –1 charged phosphate does not have this same effect (McGuffey et al., Submitted). This phenomenon coupled with the increased thiol evolution may partially disorganize hydrophobic clusters and enhance solubility at pH 6.80. More research in this pH region should be undertaken to clarify these mechanisms due to their complexity and the utilization of this pH region for many nutritional beverages.

3.4. Evolution of reactive thiol groups

The difference in pH dependence of solubility may be related to the evolution of reactive thiol groups so this was measured for both lots when heated at 95°C for various times and cooled to ~23°C (Figure 3). Both lots evolved a significant quantity of reactive thiol groups throughout the first 15 min of heating. After ~40 min, lot B had reached a plateau whereas lot A still gradually increased. At all times (including t = 0), the value for lot A was ~3× lot B. At t = 60 min, the values for both lots were ~5-6 X the quantity measured at t = 0. The calculated vs. measured thiol content of the t = 0 sample for lot A and B was 144 μM vs. 146 μM and 83 μM

vs. 48 μM, respectively. It is not clear why the lot B thiol values were not corroborated, but the calculated value (based on Table 1) may have been overestimated.

Doi et al. (1983) demonstrated a similar trend in reactive thiol concentration with α-La heated at 90°C. The concentration linearly increased and peaked at 60 min where it reached a plateau through 150 min. There is no indication that they measured the reactive thiol content of the unheated samples, but based on their extrapolation to 0 time, there is an approximately 5-6 fold increase in the thiol concentration up to their plateau value (Doi et al., 1983).

The increase and plateau values for reactive thiol concentration represent the net effect of three reactions:

$$R\text{—}S\text{-}S\text{—}R \rightarrow 2\ R\text{-}S^- \quad (1)$$

$$R\text{-}S^- + R\text{—}S_1\text{-}S_2\text{—}R \rightarrow R\text{—}S\text{-}S_1\text{—}R + R\text{-}S_2^- \quad (2)$$

$$R\text{-}S^- + R\text{-}S^- \rightarrow R\text{—}S\text{-}S\text{—}R \quad (3)$$

Reaction 1 represents the breaking of disulfide bond (i.e. reduction), which creates two mols of reactive thiol groups per mol disulfide bond. Reaction 2 represents thiol/disulfide interchange, which has no net effect on reactive thiol concentration. Reaction 3 represents thiol/thiol termination reactions (i.e. oxidation), which consume 2 mols of reactive thiol groups.

Preliminary experiments found no difference between the reactive thiol concentration of the heated samples analyzed in 8M urea or 0.1M phosphate buffer. This indicates that either the thiol groups evolved on the surface of the aggregates or that the aggregate structure permitted the rapid diffusion and reaction with DTNB. One final note regarding our methodology relative to the majority of the literature is our utilization of the heated sample (appropriately diluted, but without added DTNB) as a blank. Large aggregates scatter light significantly at 412 nm

contributing to the total absorbance and must be subtracted to obtain an accurate value for total reactive thiol groups.

3.5. Conversion of monomer to aggregates

Figure 4A shows the loss of monomer throughout the first 15 min of heating where the most reactive thiol groups evolved. Both lots had a similar trend and fit a first order kinetics model for loss of monomer ($\ln C/C_o = -kt$) with an $R_2 > 0.99$. The rate constant of monomer loss (k) was ~25% faster for lot A ($k = 0.199\ s^{-1}$) than lot B ($k = 0.159\ s^{-1}$), but both lots had a similar quantity (~5-10%) of monomer remaining after heating at 95°C for 15 min for both lots. Interestingly, despite the well established mechanism that disulfide bond formation drives the irreversible loss of monomer (Bertrand-Harb et al., 2002; Chaplin et al., 1986), the loss of monomer was not similar in magnitude to the evolution of reactive thiol groups. The first order loss kinetics of α-La have been extensively demonstrated in various environments (Anema, 2001; Anema & McKenna, 1996; Baer & Blanc, 1976; Dannenberg & Kessler, 1988; Hillier & Lyster, 1979; Lyster, 1970).

The elution profile of α-La (Lot B) heated from 0 to 15 min at 95°C is shown in Figure 4B and demonstrates the conversion of monomer into aggregates. Lot A had a similar profile (data not shown). The monomer M_w data is shown for t = 0 min and an average value of 13.9 kDa was calculated for this peak by the Astra software. This compares nicely to the commonly published value of 14.2 kDa. During the early stages of heating, there was very little build-up of low M_w aggregates (< 200 kDa) that would elute from 15-17 mL. There was a small peak at ~16.5 mL that may correspond to small α-La oligomers that were precursors to large aggregate formation. These were represented as distinct, intense bands (dimer, trimer, etc.) when observed in SDS-PAGE (data not shown). When the heating time was increased from 1.9 to 3.75 min, the

center of the mass peak shifts from ~13 to ~12.5 mL, but there was no buildup of mass at the void volume. For both of these peaks, there was a normal distribution of mass around the peak. The t = 3.75 min M_w data demonstrated a linear elution of log M_w from 2000 kDa down to ~300 kDa with an upward curvature at M_w values outside this range. The nonlinearity for larger aggregates occurs because they elute at the void volume and are excluded by the column. The nonlinear M_w elution at <300 kDa occurs either because the protein interacts with the stationary phase or it has a different shape than the linearly eluted aggregates (Jones, 2002). As the heating time was increased beyond 3.75 min, mass progressively accumulated at the void volume and the monomer was depleted.

3.6. Molecular weight distribution

Figure 5A demonstrates the cumulative weight distribution of the M_w values corresponding to the data from Figure 4B (for Lot B). In this plot, the mass distribution over the M_w range can be followed with time. The t = 1.9 min sample was the only timepoint to possess a significant quantity of mass less than 10^5 Da. It demonstrated a linear log M_w distribution from ~200 kDa up to ~1000 kDa. Both the t = 1.9 min and 3.75 min curves had a similar shape with ~20% of the mass residing in the low M_w tail. This indicates that similar growth processes occurred place throughout early heating. Upon further heating to t = 7.5 min, the low M_w material (from 200 to 600 kDa) flattened out and was comprised of less mass over a wider M_w range. This preceded a very sharp increase in slope around 800 to 900 kDa that comprised ~20% of the total mass. Larger M_w aggregates (>1000 kDa) followed the characteristic shape from earlier times with a linear profile through ~6500 kDa. The linear elution extends beyond the reported exclusion limit for this column (2000 kDa). Since the reported exclusion ranges for protein SEC columns are established using spherical standards, this indicates these aggregates

are not spherical and are more extended in conformation. At t = 15 min, there were two linear M_w elution ranges from 3500 to 5000 kDa and 5000 to 9000 kDa with each possessing about 20% of the total mass. The larger 50% of the mass was excluded into the void volume and eluted in a non-linear manner. Finally, the cumulative weight distribution curves for t = 1.9-7.5 min had an equivalent shift to the right whereas heating for 15 min resulted in a more pronounced shift to the right. Heating from 7.5 min to 15 min resulted in an increase in weight-averaged R_g from ~20 nm to ~40 nm.

Figure 5B demonstrates the cumulative weight distribution for Lot A. This lot produced a much different cumulative weight distribution time course than lot B. The linear elution for the 1.9, 3.75 and 7.5 min timepoints all began around 200-300 kDa, but broadened to 2000, 4000 and 6000 kDa, respectively. This corresponded to a polydispersity index (M_w/M_n) of 1.9, 2.2 and 3.0, respectively. It appeared that in the first 1.9 min of heating that the aggregate "primary particle" was formed and continued heating to 7.5 min resulted in the addition of denatured monomers and smaller aggregates to this particle. When the heating time was increased to 15 min, there was a dramatic increase in M_w distribution and the elution was non-linear indicating most of the protein eluted in the void volume.

Throughout the first 7.5 min of heating, the R_g values were calculated to be ~20 nm for both lots. Upon heating to 15 min, there was a sharp increase in R_g up to ~40 nm for Lot B and ~90 nm for Lot A. It should also be noted that the t = 15 min samples were the only ones that yielded excessive backpressure during filtration (0.2 μm). This indicated that some very large aggregates (Diameter > 200 nm) were formed between 7.5 and 15 min.

3.7. Analysis of shape factors

The aggregate shape can be inferred from the scaling of R_g with M_w through a power law relationship:

$$R_g = KM^{\nu} \qquad (4)$$

where ν is characteristic shape of the molecule (Burchard, 1994). The ν values for lots A and B were 0.357 ± 0.03 and 0.575 ± 0.07, respectively. The upper-end of the linear portion of the t = 7.5 min R_g and M_w curves was used because t = 15 min plots had limitations in linearity. A low value represents a dense structure with 0.33 being the lower limit for a dense sphere. The upper limit is 1.0, which represents a rigid rod. Linear or randomly branched structures typically have values between 0.50 and 0.60 depending on their degree of swelling in good (0.60) or poor solvents (0.50) (Burchard, 1994). This indicates the aggregates formed in lot A had a dense, spherical shape whereas the lot B aggregates had a more expanded architecture during early heating times. This further suggests that these two lots had different mechanisms for aggregate formation.

Patro and Przybycien (1994) utilized Monte-Carlo simulations to model the aggregate density as a function of the hydrophobic-hydrophobic contact energy. Increasing the number of hydrophobic clusters and their magnitude caused an increase in aggregate density (Patro et al., 1994). This suggests that hydrophobic attractions played a stronger role in lot A and therefore *in situ* turbidity measurements were made at 95°C to understand this.

3.8.1 Supremolecular aggregate formation and the Role of Hydrophobic Interactions

Figure 6 shows the turbidity development at 95°C ($\tau_{95°C}$) and its reversibility when cooled to room temperature (τ_{cool}) for both lots. Lot A had a sigmoidal-shaped $\tau_{95°C}$ curve with a lag time of ~15 min and a plateau value that was reached around 30 min. Throughout the initial

heating period (≤ 20 min), the τ_{cool} was actually greater than $\tau_{95°C}$. This indicates that the aggregates formed at 95°C either changed shape or further associated upon cooling. At later heating times (≥ 30 min), lot A exhibited 20% reversibility upon cooling. Lot B had a more linear turbidity development profile with essentially no lag time and a plateau value that was reached around 40-45 min. This lot exhibited a high degree of reversibility (~70%) throughout the entire heating period.

Heating both of these lots for 15 min at 95°C converted ~95% of the monomer into aggregates (Figure 5a). However, by t = 15 min, lot A had triple the reactive thiol concentration (Figure 2), triple the average M_w and more than double the τ_{cool} (Figure 6). Interestingly, these room temperature results contradict the $\tau_{95°C}$ data that indicates lot B develops larger aggregates in the first 20 min than lot A. This suggests that hydrophobic interactions were the predominant attractive force at 95°C causing the formation of large aggregates as has been suggested for both α-La (McGuffey et al., Submitted) and β-Lg (Galani & Apenten, 1997). It was not totally clear if hydrophobic interactions lead to the formation of disulfide bond formation or vice versa. McGuffey et al. (Submitted) suggested that hydrophobic interactions drove the formation of disulfide bonded oligomers in very pure α-La preparations, but this was not observed in commercial α-La in the same electrostatic conditions. Bauer, Carrotta, Rischel and Øgendal (2000) found that heated β-Lg initially forms disulfide bonded oligomers (up to tetramers) that rapidly form large aggregates through non-covalent interactions (when monomer is depleted) without a build-up of material with intermediate M_w. The evidence for the aggregation of α-La suggests a similar mechanism (Figure 7). In SDS-PAGE analysis of the samples from Figure 3A (data not shown), there were two species of aggregated material, distinct oligomeric bands (dimer, trimer, tetramers) and large aggregates that could not enter the gel matrix. This is

consistent with Figure 5 that demonstrates low concentrations of intermediate M_w material (< 200 kDa). In step 1 (Figure 7), denaturation leads to disulfide bond reduction and the formation of intermolecular disulfide bonds (step 2). These oligomers then rearrange to maximize exposure of hydrophobic clusters (step 3), resulting in rapid aggregation (step 4). The depletion of monomer (Figure 3A) was consistent with a pronounced shift in M_w cumulative weight distribution (from 7.5 to 15 min) in Figure 5. The continued development of reactive thiol groups corresponded to increasing $\tau_{95°C}$ (step 5) and they both plateau at 30-40 min. This suggests that thiol/disulfide interchange may be a prerequisite to the development of surface hydrophobicity; however hydrophobic interactions may facilitate close molecular association in the early stages of denaturation.

Finally, step 6 shows that cooling caused partially dissociation of the aggregates. When the reactive thiol curves (Figure 2) were overlaid with the τ_{cool} data (Figure 6), there was a remarkable similarity in the magnitude and shape of the trends. This indicates that aggregates associated by hydrophobic interactions either become "locked in" through further disulfide bond formation or dissociate with cooling.

Several recent studies have demonstrated that modifying/blocking the disulfide bonds leads to extensive hydrophobic aggregation and turbidity development. Reducing the disulfide bonds of α-La causes rapid aggregation through hydrophobic interactions at room temperature and this attraction is highly dependent on electrostatic interactions (Goers, Permyakov, Permyakov, Uversky & Fink, 2002; Li, Zhang & Wang, 2001; Lindner, Treweek & Carver, 2001). Kitabatake, Wada and Fujita (2001) blocked the free thiol group of β-Lg with n-ethylmaleimide, and heated it at 80°C (0.2M NaCl) and formed "huge aggregates" that could be dissociated with SDS. Essentially, they changed the pathway of aggregation from disulfide

driven (unmodified β-LG) to hydrophobically driven by blocking the free thiol groups (Kitabatake et al., 2001). This may be a global characteristic of globular protein aggregation where the only compensation for the disulfide bond restriction on conformational entropy is the minimization of free energy through hydrophobic interactions. This has been proposed in thermodynamic models of aggregation (Fields, Alonso, Stigter & Dill, 1992).

Fluorescent probe binding studies that heat α-La at temperatures ≥ 80°C in dilute solution (~1 $g \cdot L^{-1}$) observe a reduction in surface hydrophobicity with time (Eynard, Iametti, Relkin & Bonomi, 1992; Vanderheeren & Hanssens, 1994). In dilute solution, the lack of excluded volume interactions favors extensive monomer unfolding and disruption of native hydrophobic organization. Increasing the protein concentration facilitates pronounced turbidity development when heated to 95°C and precipitation of pure α-La preparations (McGuffey et al., Submitted).

3.8.2. Potential Role of Preformed Aggregates

An observation not yet described was the difference in shape between the two $\tau_{95°C}$ curves. It was possible that the slightly different composition of lot A might be causing its lag time, but titrating β-Lg or BSA into lot B did not dramatically alter its curve shape (data not shown). What seems more plausible is that the greater quantities of preformed aggregates in lot A (Figure 1) provided a nucleation site (possibly through hydrophobic interactions) for the disulfide bonded aggregates (Figure 7). It has been demonstrated that soluble aggregates dramatically enhance the aggregation and gelation of whey proteins (Puyol, Cotter & Mulvihill, 1999). Also, disulfide-reduced α-La associates with preformed aggregates from various proteins through hydrophobic interactions at 25°C (Li et al., 2001). This difference in $\tau_{95°C}$ shape also may be related to the difference in cumulative weight distribution in Figure 5. Lot A

demonstrated more of a branching phenomenon where aggregates interacted with the existing (preformed) aggregates by broadening the M_w distribution. When preformed aggregates were not present (Lot B), both cumulative weight distributions had a similar slope indicating that aggregate growth was more random. This may have also played a role in the more dense, spherical shape of Lot A aggregates where the Lot B aggregates were more expanded in conformation. Further research should be undertaken to more fully understand this phenomenon including a study that contrasts the shape of the aggregates at high temperature with room temperature.

4.1. Effect of β-Lg on α-La Solubility

Figure 8 shows the effect of increasing the relative β-Lg concentration on the solubility of α-La (Lot B) heated at 95°C for 1 hr. Lot B was investigated since it possessed less β-Lg than lot A. A commercially isolated β-Lg (Table 1) was titrated into the α-La to lower the total α-La concentration to 40 $g \cdot L^{-1}$, 35 $g \cdot L^{-1}$ and 30 $g \cdot L^{-1}$ (50 $g \cdot L^{-1}$ total protein). This corresponds to a α-La to β-Lg molar ratio (MR) of 7.4, 3.7 and 2.3, respectively. Further lowering the MR to 1.4 resulted in the formation of a gel after ~15 min. Figure 7 shows that decreasing the pH from 7.0 to 6.85 resulted in a dramatic loss of solubility for the preparations with additional β-Lg with only a ~10% loss for the control. At pH 6.95 and 7.00, the 2.3 MR was the only treatment that displayed a significant loss of solubility. At pH 6.90, the solubility decreased with increasing MR. There have been no studies that evaluated the heat stability with different ratios of the two proteins. However, whey protein solutions (1.7% total protein) heated to 96°C demonstrate enhanced stability above pH 6.9 (Rattray et al., 1997).

4.2. Effect of β-Lg on Turbidity Development

Figure 9 shows the effect of increasing the relative proportion of β-Lg on the $\tau_{95°C}$ and τ_{cool} at 30 min (at pH 7.0). The general effect of increasing β-Lg was a higher plateau turbidity value and a decreased plateau turbidity time. The presence of a 7.4 MR did not significantly alter $\tau_{95°C}$ until >25 min, whereas the 3.7 MR deviated at 10 min. The 2.3 MR (the only treatment with <80% solubility) had a very abrupt rise in $\tau_{95°C}$, but gradually tapered off. These results are consistent with the observations by Schokker et al. (2000) that indicated hydrophobic interactions are especially important in the early stages of the aggregation of α-La and β-Lg. Hydrophobic interactions (as inferred from $\tau_{95°C}$) were accentuated by the addition of β-Lg down to a 3.7 MR, but played less of a role with a 2.3 MR. This may be influenced by the evolution of reactive thiol groups, which is discussed in the next section.

The % reversibility of turbidity development was 79, 74 and 20 for 7.4, 3.7 and 2.3, respectively. This reinforces the previous observation that increasing disulfide bond formation is occurring along with hydrophobic interactions and limits the degree of reversibility. However, addition of β-Lg up to a 3.7 MR has a negligible effect on reversibility.

4.3. Effect of β-Lg on Reactive Thiol Evolution

Figure 10 shows the change in reactive thiol groups with heating at 95°C. All of the t = 0 min treatments demonstrated ~0.75 mol of thiol/ mol of β-Lg monomer, which is in reasonable agreement with the value of 0.85 found by Hoffmann and van Mil (1999). All of the treatments exhibited an initial increase, but the plateau time (defined as the first timepoint to show a decrease in value relative to the previous time) was 40, 35, 30 and 10 min for the 36, 7.4, 3.7 and 2.3, respectively. Apparently, initial heating at 95°C caused disulfide bond reduction (i.e.

breaking, reaction 1). Increasing the relative concentration of β-Lg caused an increase in the net contribution of disulfide bond oxidation (i.e. termination reactions; reaction 3). The behavior of the 2.3 MR treatment provided insight into the relationship between thiol reactivity and the development of hydrophobic interactions. The net evolution of reactive thiol groups reaches its maximum value at 10 min. Heating beyond this time caused a relative decrease in reactive thiol groups, which is indicative of a net thiol oxidation. In Figure 9, this corresponded to a pronounced increase in $\tau_{95°C}$ through 10 min that tapered of with continued heating. This reinforces the previous assertion (Figure 7; Steps 2 and 3) that evolution of free thiol groups and intermolecular disulfide bond formation precedes (and facilitates) hydrophobic interactions.

There has been no direct measurement of the reactive thiol concentration of α-La and β-Lg mixtures, but their coaggregation has been extensively studied by other methods. Livney et al. (2003) indicated that β-Lg is important in the early stages of aggregation in initiating thiol/disulfide interchange with α-La, but subsequently α-La is a good "chain carrier" for this reaction. This is consistent with Figure 10 data where the flat slope at MR ≥ 7.4 is indicative of a good chain carrier whereas lower MR favor chain termination. There was a remarkable similarity in the data trends observed in Figure 10 and the evolution of reaction thiol groups (measured by reaction with DTNB) in pure β-Lg at varying pH (Hoffmann et al., 1999). Essentially, increasing the pH towards the thiol pKa, increases the reactivity of the free thiol group in β-Lg. At pH 6.4 and 6.8, there was a gradual evolution with heating time and a relatively flat plateau after continued heating (Hoffmann et al., 1999) like the 7.4 and 36 MR treatments (Figure 10). Increasing the pH to ≥ 7.2 causes an abrupt initial rise followed by a moderate decline in reactive thiol concentration (Hoffmann et al., 1999) as observed for the 2.3 MR treatment. Apparently, the ability of α-La to carry the thiol/disulfide interchange reaction is

related to the concentration and reactivity of the free thiol groups where increasing either of these variable favors thiol oxidation, which also favors insolubilization Figure 8.

5.1. Effect of Excess Ca^{2+} on Turbidity Development and Solubility

Figure 11 shows the sensitivity of three commercial whey protein preparations to the addition of Ca^{2+} by $\tau_{95°C}$ measurement. Without any additional Ca^{2+}, whey protein isolate (WPI) and α-La formed soluble solutions whereas β-Lg formed a gel (Figure 11A). This indicated that the higher concentration of minor protein constituents in WPI was critical to maintaining solubility. However, a 1:1 MR of Ca^{2+} to α-La (Figure 11B) resulted in much higher $\tau_{95°C}$ values and it caused WPI to form a gel whereas α-La remained soluble. The enhanced stability of α-La in the presence of Ca^{2+} makes it an excellent candidate for utilization in a heat stable nutritional beverage where Ca^{2+} levels are > 20 mM.

Figure 12 shows the reduction in α-La solubility with the addition of 2, 3 and 4 MR of Ca^{2+} to α-La (Lot A). As the Ca^{2+} was increased, the solubility generally decreased as was best visualized at pH 7.2. A corresponding increase in pH was required in order to maintain protein solubility with excess Ca^{2+} and only at pH 7.5 was high solubility regained for the 4 MR treatment. These observations are consistent with general whey protein solubility trends (de Rham et al., 1984). At pH 7.0, the phosphate concentration was doubled to 20 mM (Figure 12) for the 4 MR treatment to understand its effect on solubility through its ability to chelate Ca^{2+}. This level of phosphate caused visible turbidity development in the unheated solutions due to the formation of soluble calcium phosphate complexes. In the presence of whey proteins, the size of these complexes get much larger when their concentration is increased from 10 mM (142 nm) up to 20 mM (207 nm) (O'Kennedy, Halbert & Kelly, 2001). Although, these complexes are

larger, they have the same zeta potential indicating their size is not related to their surface charge (O'Kennedy et al., 2001). It was not clear why 10 mM phosphate did not enhance solubility of even the 2 MR (6.4 mM Ca^{2+}) treatment where 20 mM phosphate provided 95% solubility of the 4 MR treatment. The presence of larger calcium phosphate particles may play a role in decreasing the frequency of aggregate collisions and/or their high surface charge may cause electrostatic stabilization. Further research should be undertaken to understand this interrelationship in order to optimize / manipulate protein solubility.

CONCLUSIONS

When heated at 95°C, α-La evolved reactive thiol groups that lead to the formation of disulfide bonds, which appeared to facilitate hydrophobic interactions. Aggregates formed at 95°C partially dissociated with cooling and this process was correlated to the evolution of free thiol groups. The presence of preformed aggregates altered both the molecular weight distributions and turbidity development. Increasing the concentration of β-Lg decreased solubility and these aggregates were much more sensitive to reductions in surface charge. The presence of excess calcium causes a pronounced decrease in solubility at pH 7.0 that required an increase in protein surface charge or chelation of this calcium with 20 mM phosphate in order for the protein to remain soluble.

Table 1

Protein composition for two industrial α-lactalbumin lots and a commercial β-Lg lot as determined by reverse phase HPLC

	Percent Weight of Total Protein					
Lot	**α-La**	**β-Lg**	**BSA**	**IgG**	**GMP**	**PP**
A	89.7	4.9	1.3	2.2	0.4	1.6
B	92.5	2.8	0.8	1.1	0.6	2.2
β-Lg	2.6	92.7	0.0	2.6	1.5	0.7

a) β-Lg = β-lactoglobulin; BSA = bovine serum albumin; IgG = immunoglobulin; GMP = glycomacropeptide; PP = proteose peptone

List of Figures

Fig. 1. Native PAGE of unheated α-La lots. For lanes 2-9, even numbered lanes are lot A and odd numbered lanes are lot B: Lane 2 & 3: 20 μg TP; Lanes 4 & 5: 40 μg TP; Lanes 6 & 7; 80 μg TP; Lanes 8 & 9 160 μg TP. Lanes 1 is the M_w marker and lane 10 contains 30 μg whey protein isolate.

Fig. 2. pH-dependence of protein solubility for lot A (filled bars) and B (open bars) α-La (50 $g \cdot L^{-1}$ TP) heated at 95°C for 1 hour then centrifuged at 30,000 $\times g$ for 30 min at 20°C. The solutions contained 1:1 MR of calcium to α-La, 5 mM sodium phosphate, 5 mM potassium phosphate and 30 mM total Na^+ and K^+ (including what is provided by the phosphate solution).

Fig. 3. Time-dependent reactive thiol evolution when α-La lots A (□) and B (○) are heated to 95°C in the conditions described in Fig 2. Solutions were cooled to room temperature, reacted with DTNB then the $Abs_{412\ nm}$ was measured.

Fig. 4. Time dependent loss of monomer (Panel A) for α-La lot A (filled symbols) and B (open symbols) heated at 95°C in the conditions described in Fig 2 and analyzed by SEC. In panel B, the complete SEC-RI chromatograms (black circles) obtained by heating α-La (lot B) at 95°C for 0, 1.875, 3.75, 7.5 and 15 min. The native peaks decrease and the aggregate peaks (at 11 mL) increase in that order (t = 0 aggregate peak not shown). The M_w data (grey circles) is shown for t = 0 (under native peak) and t = 3.75 min (over aggregate peaks) treatments.

Fig. 5. Cumulative M_w distributions for the lot B (Panel A) and lot A (Panel B) aggregate data as determined by SEC-MALLS. The curves correspond to heating times (from left to right) of t = 1.875, 3.75, 7.5 and 15 min in the conditions described in Fig 2.

Fig. 6. Time-dependent turbidity development at 95°C (□,○) and its reversibility when cooled to room temperature (Ù,Ð) for α-La heated in the conditions described in Fig 2. Lot A is

represented by filled symbols and lot B by open symbols for both figures. All turbidity measurements were made at a wavelength of 400 nm.

Fig. 7. Cartoon describing the role (and interrelationship) of disulfide bond formation, hydrophobic interactions and preformed aggregates on the formation and reversibility of the α-La heat-induced aggregation process at neutral pH for lot A and lot B. Minor protein constituents are not represented for the sake of simplicity.

Fig. 8. The pH dependence (from 6.85 to 7.00) of protein solubility for varying proportions of α-La (Lot B) to β-Lg containing 50 $g \cdot L^{-1}$ total protein, heated at 95°C for 1 hour in the conditions described in Fig 2. The treatments for each pH corresponded to (from left to right) molar ratios of 2.3, 3.7, 7.4 and 36 α-La to β-Lg with the latter treatment being the data from Figure 2 provided as a reference.

Fig. 9. Time dependent turbidity development at 95°C (open symbols) and its reversibility when cooled (closed symbols) for the 2.3 (♦), 3.7 (▲), 7.4 (Ỳ) molar ratios of α-La to β-Lg heated in the conditions described in Fig 2. The 36:1 molar ratio from Figure 6 was added (○) as a reference.

Fig. 10. Time dependent thiol evolution for the 2.3 (♦), 3.7 (▲) and 7.4 (Ỳ) molar ratios of α-La to β-Lg heated in the conditions described in Fig 2. The 36:1 molar ratio from Figure 6 was added (○) as a reference. Lines were drawn to guide the eye.

Fig. 11. – Time dependent turbidity development for a WPI (▲), β-Lg (Ỳ) and α-La solutions (đ) heated at 95°C with no Ca^{2+} added (a) and a 1:1 molar ratio of Ca^{2+} to α-La (b) in the electrostatic conditions described in Fig 2.

Fig. 12. – pH dependence of α-La solubility (Lot A; 50 g L^{-1} total protein) containing 10 mM sodium phosphate, 2, 3 and 4 molar ratios of Ca^{2+}:α-La (from left to right at each pH), with NaCl

and KCl being decreasing to account for the ionic strength increase with additional $CaCl_2$. At pH 7.0, the bar on the far right represents 20 mM sodium phosphate.

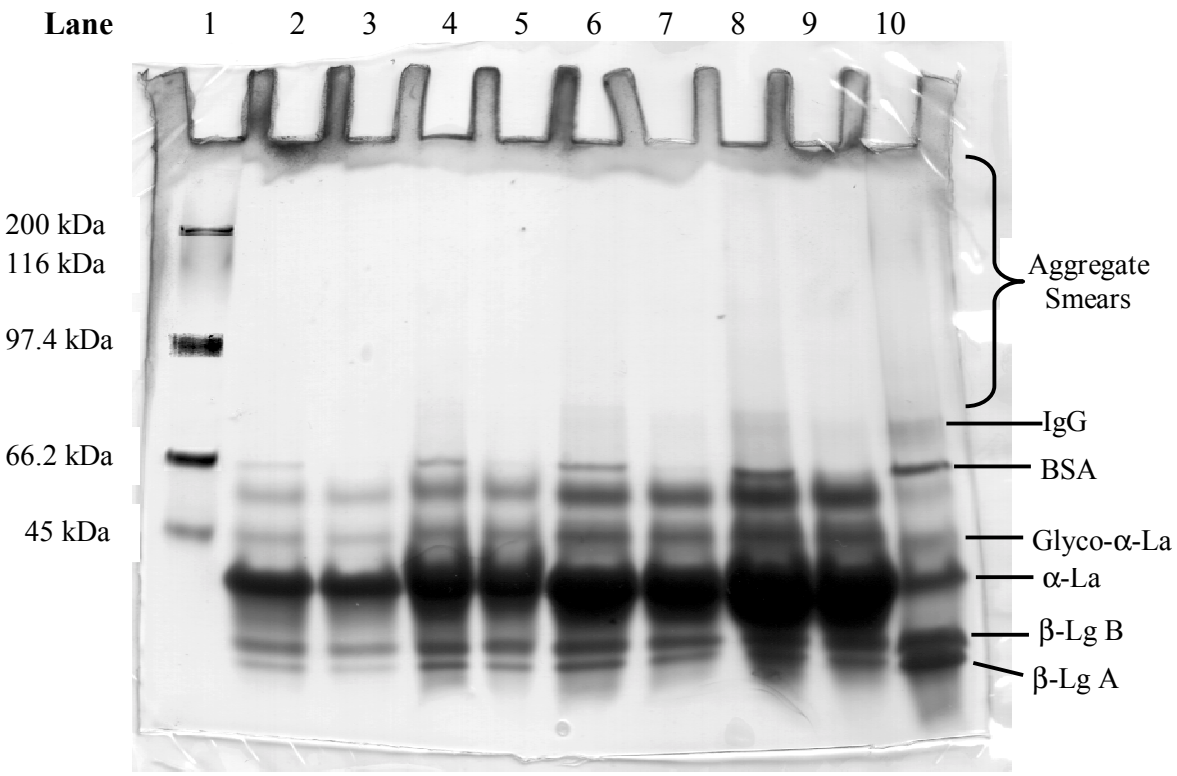
Lane
1
2
3
4
5
6
7
8
9
10
200 kDa
116 kDa
97.4 kDa
66.2 kDa
45 kDa
Aggregate Smears
IgG
BSA
Glyco-α-La
α-La
β-Lg B
β-Lg A

Figure 1

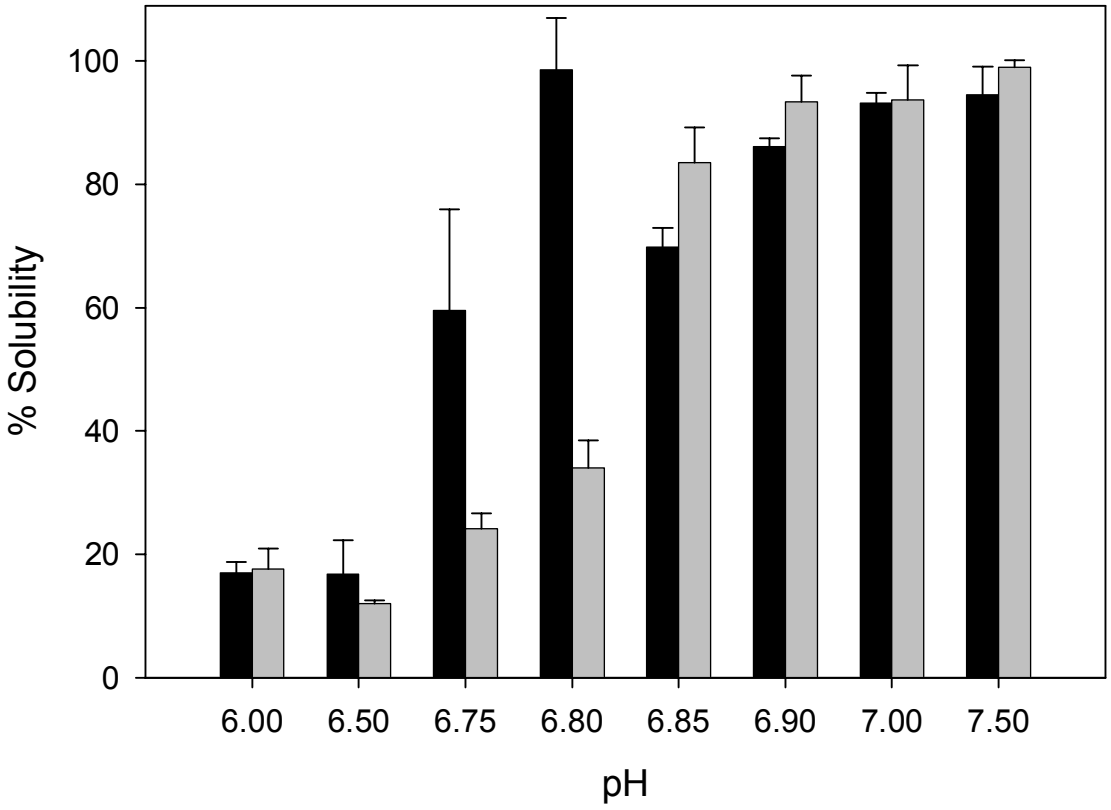

Figure 2

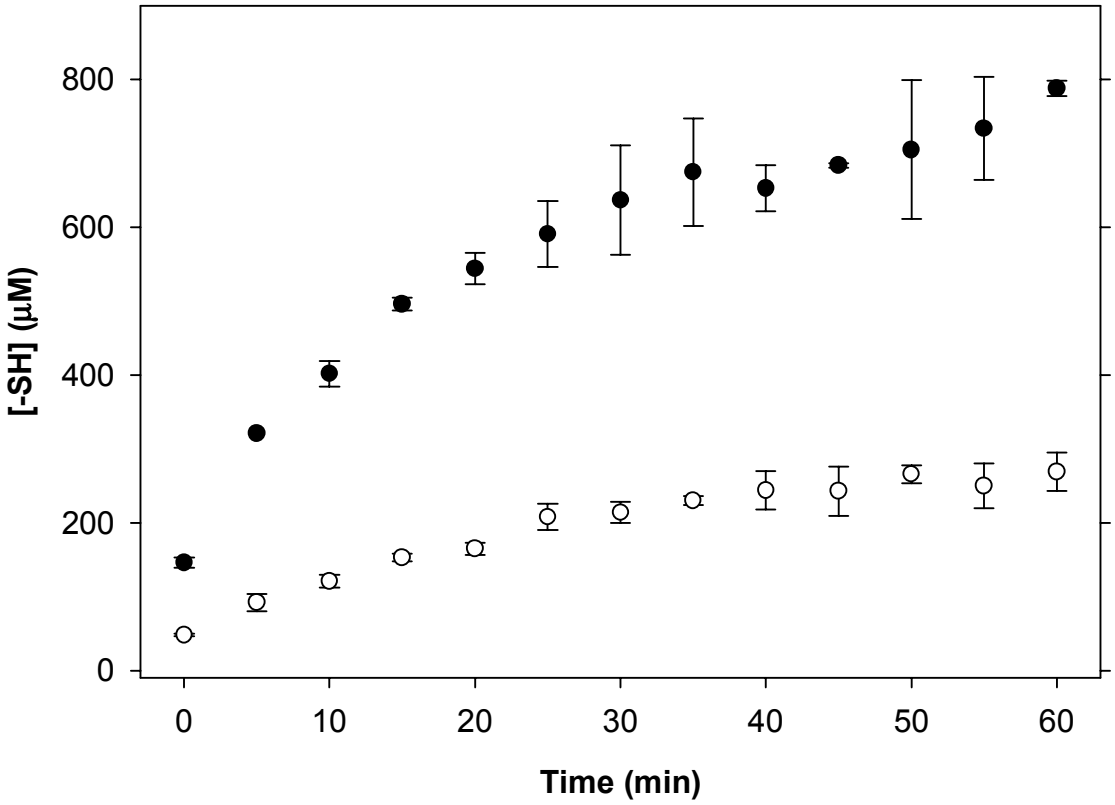

Figure 3

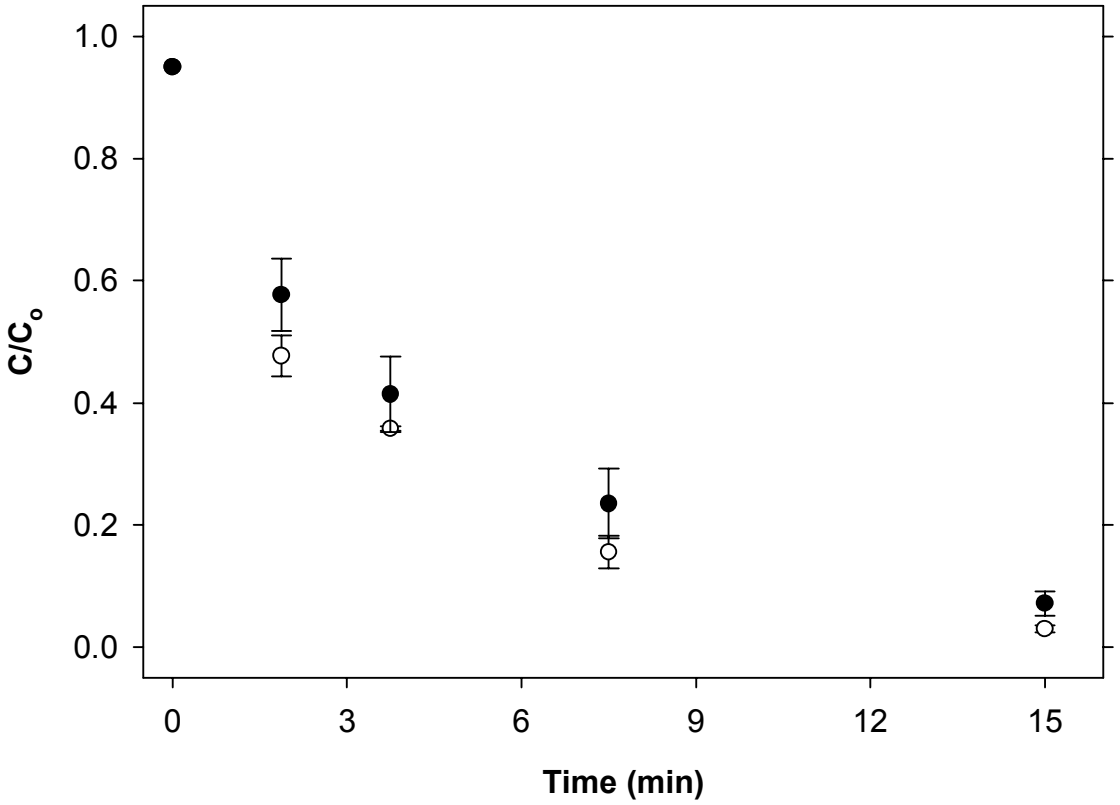

Figure 4A

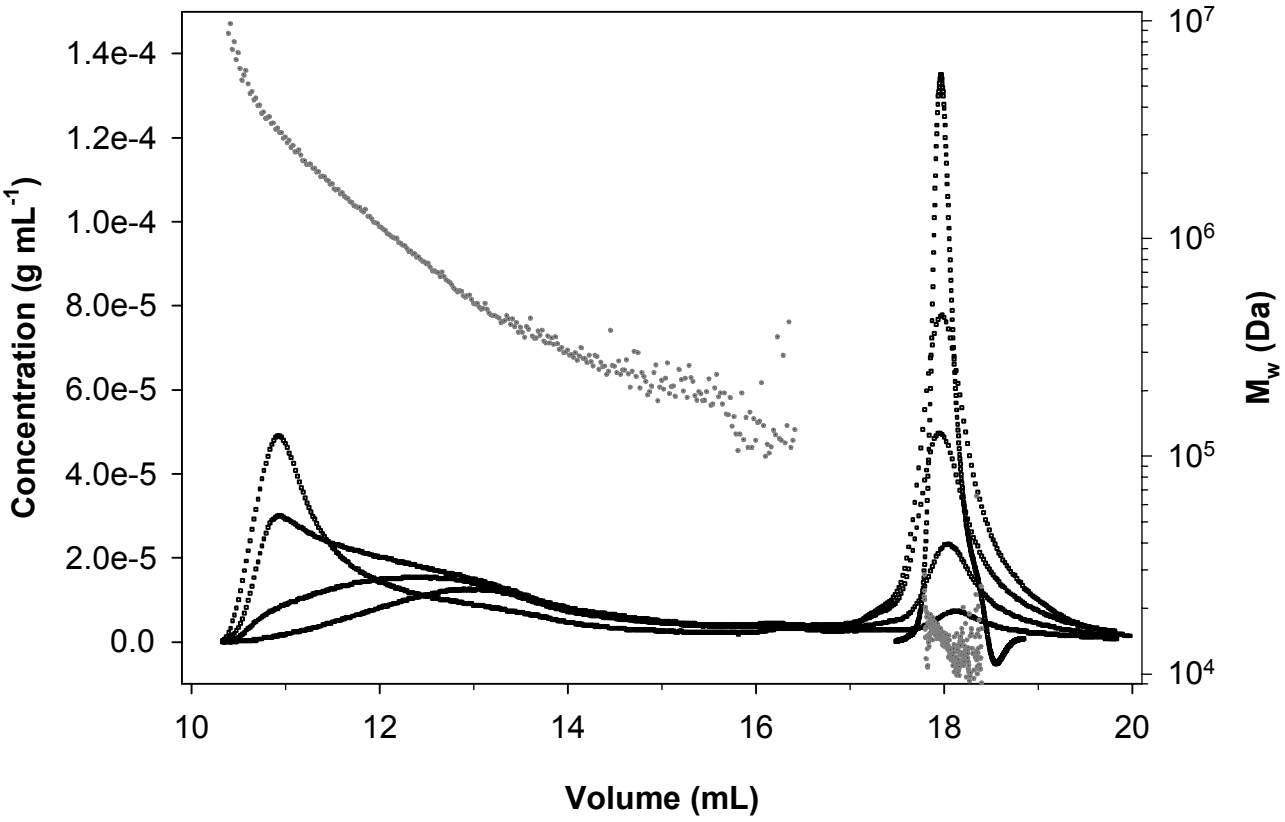
Concentration (g mL^{-1})
1.4e-4
1.2e-4
1.0e-4
8.0e-5
6.0e-5
4.0e-5
2.0e-5
0.0
10^7
10^6
10^5
10^4
M_w (Da)
10
12
14
16
18
20
Volume (mL)

Figure 4B

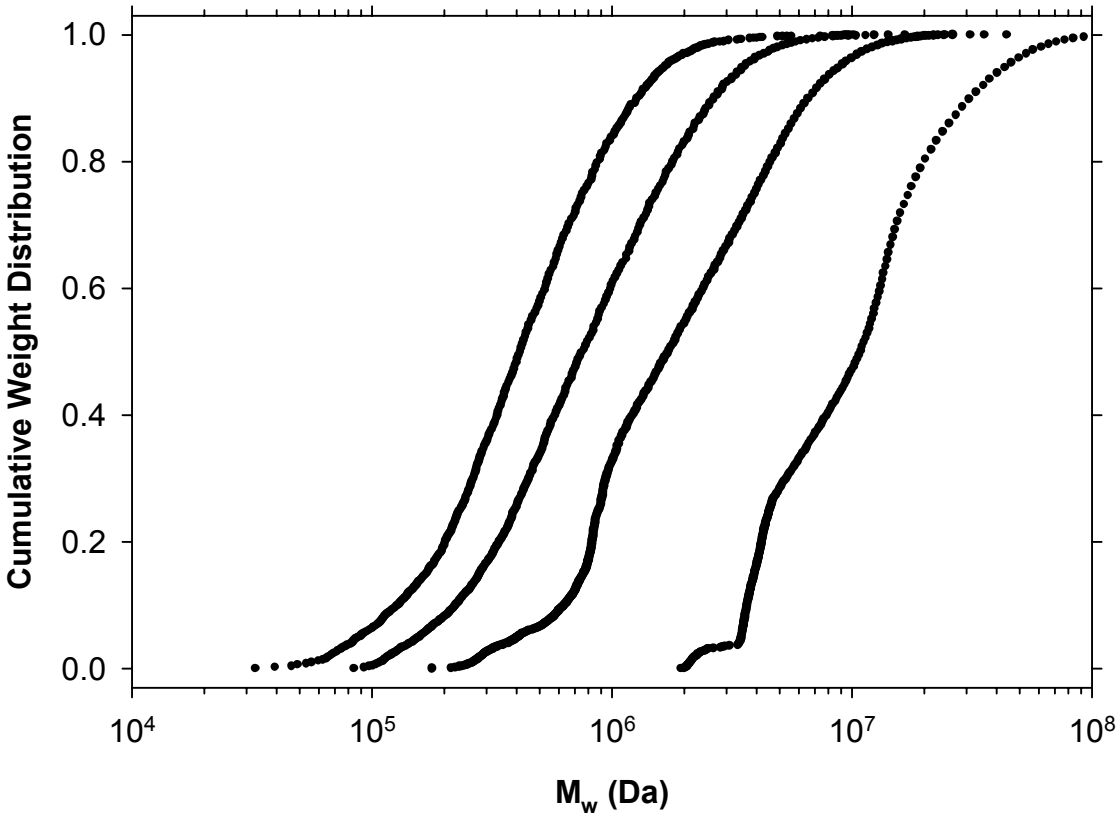
Cumulative Weight Distribution
1.0
0.8
0.6
0.4
0.2
0.0
10^4
10^5
10^6
10^7
10^8
M_w (Da)

Figure 5A

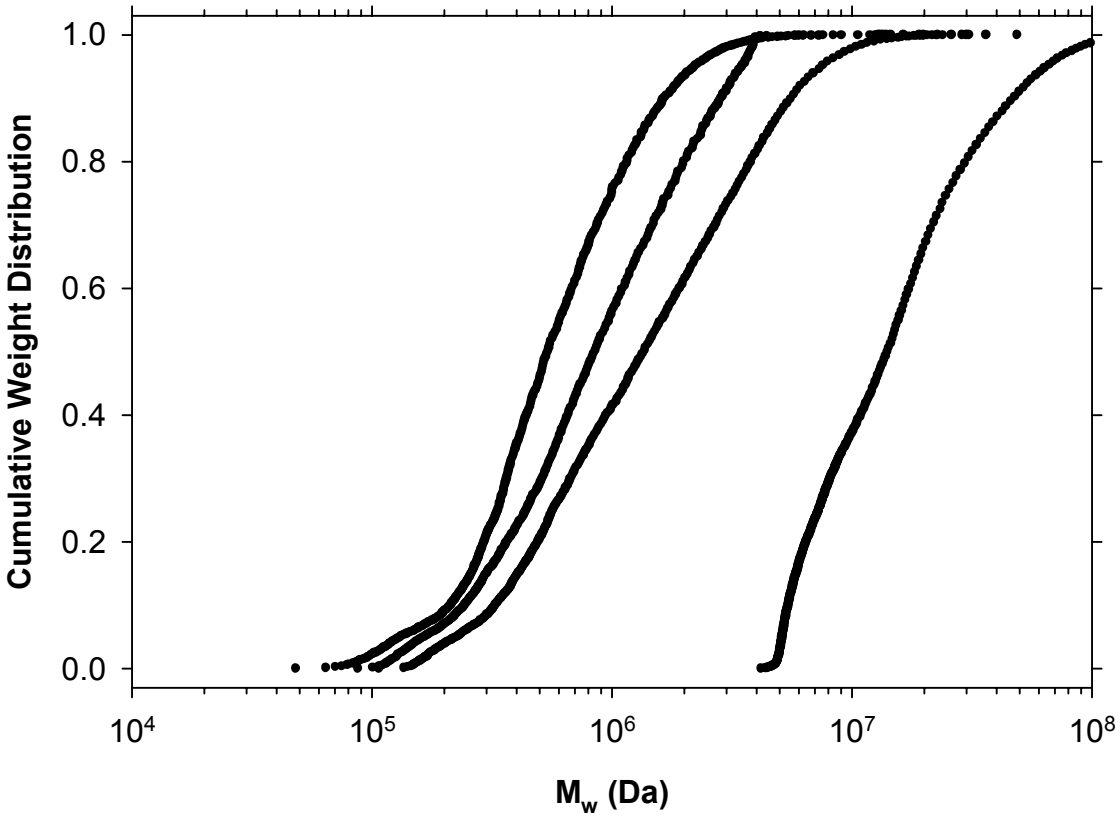
Cumulative Weight Distribution
1.0
0.8
0.6
0.4
0.2
0.0
10^4
10^5
10^6
10^7
10^8
M_w (Da)

Figure 5B

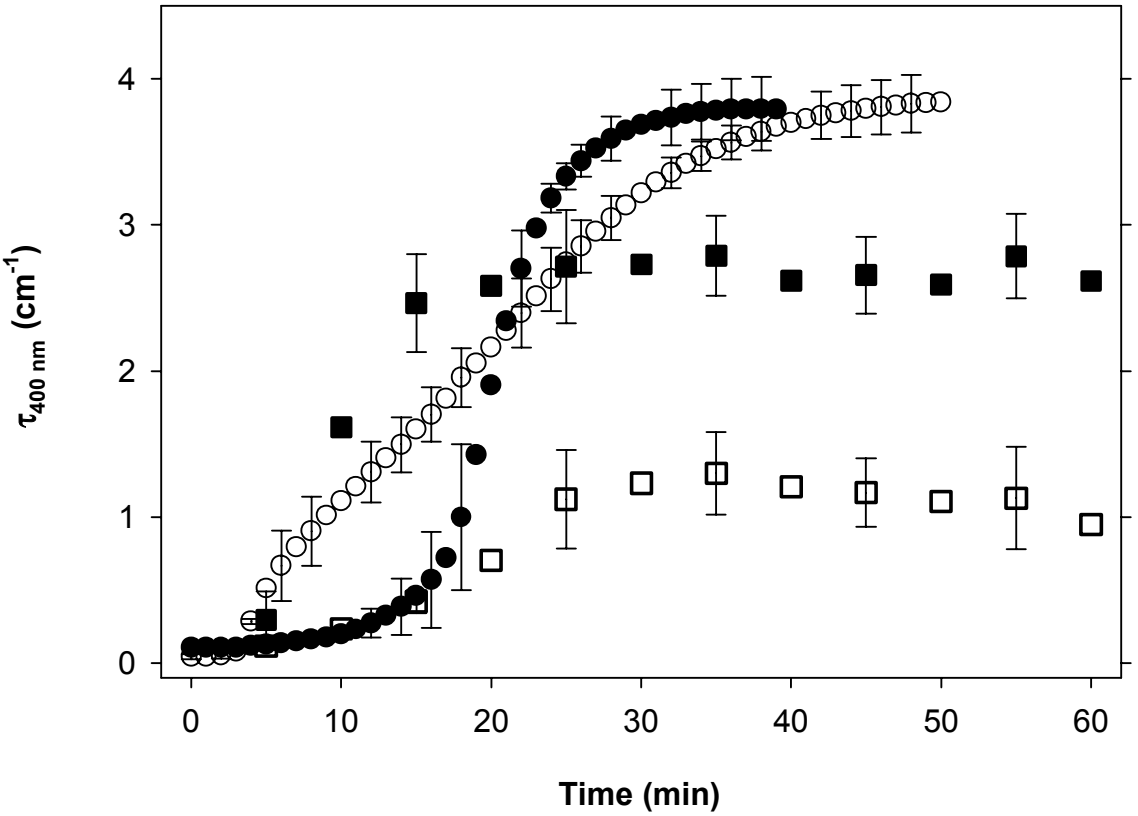

Figure 6

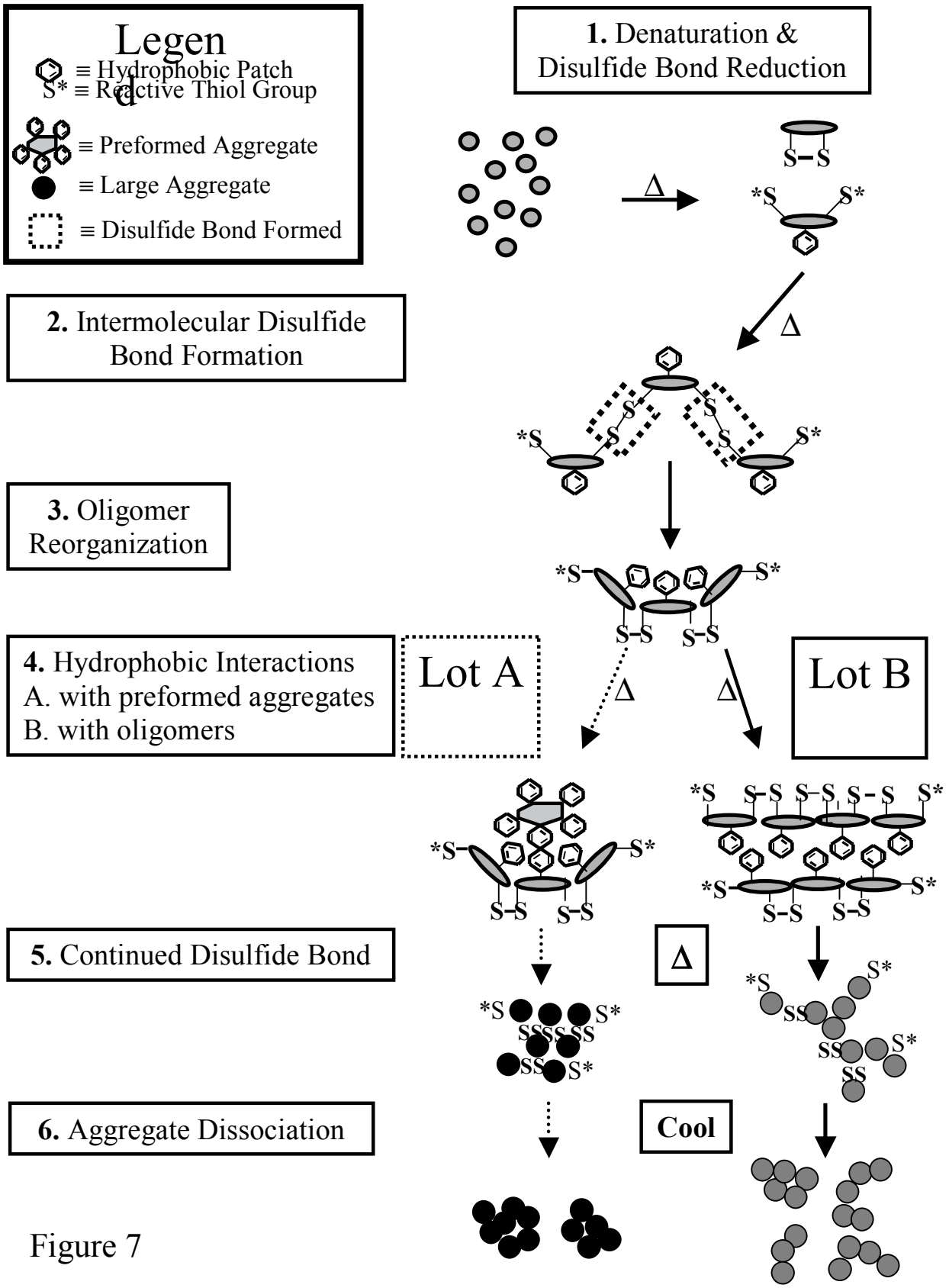
Legend
≡ Hydrophobic Patch
S* ≡ Reactive Thiol Group
≡ Preformed Aggregate
≡ Large Aggregate
≡ Disulfide Bond Formed
1. Denaturation & Disulfide Bond Reduction
2. Intermolecular Disulfide Bond Formation
3. Oligomer Reorganization
4. Hydrophobic Interactions
A. with preformed aggregates
B. with oligomers
Lot A
Lot B
5. Continued Disulfide Bond
6. Aggregate Dissociation
Cool
Δ
S–S
*S
S*

Figure 7

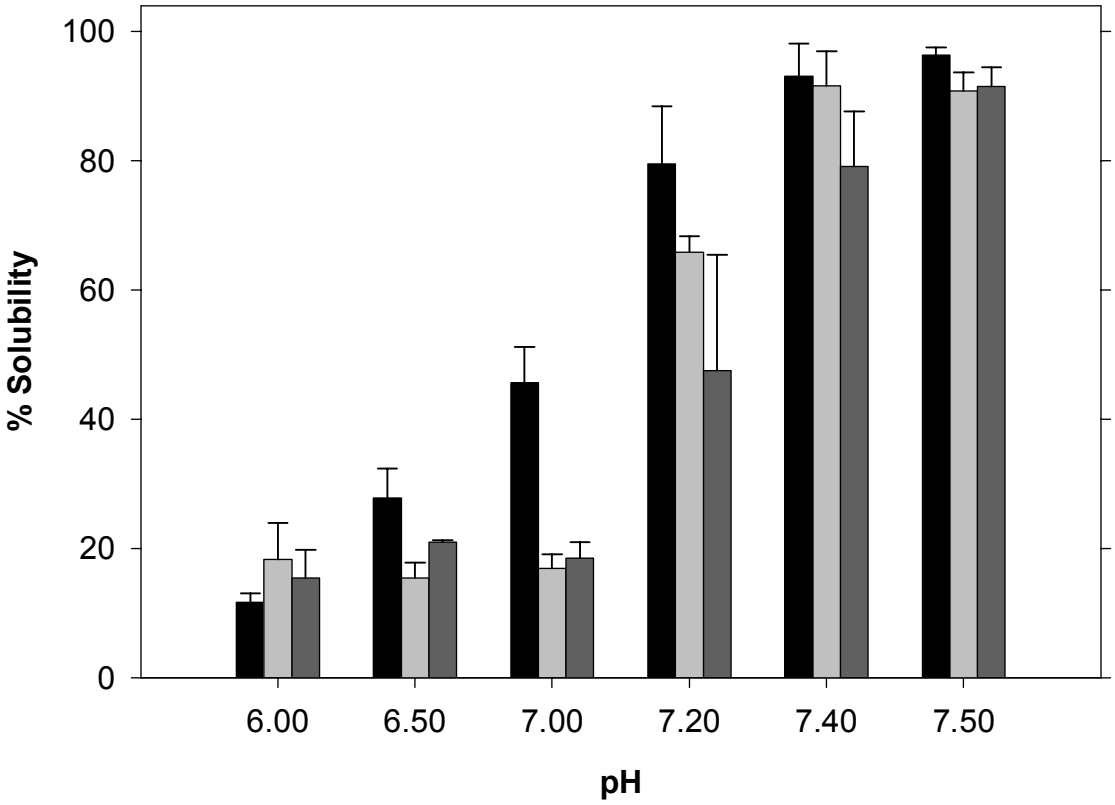

Figure 8

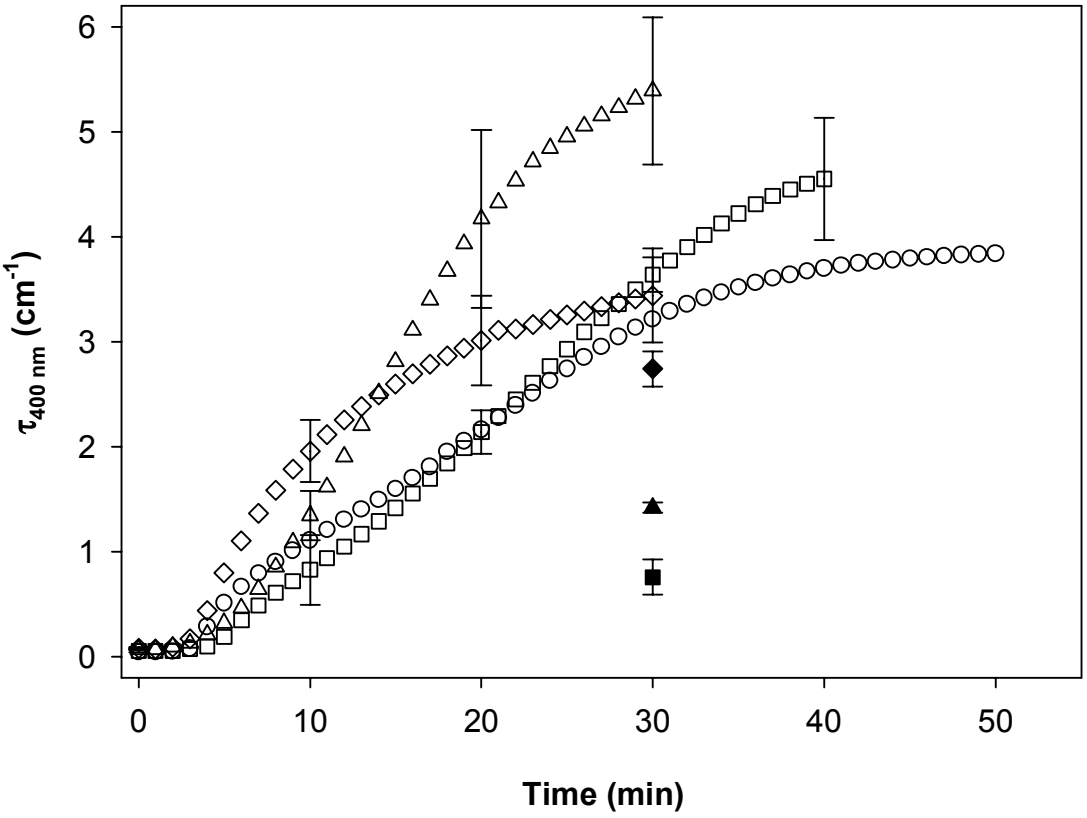

Figure 9

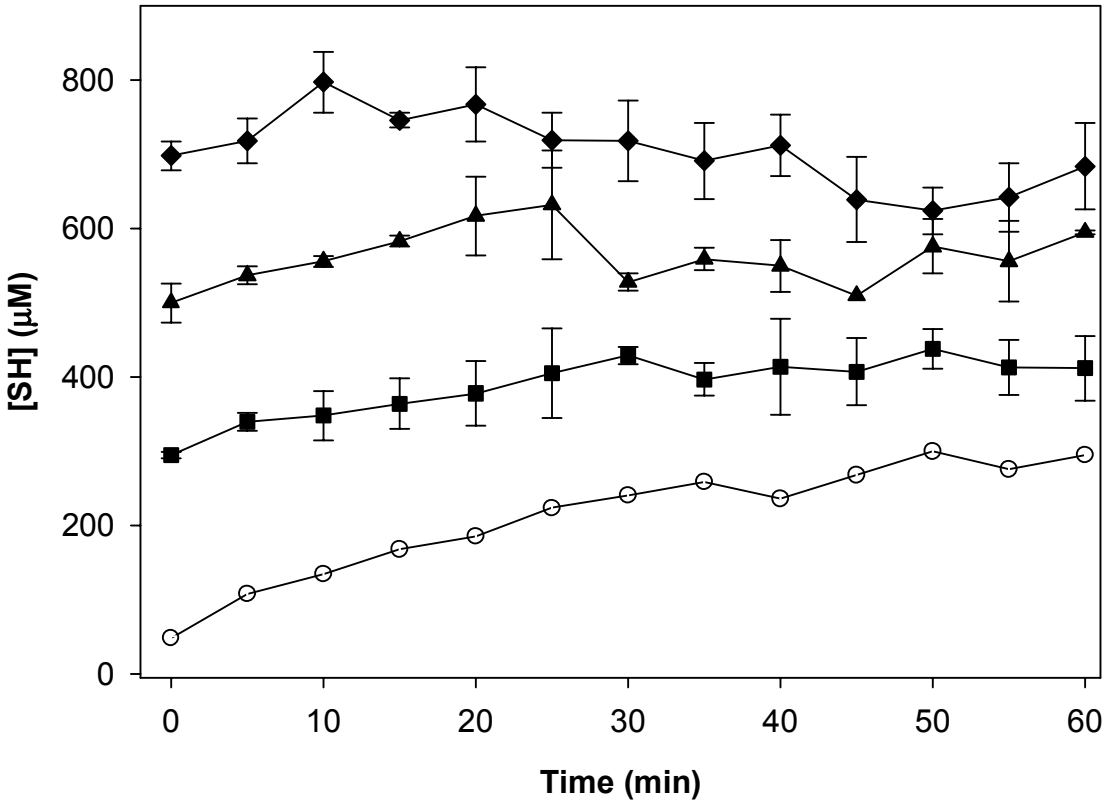

Figure 10

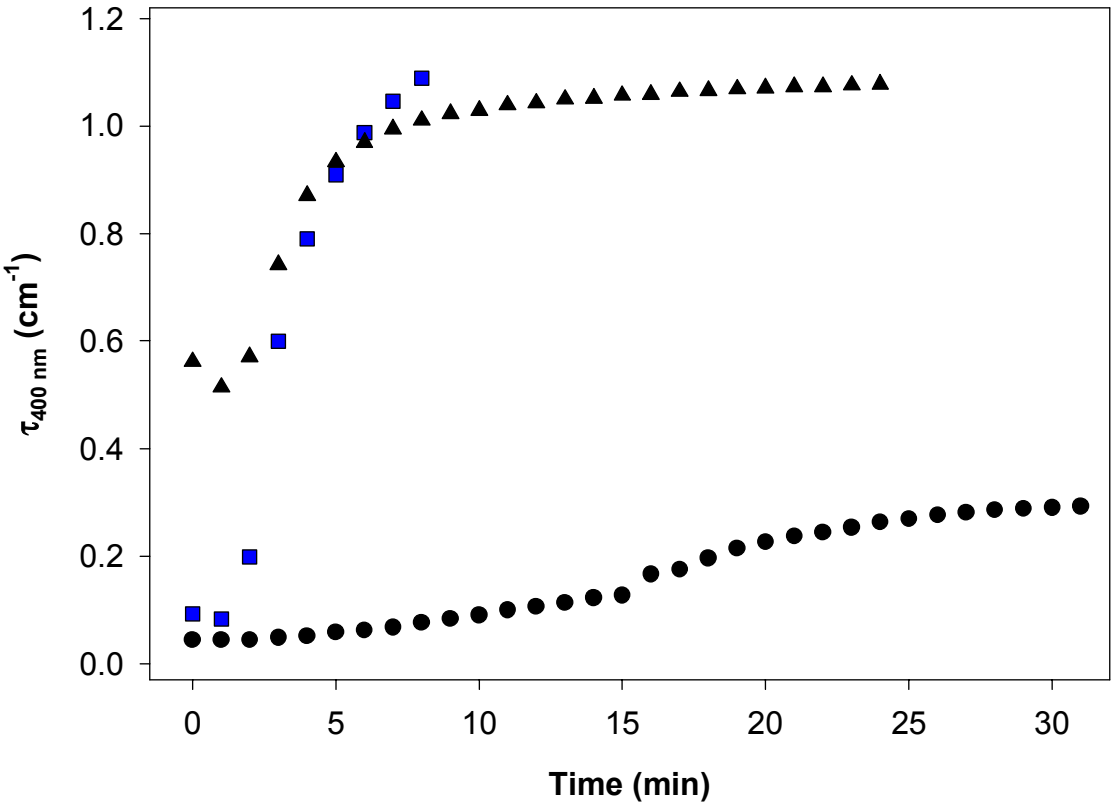

Figure 11a

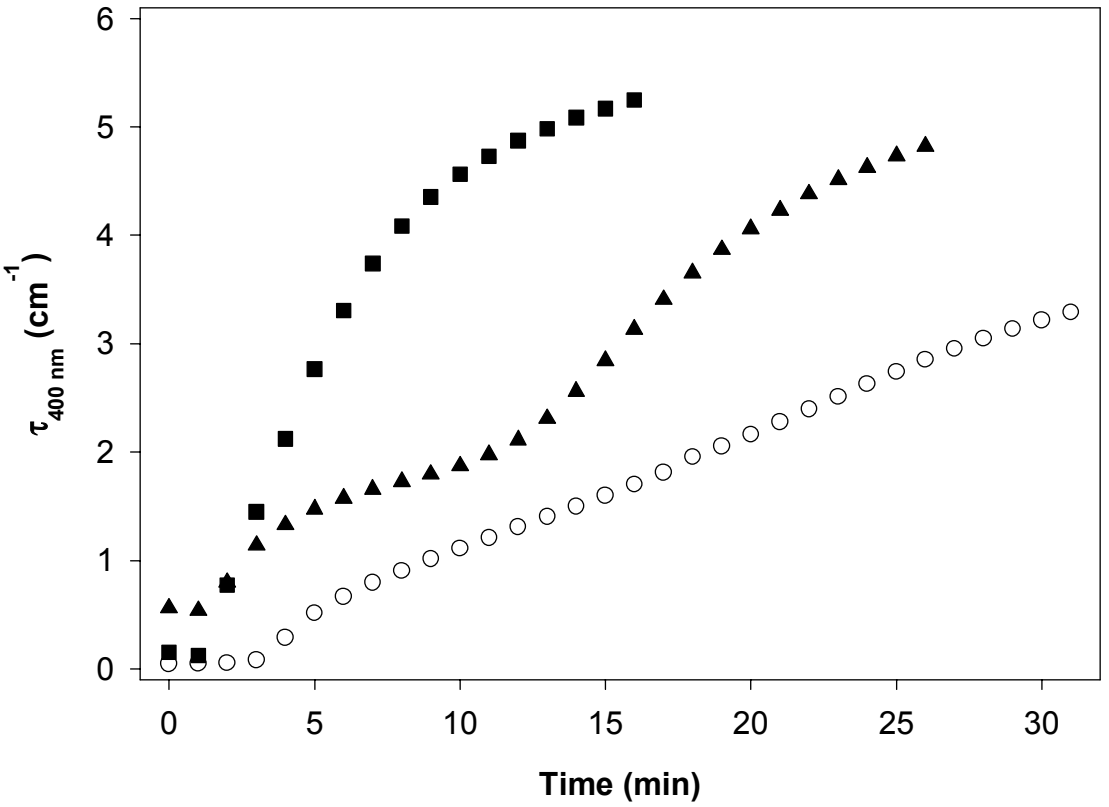

Figure 11b

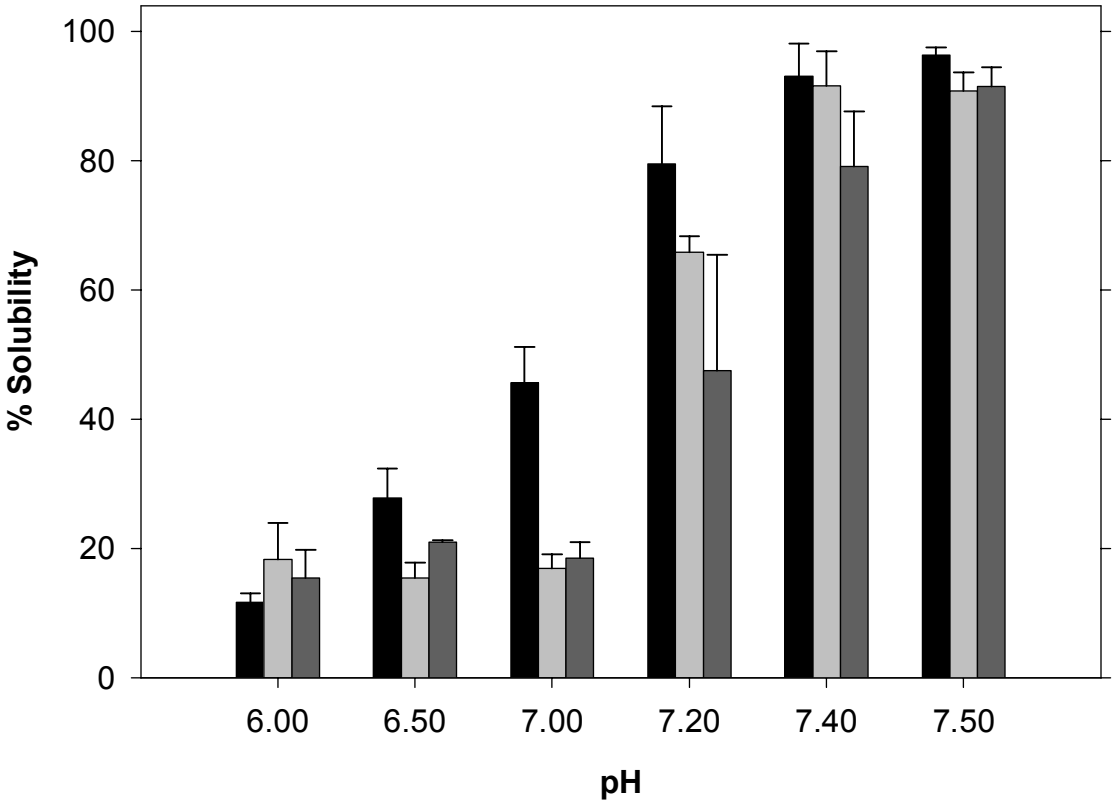

Figure 12

LITERATURE CITED

Anema, S. G. (2001). Kinetics of the irreversible thermal denaturation and disulfide aggregation of α-lactalbumin in milk samples of various concentrations. *Journal of Food Science*, 66(1), 2-9.

Anema, S. G. & McKenna, A. B. (1996). Reaction kinetics of thermal denaturation of whey proteins in heated reconstituted whole milk. *Journal of Agricultural and Food Chemistry*, 44(2), 422-428.

Baer, M. O. & Blanc, B. (1976). Serological studies on heat-induced interactions of α-lactalbumin and milk proteins. *Journal of Dairy Research*, 43, 419-423.

Bauer, R., Carrotta, R., Rischel, C., & Ogendal, L. (2000). Characterization and Isolation of Intermediates in beta -Lactoglobulin Heat Aggregation at High pH. *Biophys. J.*, 79(2), 1030-1038.

Bell, K. & McKenzie, H. A. (1967). Isolation and properties of bovine β-lactoglobulin C. *Biochimica Et Biophysica Acta*, 147(1), 109-&.

Bertrand-Harb, C., Baday, A., Dalgalarrondo, M., Chobert, J. M., & Haertle, T. (2002). Thermal modifications of structure and co-denaturation of α-lactalbumin and β-lactoglobulin induce changes of solubility and susceptibility to proteases. *Nahrung-Food*, 46(4), 283-289.

Boye, J. I. & Alli, I. (2000). Thermal denaturation of mixtures of α-lactalbumin and β-lactoglobulin: a differential scanning calorimetric study. *Food Research International*, 33(8), 673-682.

Brew, K. & Grobler, J. A. (1992). α-Lactalbumin. In P. F. Fox, (Ed). Advanced dairy chemistry: proteins. (pp. 191-229). Vol. 1. Elsevier Applied Science: New York.

Burchard, W. (1994). Light Scattering Techniques. In S. B. Ross-Murphy, (Ed). Physical Techniques for the Study of Food Biopolymers. Blackie: New York.

Calvo, S., Leaver, J., & Banks, J. M. (1993). Influence of other whey proteins on the heat-induced aggregation of α-lactalbumin. *International Dairy Journal*, 3, 719-727.

Chaplin, L. C. & Lyster, R. L. J. (1986). Irreversible heat denaturation of bovine α-lactalbumin. *Journal of Dairy Research*, 53, 249-258.

Creighton, T. E. (1993). Proteins. structures and molecular properties. 2nd ed. W.H. Freeman and Co., New York.

Dalgleish, D. G., Senaratne, V., & Francois, S. (1997). Interactions between α-lactalbumin and β-lactoglobulin in the early stages of heat denaturation. *Journal of Agricultural and Food Chemistry*, 45(9), 3459-3464.

Dannenberg, F. & Kessler, H.-G. (1988). Reaction kinetics of the denaturation of whey proteins in milk. *Journal of Food Science*, 53(1), 258-263.

de Rham, O. & Chanton, S. (1984). Role of ionic environment in insolubilization of whey proteins during heat treatment of whey products. *Journal of Dairy Science*, 67(5), 939-949.

de Wit, J. N. & Klarenbeek, G. (1984). Effects of various heat treatments on structure and solubility of whey proteins. *Journal of Dairy Science*, 67(11), 2701-2710.

Doi, H., Tokuyama, T., Kuo, F.-H., Ibuki, F., & Kanamori, M. (1983). Heat-induced complex formation between κ-casein and α-lactalbumin. *Agricultural and Biological Chemistry*, 47(12), 2817-2824.

Dolgikh, D. A., Abaturov, L. V., Bolotina, I. A., Brazhnikov, E. V., Bychkova, V. E., Gilmanshin, R. I., Lebedev, Y. O., Semisotnov, G. V., Tiktopulo, E. I., & Ptitsyn, O. B. (1985). Compact state of a protein molecule with pronounced small-scale mobility - bovine α-lactalbumin. *European Biophysics Journal*, 13(2), 109-121.

Elgar, D. F., Norris, C. S., Ayers, J. S., Pritchard, M., Otter, D. E., & Palmano, K. P. (2000). Simultaneous separation and quantitation of major bovine whey proteins including proteose peptone and caseinomacropeptide by reversed-phase high-performance liquid chromatography on polystyrene-divinylbenzene. *Journal of Chromatography A*, 878(2), 183-196.

Ellman, G. L. (1959). Tissue sulfhydryl groups. *Archives in Biochemistry and Biophysics*, 82, 70-77.

Eynard, L., Iametti, S., Relkin, P., & Bonomi, F. (1992). Surface hydrophobicity changes and heat-induced modifications of α-lactalbumin. *Journal of Agricultural and Food Chemistry*, 40(10), 1731-1736.

Fang, Y. & Dalgleish, D. G. (1998). The conformation of α-lactalbumin as a function of pH, heat treatment and absorption at hydrophobic surfaces studied by FTIR. *Food Hydrocolloids*, 12, 121-126.

Fields, G. B., Alonso, D. O. V., Stigter, D., & Dill, K. A. (1992). Theory for the aggregation of proteins and copolymers. *Journal of Physical Chemistry*, 96, 3974-3981.

Foegeding, E. A., Davis, J. P., Doucet, D., & McGuffey, M. K. (2002). Advances in modifying and understanding whey protein functionality. *Trends in Food Science & Technology*, 13, 151-159.

Galani, D. & Apenten, R. K. O. (1997). The comparative heat stability of bovine b-lactglobulin in buffer and complex media. *J. Sci. Food Agric.*, 74, 89-98.

Gezimati, J., Creamer, L. K., & Singh, H. (1997). Heat-induced interactions and gelation of mixtures of β-lactoglobulin and α-lactalbumin. *Journal of Agricultural and Food Chemistry*, 45(4), 1130-1136.

Goers, J., Permyakov, S. E., Permyakov, E. A., Uversky, V. N., & Fink, A. L. (2002). Conformational prerequisites for α-lactalbumin fibrillation. *Biochemistry*, 41(41), 12546-12551.

Havea, P., Singh, H., & Creamer, L. K. (2000). Formation of new protein structures in heated mixtures of BSA and α-lactalbumin. *Journal of Agricultural and Food Chemistry*, 48(5), 1548-1556.

Hillier, R. M. & Lyster, R. L. J. (1979). Whey protein denaturation in heated milk and cheese whey. *Journal of Dairy Research*, 46, 95-102.

Hoffmann, M. A. M. & van Mil, P. J. J. M. (1999). Heat-induced aggregation of β-lactoglobulin as a function of pH. *J. Agric. Food Chem.*, 47, 1898-1905.

Hollingsworth, P. (2003). Food and the aging consumer. *Food Technology*, 57(7), 28-30.

Hong, Y. H. & Creamer, L. K. (2002). Changed protein structures of bovine β-lactoglobulin B and α-lactalbumin as a consequence of heat treatment. *International Dairy Journal*, 12(4), 345-359.

Jegouic, M., Grinberg, V. Y., Guingant, A., & Haertle, T. (1996). Thiol-induced oligomerization of α-lactalbumin at high pressure. *Journal of Protein Chemistry*, 15(6), 501-509.

Jones, W. R. (2002). Dynamic and Rayleigh laser light scattering detection modes in size exclusion chromatography as a means to characterize therapeutic proteins and as a methods development tool. *American Biotechnology Laboratory*, 20(2), 36-38.

Karman, A. H. & van Boekel, M. A. J. S. (1986). Evaluation of the Kjeldahl factor for conversion of the nitrogen content of milk and milk products to protein content. *Neth. Milk Dairy J.*, 40, 315-336.

Kitabatake, N., Wada, R., & Fujita, Y. (2001). Reversible conformatinal change in β-lactoglobulin A modified with n-ethylmaeimide and resistance to molecular aggregation on heating. *Journal of Agriculture and Food Chemistry*, 49(8), 4011-4018.

Kronman, M. J. (1989). Metal-ion binding and the molecular conformational properties of α-lactalbumin. *Critical Reviews in Biochemistry and Molecular Biology*, 24(6), 565-667.

Li, J., Zhang, S., & Wang, C. C. (2001). Only the reduced conformer of α-lactalbumin is inducible to aggregation by protein aggregates. *Journal of Biochemistry*, 129(5), 821-826.

Lindner, R. A., Treweek, T. M., & Carver, J. A. (2001). The molecular chaperone α-crystallin is in kinetic competition with aggregation to stabilize a monomeric molten- globule form of α-lactalbumin. *Biochemical Journal*, 354, 79-87.

Livney, Y. D., Verespej, E., & Dalgleish, D. G. (2003). Steric effects governing disulfide bond interchange during thermal aggregation in solutions of beta-lactoglobulin B and alpha-lactalbumin. *Journal of Agricultural and Food Chemistry*, 51(27), 8098-8106.

Lyster, R. L. (1970). The denaturation of α-lactalbumin and β-lactoglobulin in heated milk. *Journal of Dairy Research*, 37, 233-243.

McGuffey, M. K., Epting, K. L., Kelly, R. M., & Foegeding, E. A. (Submitted). Denaturation and aggregation of 3 α-lactalbumin preparations at neutral pH. *Journal of Agricultural and Food Chemistry*.

McSweeney, S. L., Mulvihill, D. M., & O'Callaghan, D. M. (2004). The influence of pH on the heat-induced aggregation of model milk protein ingredient systems and model infant formula emulsions stabilized by milk protein ingredients. *Food Hydrocolloids*, 18(1), 109-125.

Morr, C. V. & Foegeding, E. A. (1990). Composition and functionality of commercial whey and milk protein concentrates and isolates: A status report. *Food Technology*, 44(4), 100, 102-104, 106, 108, 110 & 112.

Okazaki, A., Ikura, T., Nikaido, D., & Kuwajima, K. (1994). The chaperonin GroEL does not recognize apo-α-lactalbumin in the molten globule state. *Nature Structural Biology*, 1, 439-446.

O'Kennedy, B. T., Halbert, C., & Kelly, P. M. (2001). Formation of whey protein particles using calcium phosphate and their subsequent stability to heat. *Milchwissenschaft-Milk Science International*, 56(11), 625-628.

Patro, S. Y. & Przybycien, T. M. (1994). Simulations of kinetically irreversible protein aggregate structure. *Biophysical Journal*, 66, 1274-1289.

Permyakov, E. A., Morozova, L. A., Kalinichenko, L. P., & Derezhkov, V. Y. (1988). Interaction of α-lactalbumin with Cu^{2+}. *Biophysical Chemistry*, 32, 37-42.

Peters, T. (1985). Serum-Albumin. *Advances in Protein Chemistry*, 37, 161-245.

Puyol, P., Cotter, P. F., & Mulvihill, D. M. (1999). Thermal gelation of commercial whey protein concentrate: influence of pH 4.6 insoluble protein on thermal gelation. *International Journal of Dairy Technology*, 52(3), 81-91.

Rattray, W. & Jelen, P. (1997). Thermal stability of skim milk whey protein solution blends. *Food Research International*, 30(5), 327-334.

Robbins, F. M., Andreott, R., Holmes, L. G., & Kronman, M. J. (1967). Inter- and Intramolecular Interactions of α-Lactalbumin. 7. Hydrogen Ion Titration Curve of α-Lactalbumin. *Biochimica Et Biophysica Acta*, 133(1), 33-&.

Schokker, E. P., Singh, H., & Creamer, L. K. (2000). Heat-induced aggregation of β-lactoglobulin A and B with α-lactalbumin. *International Dairy Journal*, 10(12), 843-853.

Schorsch, C., Jones, M. G., & Norton, I. T. (1999). Thermodynamic incompatibility and microstructure of milk protein/locust bean gum/sucrose systems. *Food Hydrocoll.*, 13, 89-99.

Swaisgood, H. E. (1982). Developments in dairy chemistry. In P. F. Fox, (Ed). Developments in dairy chemistry. (pp. 132-147). Vol. 1. Elsevier Applied Science Publishers: London.

Vanderheeren, G. & Hanssens, I. (1994). Thermal unfolding of bovine α-lactalbumin. *Journal of Biological Chemistry*, 269(10), 7090-7094.

Veprintsev, D., Permyakov, E. A., Kalinichenko, L. P., & Berliner, L. J. (1996). Pb^{2+} and Hg^{2+} binding to α-lactalbumin. *Biochemistry and molecular biology international*, 39(6), 1255-1265.

Winder, A. F. & Gent, W. L. G. (1971). Correction of light-scattering errors in spectrophotometric protein determinations. *Biopolymers*, 10, 1243-1251.

Xiong, Y. L. (1992). Influence of pH and ionic environment on thermal aggregation of whey proteins. *J. Agric. Food Chem.*, 40, 380-384.